



รายงานการวิจัย

ทุนงบประมาณแผ่นดิน ประจำปี พ.ศ. ๒๕๕๘

หมวดผลผลิตเพื่อสร้างองค์ความรู้

หัวข้อ

การใช้ศักย์ไฟฟ้ากระตุ้นการยืดเส้นแอกซอนและการเกาะติดของเซลล์ประสาท
บนแผ่นทองขนาดเล็ก

On-media axon branching and adhesion investigation of
neurons as stimulated by modulated potentials on micro-
patterned gold substrate

ผู้วิจัย

รองศาสตราจารย์ ดร.ศักดิ์นันทน์ พงศ์พันธุ์ผู้ภักดี
อาจารย์ ดร.บุญรัตน์ โล่ห์วงศ์วัฒน์
ศาสตราจารย์ นายแพทย์อนันต์ ศรีเกียรติขจร
คณะแพทยศาสตร์ จุฬาลงกรณ์มหาวิทยาลัย

หัวหน้าโครงการวิจัย
อาจารย์ผู้วิจัยร่วม
ที่ปรึกษาโครงการ

สารบัญเรื่อง

กิตติกรรมประกาศ (Acknowledgement) ที่ระบุนการรับทุนอุดหนุนการวิจัย.....	4
บทความที่เผยแพร่ในวารสารวิชาการนานาชาติ	
การนำเสนอผลงานวิชาการระดับนานาชาติ	
การนำเสนอผลงานวิชาการระดับชาติ	
ผลผลิตอื่นๆ.....	5
บทความวิชาการ และหนังสืออิเล็กทรอนิกส์	
บุคลากรผู้เข้าร่วมโครงการ	
บัณฑิตศึกษาผู้เข้าร่วมโครงการ	
นิสิตแพทย์ผู้เข้าร่วมวิจัย	
แพทย์ต่อยอดผู้เข้าร่วมวิจัย	
อาจารย์ผู้เข้าร่วมวิจัย	
บทคัดย่อภาษาไทย.....	6
บทคัดย่อภาษาอังกฤษ.....	6
บทนำ (Introduction).....	7
วัตถุประสงค์ (Objectives).....	10
วิธีดำเนินการวิจัย (Materials & Methods).....	10
Substrate Fabrication	
Substrate Characterization	
Substrate Patterning	
Cell Culture	
Statistical Analysis	
ผลการวิจัย (Results).....	12
Substrate Fabrication	
Atomic Force Microscopy	
Cell Culture	
อภิปราย/วิจารณ์ (Discussion).....	20
สรุปและเสนอแนะเกี่ยวกับการวิจัย	
ประโยชน์ในทางประยุกต์ของผลงานวิจัย	
บรรณานุกรม (Bibliography).....	22
ประวัตินักวิจัยและคณะ.....	24
รองศาสตราจารย์ ดร.ศักดิ์นันทน์ พงศ์พันธุ์ผู้ภักดี	หัวหน้าโครงการวิจัย
อาจารย์ ดร.บุญรัตน์ โฉ่ววงศ์วัฒน์	อาจารย์ผู้วิจัยร่วม
ศาสตราจารย์ นายแพทย์อนันต์ ศรีเกียรติขจร	ที่ปรึกษาโครงการ
ภาคผนวก (Appendix).....	35

สารบัญภาพ (List of Illustrations)

Figure 1.	12
Batch A: Gold thin-film; thermally evaporated onto surface modified glass substrate	
Figure 2.	13
Batch B: Gold thin-films; thermally evaporated onto surface modified glass substrate	
Figure 3.	14
Top well – peeling problem was observed for gold thin-film substrate; bottom well – attachment of film was improved for gold-chromium thin-film substrate	
Figure 4.	15
AFM 3-D image of surface treated glass substrate	
Figure 5.	15
AFM 2-D image of surface treated glass substrate	
Figure 6.	15
AFM 2-D image of gold thin-film on glass substrate after coating by thermal evaporation	
Figure 7.	16
AFM3-D image of gold thin-film on glass substrate after coating by thermal evaporation	
Figure 8.	16
AFM 2-D image of chromium-gold thin-film after coating by thermal evaporation	
Figure 9.	16
AFM 3-D image of chromium-gold thin-film after coating by thermal evaporation	
Figure 10.	17
AFM images: Micro-patterned gold on polyimide substrate	
Figure 11.	17
3-D AFM image of micro-patterned gold on polyimide	
Figure 12.	18
Cell adhesion Test (Day 0 after 4 hours)	
Figure 13.	18
Adhesion Test (Day 0 after 4 hours): Quantitative comparisons of all substrates tested	
Figure 14.	18
Cell Proliferation (0% serum)	
Figure 15.	18
Cell Proliferation (5% serum)	
Figure 16.	19
Differentiated Neuro2A on gold thin-film	
Table 1.	13
Coefficient of linear thermal expansion and coefficient of volumetric thermal expansion of glass and gold	

กิตติกรรมประกาศ (Acknowledgement) ที่ระบุนการรับทุนอุดหนุนการวิจัย

บทความที่เผยแพร่ในวารสารวิชาการนานาชาติ จำนวน 4 บทความ

- Hansrivijit P, Vibulyaseck S, Maneepark M, Srikiatkachorn A, Bongsebandhu-phubhakdi S. Cortical spreading depression increases NR2A/NR2B ratio by altering numbers of nr2a and nr2b subunit-containing nmda receptors in the hippocampus. *The Journal of Headache and Pain*. 2014; 15 (Suppl 1): F8.
- Hansrivijit P, Vibulyaseck S, Maneepark M, Srikiatkachorn A, Bongsebandhu-phubhakdi S. GluN2A/B ratio elevation induced by cortical spreading depression: Electrophysiological and quantitative studies of the hippocampus. *Journal of Physiological sciences*. 2015; Accepted
- Saleeon W, Jansri U, Srikiatkachorn A, Bongsebandhu-phubhakdi S. The estrous cycle modulates voltage-gated ion channels in TG neurons. *Journal of Physiological sciences*. 2015; Accepted
- Saleeon W, Jansri U, Srikiatkachorn A, Bongsebandhu-phubhakdi S. Estrous cycle induces peripheral sensitization in TG neurons: An animal model of menstrual migraine. *Journal of Medical Association Thailand*. 2015; Accepted

การนำเสนอผลงานวิชาการระดับนานาชาติ จำนวน 2 เรื่อง

- Hansrivijit P, Vibulyaseck S, Maneepark M, Bongsebandhu-phubhakdi S, Srikiatkachorn A. GluN2A/B ratio elevation induced by cortical spreading depression: Electrophysiological and quantitative studies of the hippocampus. 8th Federation of the Asian and Oceanian Physiological Society – FAOPS 2015, Bangkok Thailand, 22nd – 25th November, 2015.
- Saleeon W, Jansri U, Srikiatkachorn A, Bongsebandhu-phubhakdi S. The estrous cycle modulates voltage-gated ion channels in TG neurons. 8th Federation of the Asian and Oceanian Physiological Society – FAOPS 2015, Bangkok Thailand, 22nd – 25th November, 2015.

การนำเสนอผลงานวิชาการระดับชาติ จำนวน 2 เรื่อง

- นายวชิรพงศ์ สลิอ่อน เรื่อง “The estrogen oscillation in estrous cycle modulates electrophysiological properties in trigeminal ganglion neurons” 4 มิถุนายน 2558 ในการประชุม Joint Conference in Medical Sciences 2015: Chula-Rama-Siriraj ณ โรงแรมเซ็นทารา แกรนด์ แอท เซ็นทรัลเวิลด์ กรุงเทพมหานคร
- รองศาสตราจารย์ ดร.ศักดิ์นัน พงศ์พันธุ์ผู้ภักดี เรื่อง “ASICs channel modulation in migraine attack” 22 เมษายน 2558 ในการประชุม The 7th Chula Neuroscience forum 2015 ณ อาคาร อปร คณะแพทยศาสตร์ จุฬาลงกรณ์มหาวิทยาลัย

ผลผลิตอื่นๆ

บทความวิชาการ จำนวน 2 บทความ

- รองศาสตราจารย์ ดร.ศักดิ์นันทน์ พงศ์พันธุ์ผู้ภักดี เรื่อง “ASICs channel modulation in migraine attack” ในหนังสือ 7th Basic and Clinical Neuroscience
- นายวชิรพงศ์ สลืออ่อน และ รองศาสตราจารย์ ดร.ศักดิ์นันทน์ พงศ์พันธุ์ผู้ภักดี เรื่อง “The estrogen oscillation in estrous cycle modulates electrophysiological properties in trigeminal ganglion neurons” ในหนังสือ Joint Conference in Medical Sciences 2015: Chula-Rama-Siriraj

หนังสืออิเล็กทรอนิกส์ 2 เล่ม

- รองศาสตราจารย์ ดร.ศักดิ์นันทน์ พงศ์พันธุ์ผู้ภักดี และศาสตราจารย์ นายแพทย์อนันต์ ศรีเกียรติขจร “MDCU-Neurophysiology” สำหรับการเรียนการสอนรายวิชา 3000278 Neuroscience คณะแพทยศาสตร์ จุฬาลงกรณ์มหาวิทยาลัย
- รองศาสตราจารย์ ดร.ศักดิ์นันทน์ พงศ์พันธุ์ผู้ภักดี “GI hormones and Control of food intake” สำหรับการเรียนการสอนรายวิชา 3000268 Alimentary System I คณะแพทยศาสตร์ จุฬาลงกรณ์มหาวิทยาลัย

บุคลากรผู้เข้าร่วมโครงการ

บัณฑิตศึกษาผู้เข้าร่วมโครงการ จำนวน 5 คน

- อาจารย์ ทันทแพทย์หญิงปราณี พงษ์วิรัตน์นันทน์ ระดับปริญญาเอก ชั้นปีที่ 4
- นายวชิรพงศ์ สลืออ่อน ระดับปริญญาโท ชั้นปีที่ 3
- นางสาวมานิตา ลินพรหม ระดับปริญญาโท ชั้นปีที่ 2
- นางสาวสุภารัตน์ อุดมเลิศปรีชา ระดับปริญญาโท ชั้นปีที่ 3
- นางสาวสินีนาง ทุมรสุนทร ระดับปริญญาโท ชั้นปีที่ 3

นิสิตแพทย์ผู้เข้าร่วมวิจัย จำนวน 2 คน

- นายภานุพงศ์ ห่านศรีวิจิตร ชั้นปีที่ 5
- นางสาวภาลดา พิทักษ์กิจนุกร ชั้นปีที่ 3
- นางสาวภาสินี ตั้งจิตดี ชั้นปีที่ 3

แพทย์ต่อยอดผู้เข้าร่วมวิจัย 1 คน

- แพทย์หญิงพัชรินทร์ เกียรติสารพิภพ แพทย์ต่อยอด ชั้นปีที่ 1 ภาควิชาสูติรีเวชศาสตร์ คณะแพทยศาสตร์ จุฬาลงกรณ์มหาวิทยาลัย

อาจารย์ผู้เข้าร่วมวิจัย 7 คน

- อาจารย์ ดร.อารี วนสุนทรวงศ์ ภาควิชาสรีรวิทยา คณะทันตแพทยศาสตร์ มหาวิทยาลัยมหิดล
- อาจารย์ นายแพทย์ศรัณย์ ตันติวิสุทธิ ภาควิชาออร์โธปิดิกส์ คณะแพทยศาสตร์ จุฬาลงกรณ์มหาวิทยาลัย
- อาจารย์ ดร.เดภิชา จินดาทิพย์ ภาควิชากายวิภาคศาสตร์ คณะแพทยศาสตร์ จุฬาลงกรณ์มหาวิทยาลัย
- อาจารย์ ดร.เทวฤทธิ์ สาระชนะ ภาควิชาเคมีคลินิก คณะสหเวชศาสตร์ จุฬาลงกรณ์มหาวิทยาลัย

- อาจารย์ ดร.ธีระพล สลึงค์ ภาควิชาคณิตศาสตร์ คณะวิทยาศาสตร์ มหาวิทยาลัยเทคโนโลยีพระจอมเกล้าธนบุรี
- อาจารย์ ดร.มนตรี มณีภาค ภาควิชาชีววิทยา คณะวิทยาศาสตร์ มหาวิทยาลัยศรีนครินทรวิโรฒ
- อาจารย์ ดร.ธรรศ พิศลย์กุลเกษม ภาควิชาสรีรวิทยา คณะวิทยาศาสตร์การแพทย์ มหาวิทยาลัยนเรศวร

บทคัดย่อภาษาไทย

วัตถุประสงค์หลักของงานวิจัยนี้ คือการทดสอบการยึดเส้นแอกซอนและการเกาะติดของเซลล์ประสาท โดยการกระตุ้นด้วยศักย์ไฟฟ้าบนแผ่นทองขนาดเล็ก เนื่องจากขั้นตอนการบูรณะเส้นประสาทที่เสียหายในปัจจุบัน จำเป็นต้องใช้เวลาอันยาวนานและมีประสิทธิภาพค่อนข้างน้อย ดังนั้นการผสมผสานปัจจัยและเทคนิคใหม่ๆ ประยุกต์ใช้ในการเพิ่มประสิทธิภาพการส่งสัญญาณระหว่างเซลล์ต่อเซลล์ หรือเซลล์ต่อโลหะ อาจเป็นมิติใหม่ในงานวิจัยสาขานี้ ซึ่งจะนำไปสู่การพัฒนาตัวเลือกใหม่สำหรับการผ่าตัดเพื่อฟื้นฟูการทำงานของเส้นประสาท

ขั้นตอนแรก กลุ่มวิจัยสังเกตการณ์การเจริญเติบโตของเซลล์ปรกติ โดยเลี้ยงเซลล์ Neuro2A ตามกระบวนการและสังเกตการณ์การเจริญเติบโตรวมถึงการแบ่งตัวเพิ่มจำนวนของเซลล์ จากนั้นนำเซลล์ทั้ง 2 ชนิดข้างต้นมาปลูกถ่ายเลี้ยงในแผ่นทองที่ไม่ได้จัดรูปแบบและจัดรูปแบบ โดยที่แผ่นทองที่ไม่ได้จัดรูปแบบจะผ่านการเคลือบทองลงเป็นฟิล์มบางบนแผ่นโพลีสไตรีนโดยเทคนิค “Cathode Arc Sputtering” และ “Magnetron Sputtering” ซึ่งจะมีกระบวนการวิเคราะห์คุณภาพการเคลือบควบคู่กับการเจริญเติบโตและการแบ่งตัวเพิ่มจำนวนของเซลล์ ในขณะที่แผ่นทองที่ได้รับการจัดรูปแบบจะเคลือบทองโดยเทคนิค “Stencil Patterning” และ “Microcontact Printing” ซึ่งเป็นเทคนิคเคลือบให้เป็นลายเส้นฟิล์มบางบนพื้นผิว อีกทั้งมีการปล่อยกระแสไฟฟ้าเพื่อเปลี่ยนศักย์ไฟฟ้ารอบข้างเซลล์ประสาทเพื่อทำให้เกิดสนามแม่เหล็กไฟฟ้า ทำให้การจัดรูปแบบมีมิติที่ 3 เกิดขึ้น คาดเดาได้ว่ารูปแบบลายเส้นและสนามแม่เหล็กไฟฟ้าน่าจะมีผลต่อการยึดแอกซอน

เป้าหมายของงานวิจัยนี้ คือการสร้างองค์ความรู้ใหม่เกี่ยวกับการยึดแอกซอนและการสร้างวงจรประสาทบนแผ่นทอง ความคาดหวังที่ยิ่งใหญ่ที่สุดของงานวิจัยนี้ไม่เพียงแต่จะให้เกิดการพัฒนาเทคนิคที่มีในปัจจุบันเท่านั้น แต่ยังก้าวไกลไปถึงนวัตกรรมที่มีประสิทธิภาพสูงสุดในการบูรณะเส้นประสาท

บทคัดย่อภาษาอังกฤษ

The main focus of this research paper is on-media axon branching and adhesion investigation of neurons as stimulated by modulated potentials on micro-patterned gold substrate. Due to the prolonged and inefficient procedures of nerve repair, it is essential that we effectively incorporate different parameters and techniques as well as investigate cell-cell and cell-substrate interactions to explore new boundaries. This could lead to more operational options for nerve regeneration.

Initially, the behavior of cell growth is first observed. 3T3 and Neuro2A cells are grown according to specific protocols allowing the observations of appropriate parameters needed to

optimize the cells' development and proliferation. After thorough examination, the two cell subjects will be grown on patterned and non-patterned gold-coated substrates. Previously, "Cathode Arc Sputtering" and "Magnetron Sputtering" techniques are used to coat gold particles on polystyrene substrates and distributions of the thin films are then analyzed. Different patterning techniques, such as "Stencil Patterning" and "Microcontact Printing" are then applied to create a number of patterns on the substrates. Furthermore, 3D patterns will be induced by electrical potentials to generate magnetic fields near neurons. Various structured patterns as well as the overall shapes of the magnetic fields are speculated to have different effects on neural behaviors. Thus, cell-substrate adhesion interactions, manipulation of neuronal growth and proliferation using electrical potentials will be explored on pure gold substrates in this research.

Specifically, the ambition of this research is to contribute to the development of neuron circuits that will allow more efficient procedures for nerve repair. This research's greatest hope is not only to provide current developments with extensive data for further improvements, but also to comprehend better the constraints restraining the breakthroughs of novel technologies.

บทนำ (Introduction)

The nervous system consists of the brain, spinal cord, peripheral nerves, and autonomic nerves. It is responsible for all movements, thoughts, and sensations of the human body, provided by the electrochemical signals. Each electrochemical impulse is sent along the axon of the neuron. Minor to moderate injuries most often impair peripheral nerves, which are responsible for connecting the spinal cords with the limbs. Matured nerve cells have almost no ability to regenerate themselves because there are barely any cellular replication activities; therefore, the primary goal in nerve repair is to provide restoration techniques for functions of sensory, motor, and autonomic axons.

Kelsy (1997) stated that peripheral nerve injury is common in both military and civil accidents and approximately 100,000 patients undergo peripheral nerve surgery yearly in Europe and the United States. In the United States alone, more than 20 million Americans are afflicted with peripheral nerve damage. This type of damage becomes increasingly more common with age. In one out of every three people with peripheral nerve damage, the damage comes from diabetes. In another third, the causes of the nerve damage are from accidents and the rest remains unknown. Nerve cells are extremely fragile and can be damaged by pressure, cutting, or even stretching. Nerve fibers that carry information can break and cease to transmit due to pressure and stretching injuries. However, when a nerve is injured

by a cut, both the insulation layer and the nerve itself are broken. All nerve injuries can result in the loss of signal transmission between the brain and the limbs causing morbidity and paralysis in specific areas.

Until now, modern nerve repair technology has only provided us with three main options for nerve injuries; direct repair, nerve grafting, and applications of nerve conduits. Although these approaches are still limited in various ways, they are the best options for today's nerve regeneration.

Direct repair of nerves involve direct connection of two nerve surfaces allowing recoveries of a torn or damaged nerve. However this method is confined to a small nerve gap of only a few centimeters where the ends of the nerve have minimal tension. Dvali and Mackinnon (2003) found that for the optimal nerve regeneration to occur, nerve ends must be accurately aligned, tension-free and also with minimal number of sutures. There are two modes of direct repair, namely "End-to-End Repair" and "End-to-Side Repair".

Nerve grafts are considered the best method for dealing with nerve injuries. Normally, a nerve is taken from the sural (outer part of the leg) to replace the part of the nerve that has been torn or damaged. This will most probably give the best return of nerve function, but will cause a loss of feeling in the area of the donor site. Autografts and allografts are the two popular procedures used in the applications of nerve repair.

The main influence that inspired the advancement of nerve guiding conduits is the disadvantage of nerve injury gap repair with autografts such as donor site morbidity and extended surgical intervals. Successful models of nerve conduits are able to offer appropriate surroundings that will promote axon and Schwann cell growth in addition with neurotrophic stimulation. However, this entubulation development is only limited to only the repairing of small nerve injuries that is no bigger than a few centimeters wide. Nerve conduits are separated into two categories; biological and artificial conduits.

Artificial conduits are a subset of synthetic materials used for nerve regeneration processes. Synthetic materials could be made from organic or inorganic compounds as well as a combination of both. One popular metal which has been increasingly chosen is gold. Gold is chosen due to its facile methods of synthesis, high degree of control over shape and size, long-term stability in a wide variety of solvents and pH conditions, and most importantly in the study regarding neurons, its conductive nature toward surface molecule interaction and modification. Currently, gold is also being tested and extensively developed as biomaterials in dental and drug delivery applications as well as compounds in treatments of cancer.

Lin et al., (2008) explored the application of chitosan-gold nano-composites for nerve conduits. Chitosan is a natural polysaccharide with excellent bacteriostatic (inhibition of

bacterial growth) and hemostatic (enhancement of the stagnation of blood) properties. In addition, chitosan can be degraded by enzymes to absorbable oligosaccharides. However, like most natural polymers, chitosan exhibits low mechanical strength. Therefore, gold, as a material with high mechanical strength and good biocompatibility, was blended with chitosan to produce chi-Au nano-composites. Results from the study showed that mechanical strength increased with the amount of gold in the chitosan. This trend was also observed for cell proliferation and gene expression but the addition of gold more than 50 ppm decreased the stimulatory effects. Addition of gold nanoparticles changes the microstructure of chitosan and this was suggested as the reason why gold nanoparticles can modulate cellular response. However, the in vivo toxicity especially for a longer term of gold nano-particle remains unknown and was not investigated in the experiments.

Lin et al., (2008) also inspected the influence of micro-pattern on cell alignment. Micro-patterning allows the control of the shape and size of cell adhesion, the control of cell migration, cell differentiation and interactions between different types of cells (Wen-wen et al., 2009). In neurology, micro-patterning is widely used as a method to investigate the interactions of ECM proteins with neurons and glia (Corey et al., 2003). Several techniques are available for cell micro-patterning such as photolithography and soft lithography which includes "Microcontact Printing", "Microfluidic Patterning" and "Stencil Patterning". In the study done by Lin et al., (2008), it was observed that most of the neural stem cells appeared multipolar on non-patterned substrates and bipolar of microgrooved substrates. On non-patterned substrates the NSC exhibit extended processes in a radial fashion while those on the micro-patterned surfaces had elongated processes oriented parallel to the grooves of the patterned substrates.

Many studies have shown that an imposed electrical field can enhance and direct nerve growth. Both direct current and alternating current stimulation have the potential to induce the terminal sprouting of intact nerves into the denervated zones of the extremity. Rozman et al., (2000) conducted an experiment to study the effect of biphasic electric fields on nerve regeneration that follows injury to the radial nerve of a dog. Functional regeneration of damaged nerves was evaluated using electromyography. It was found that after 2 months, a greater functional regeneration occurred at the left stimulated radial nerve than at the right control (unstimulated) nerve. It is our interest to examine whether magnetic fields can induce similar effects on neurons.

เนื้อเรื่อง (Main Body)

วัตถุประสงค์ (Objectives)

- 1) To grow metallic glass alloys and ordinary metals on substrate to be used as bio-media.
- 2) Different patterning processes of bio-media and operating parameters will be explored.
- 3) Study of neuronal differentiation induced by electrical potentials across neuron cells and by magnetic field around neuron cells.

วิธีดำเนินการวิจัย (Materials & Methods)

As a clarification of the overall process of the methodology of this research, the major steps that will be taken are mentioned here. Initially, the substrates used in this research are obtained as polystyrene samples are coated with gold particles in the fabrication process. A number of substrates will be patterned using “Stencil Patterning” methods in this part of our methodology. After obtaining the substrates with the desired patterns, cells will be grown on the substrates and observed under the confocal microscope. Cell-cell interactions and cell-substrate adhesion/proliferation will be investigated while the best parameter conditions will be chosen for the preceding parts of this research. The manipulation of cell-cell interactions, cell-substrate adhesion and proliferation via electrical and magnetic stimulations will then be examined. Overall, this research’s methodology consists mainly of three parts, substrate fabrication, substrate characterization, and applications of electrical and magnetic stimulations.

Substrate Fabrication

Ion Beam Sputtering

Sputtering is mainly the removal of atoms from the surface of solids through impacts of energetic particles; ions. This process is commonly used in the production of thin films on sample surfaces. Ion Sputtering is used in the substrate fabrication process of this research. Polystyrene substrate is coated with gold particles using Ion Sputtering before further characterization processes can take place. The duration of sputtering will be varied. The advantage of this process is its speed and the fact that the conditions of the ion sputtering system could be controlled. However, a slight drawback is that the samples being coated with gold will be heated at elevated temperatures and possible damage could be done to the polystyrene samples.

Substrate Characterization

1. Secondary Electron Microscopy (SEM)

Secondary electron microscope (SEM) is used to characterize the prepared substrate samples. Since the samples are gold coated glass slides, they are conductive, non-volatile, and are thin enough for electron transmission and can hence be viewed under SEM. SEM is

used to examine the thickness of the gold film, the distribution of gold particles and the surface morphology of the sample.

2. Confocal Microscopy

The two main modes of the confocal microscopy involve either reflecting light off the specimen or by stimulating fluorescence from dyes (fluorophores) applied to the specimen. In this research fluorescence confocal microscopy is utilized as it is the mode that is most commonly used in biological applications. Since the gold coated substrate samples are opaque, fluorescence confocal microscopy are suitable since the technique does not require the transmission of light through the sample. Fluorophores can also be attached to nerve cells cultured on the substrates allowing the detection of labeled cells and the monitoring of cellular integrity. The resolution of the fluorescence confocal microscopy is about 200 nm, which is appropriate for viewing neurons as the soma or the central part of a neuron typically varies from 4 to 100 micrometers in diameter. However, the prolonged exposure of the focused high intensity excitation light may cause photo-damage on the specimen as well as causing the fluorophores to undergo photo-bleaching where they fade irreversibly. These limitations are taken into account in this research.

3. Atomic Force Microscopy (AFM) and Scanning Probe Microscope (SPM)

Atomic Force Microscopy (AFM) was used to determine the topographic information of the thin film substrates. Surface roughness and profiles were determined by the interaction between the tip and the sample. Specifically for AFM, tip sample forces such as friction, electric, magnetic, or atomic, are investigated to produce such results (M.Q.Li, 1999, Appl. Phys. A 68, 255-258). There have been investigations that apply SPM to biology. An experiment by M.Q.Li has revealed a new DNA conformation called the parallel-stranded DNA. However in this research, SPM was responsible for determining the thickness, surface topology, and roughness of the thin-film coated substrates. The machine used in this process was manufactured by Di Digital Instruments, Veeco Metrology Group. This AFM machine was provided at the Scientific and Technological Research Equipment Centre of Chulalongkorn University.

Substrate Patterning

Chemical etching can be used for patterning of gold substrates. Wet chemical etching of gold requires a strong oxidizer for the separation of the unpaired valence electron, as well as a complexing agent which suppresses the reassembly of oxidized gold atoms back into the crystal. Several gold etchants are available and the most suitable etchant will be determined and utilized in the research. Different patterned photoresist masks together with the chemical etching technique will be implemented to create different patterns of gold on the

polystyrene substrates. It is anticipated that different patterns will induce difference effects on the growth, proliferation, and branching of neurons. Furthermore, each pattern is expected to encourage different outcomes once electrical and magnetic stimuli are applied.

Cell Culture

Neuro2A cell lines are used in this research. The culture media consists of 4 components: Minimum Essential Medium with Earle's Balanced Salt Solution (MEM/EBSS), Fetal Bovine Serum (FBS), L-glutamine and Penicillin Streptomycin. The protocol for culturing of Neuro2A cell lines is provided by the stem cell laboratory, Department of Medicine, Neurovirology Division, Faculty of Medicine, Chulalongkorn University Hospital.

Statistical Analysis

All data are presented as means \pm standard deviation (SD). Statistical analysis is performed using ANOVA test. A probability value (p value) of < 0.05 is accepted as indicative of a statistically significant difference.

ผลการวิจัย (Results)

Substrate Fabrication

Thin film substrates were prepared by the LEYBOLD UNIVEX 300 thermal evaporator in vacuum condition of approximately 10^{-4} Pa. Two types of substrates were prepared on pretreated glass slides; gold and chromium-gold thin-films, where chromium acts as the adhesion layer.

In Batch A, gold thin-film with thickness of 29.0 nm; approximately 103 mg of gold was used. The first trial of thermal evaporation yielded gold thin-films that have a thickness that allows only small amounts of light to penetrate. This caused an obstacle once the sample is observed under the inverted microscope. Consequently from low light penetration through the sample, the ability to focus a clear image is reduced, therefore obtaining images that are unclear or underexposed (Figure 1).

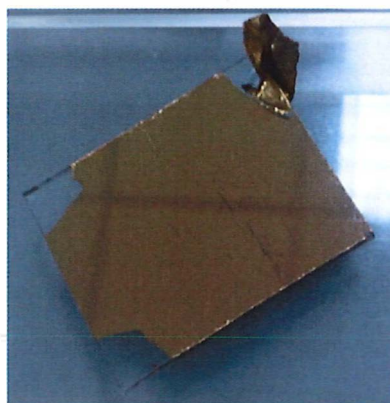


Figure 1. Batch A: Gold thin-film; thermally evaporated onto surface modified glass substrate

In Batch B, gold thin-film with thickness of 12.0 nm; approximately 37.2 mg of gold was used. By reducing the amount of gold used to evaporate onto the glass substrates, we eliminate the problem of low light penetration while using the inverted microscope. This permits a solid and clear image of cultured cells (Figure 2).

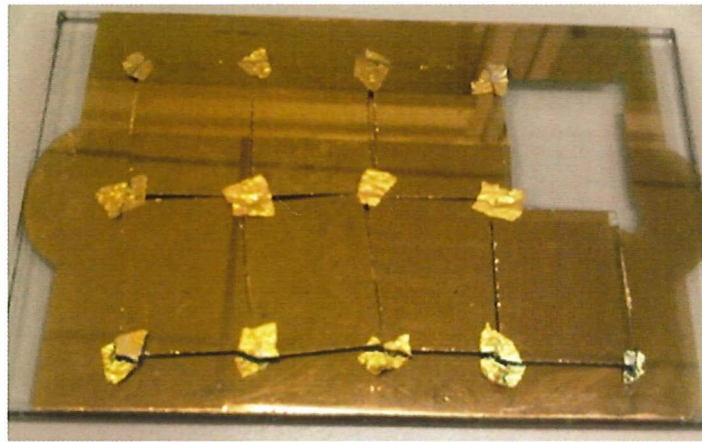


Figure 2. Batch B: Gold thin-films; thermally evaporated onto surface modified glass substrate

As seen from table 1 in the following page, we are able to see the major differences in the values of both the coefficients of linear and volumetric thermal expansion. In thermodynamics, the coefficient of volumetric thermal expansion is referred to as the compressibility (β), which is inversely related to the bulk modulus of a material. Although the coefficients of volumetric thermal expansion are able to quantitatively represent the changes of materials in bulk form relative to changes in temperature, they are not able to quantitatively represent that of thin-film materials. Since coefficients of linear thermal expansion (α) relates to the changes in materials' linear dimensions in response to changes in temperature, they significantly relate to thin-film characteristics. Therefore, it is important to note that the coefficients of linear thermal expansion are most significant in explaining the obstacle faced here. So since there were conditions in the investigations that required temperature changes, it is believed that the difference of the coefficients of linear thermal expansions of glass and gold were responsible for the peeling of gold thin-film from the glass substrate. To tackle this obstacle, in the following trial, we incorporate an adhesive layer between the glass substrate and gold thin-film.

MATERIAL	Coefficient of Linear Thermal Expansion (α) [$10^{-6}/C^{\circ}$ at 20 $^{\circ}C$]	Coefficient of Volumetric Thermal Expansion (β) [$\beta(\approx 3\alpha)$, $10^{-6}/C^{\circ}$ at 20 $^{\circ}C$]
Glass	8.5	25.5
Gold (Au)	13 - 15	42

Table 1. Coefficient of linear thermal expansion and coefficient of volumetric thermal expansion of glass and gold

In Batch C, gold thin-film with a thickness of 27.0 nm; approximately 7.38 mg of gold, and Chromium-gold thin-film with a thickness of 13.0 nm of chromium layer and 8.90 nm of gold layer; approximately 17.5 mg of chromium and 28.5 mg of gold were used.

We incorporated a variation in the third attempt of thermal evaporation to improve the adhesion of gold onto the glass substrate. Chromium acts as an adhesive layer between gold and the glass substrate. The peeling problem of the coating layer was reduced for chromium-gold thin-films; however observations of cells were consequently harder due to a lower contrast of cells and substrate which resulted from the increase in the overall thickness of the thin-film.



Figure 3. Top well – peeling problem was observed for gold thin-film substrate; bottom well – attachment of film was improved for gold-chromium thin-film substrate

Atomic Force Microscopy

Atomic Force Microscope (AFM) was used to determine the surface topology; specifically the roughness and the thickness of gold and chromium-gold thin-films after the materials were fabricated. From the AFM techniques Figure 4 and Figure 5 display the surface structure of surface treated glass substrate using the Piranha Solution. It was determined by AFM that the roughness of glass surface is approximately 2.415 nm.

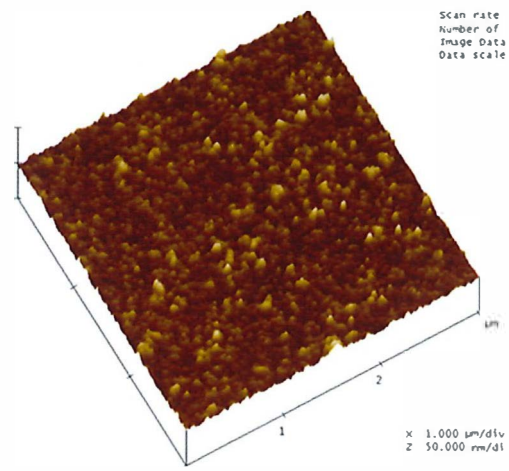


Figure 4. AFM 3-D image of surface treated glass substrate

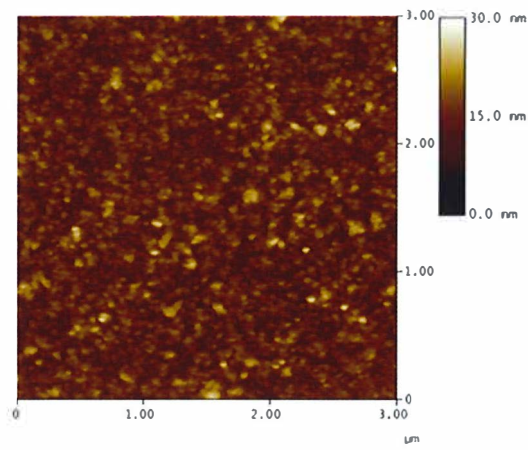


Figure 5. AFM 2-D image of surface treated glass substrate

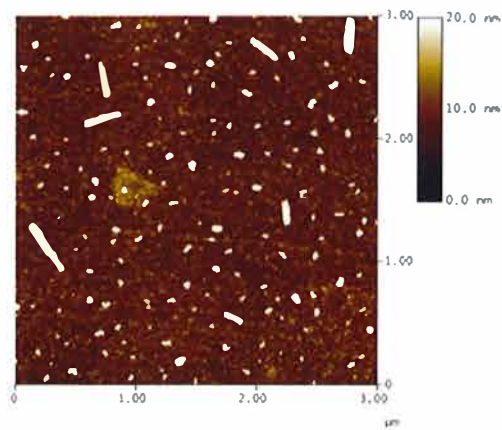


Figure 6. AFM 2-D image of gold thin-film on glass substrate after coating by thermal evaporation

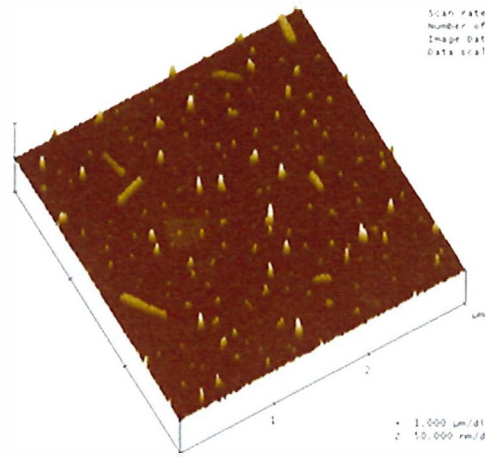


Figure 7. AFM3-D image of gold thin-film on glass substrate after coating by thermal evaporation

Figure 6 and Figure 7 display the surface of gold thin-film after thermal evaporation. Figure 4 shows the surface in 3D and it was observed that gold thin-film surface had cylindrical or rod-like structures on its surface. The thickness of gold was measured and approximated to be in the range of 13-17 nm and roughness estimated to be 2 nm.

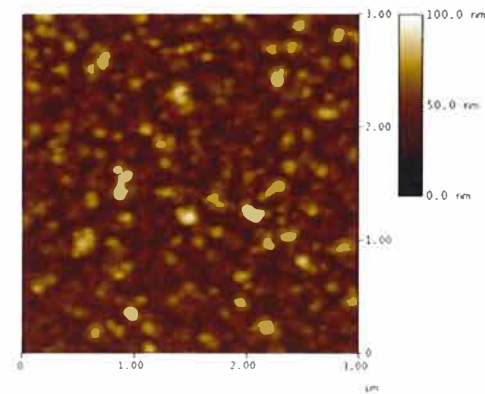


Figure 8. AFM 2-D image of chromium-gold thin-film after coating by thermal evaporation

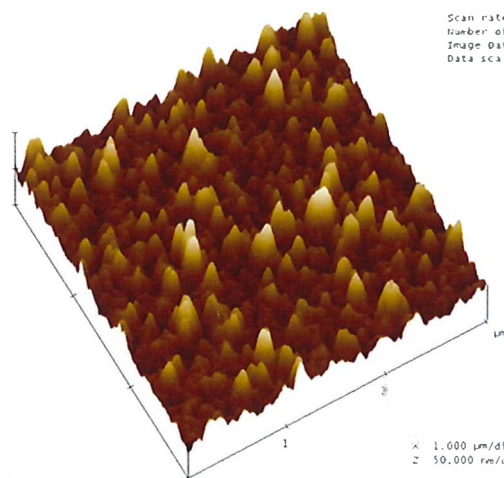


Figure 9. AFM 3-D image of chromium-gold thin-film after coating by thermal evaporation

Figure 8 and Figure 9 display the surface of gold that has been adhered on the glass surface using chromium. The roughness of chromium-gold thin-film shows a significant increase once compared to glass surface and gold thin-film. The thickness of chromium was estimated by AFM to be in the range of 116-123 nm. The roughness and thickness of gold that was coated on chromium were approximately to be 10 nm and in the range of 25-28 nm, respectively.

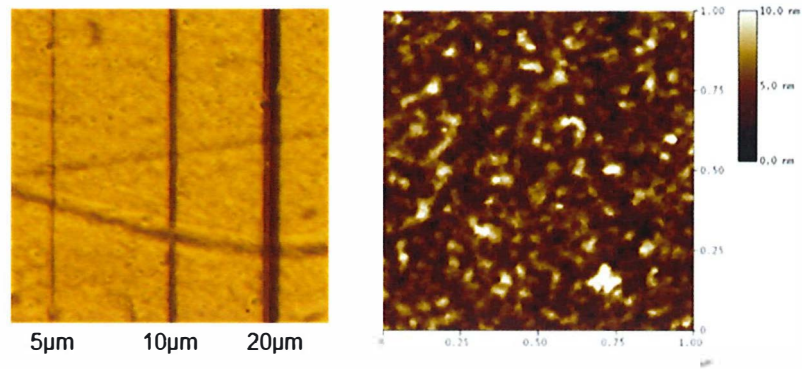


Figure 10. AFM images: Micro-patterned gold on polyimide substrate (Left). 2-D image of micro-patterned gold line (20µm) achieved by lithium dodecylsulfate (LDS) (Right).

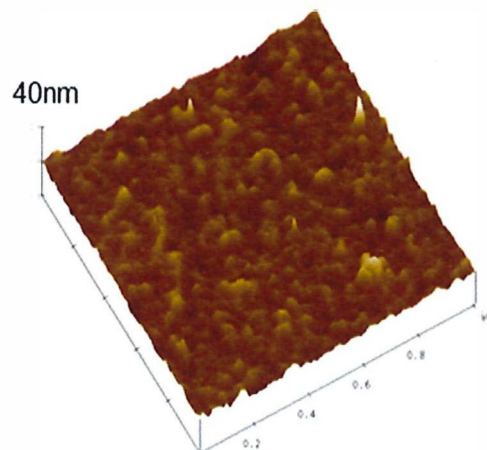


Figure 11. 3-D AFM image of micro-patterned gold on polyimide

Figure 10 and Figure 11 are AFM images that display the overall topology of the micro-patterned gold on polyimide substrates. It was investigated that the surface of the micro-patterned gold on polyimide are layers of porous depositions on gold.

Cell Culture

Once the number of cells in the culture dish accumulated and the density seemed too high indicating an inappropriate condition for sustaining the proliferation and development of

Neuro2A cells, the dish must be sub-cultured. The objective of this process is to divide the total number of cells into three new culture dishes.

Cell sub-culture procedure initiated with the removal of old media entirely and replaced with 5 ml of PBS. The amount of PBS is removed and 2 ml of 0.25% trypsin EDTA is added to the culture dish. Trypsin functions to segregate the cells into individual neuron cell. After the application of trypsin, the dish is kept in the incubator for 2 minutes before removing the dish from the incubator and then the addition of 2 ml of Neuro2A media to stop the segregation reaction. This is followed by micro-pipetting the entire solution out and injecting it into the 15 ml tube. Then centrifuge the tube at 1000 rpm for 5 minutes to allow the cells to settle at the bottom of the tube. Once completed, pour out the media solution leaving behind the cell sedimentation. Re-suspension of the cell is then done after adding 1 ml of media into the tube. Prepare 10 ml of Neuro2A media in each cell culture dish and place equal amounts of resuspended cells in each culture dish. Lastly, the dishes are placed inside the incubator at 37°C.

Two conditions were investigated using serum-free media and 5% serum media where cell adhesion and cell proliferation tests were conducted. Cells were cultured on different substrates. Gold thin-film substrates used were obtained from batch A. Observable through the comparison of Figure 12, the number of cell adhesion after 4 hours were higher and the Neuro2A on gold surfaces had relatively higher densities compared to the controlled group.

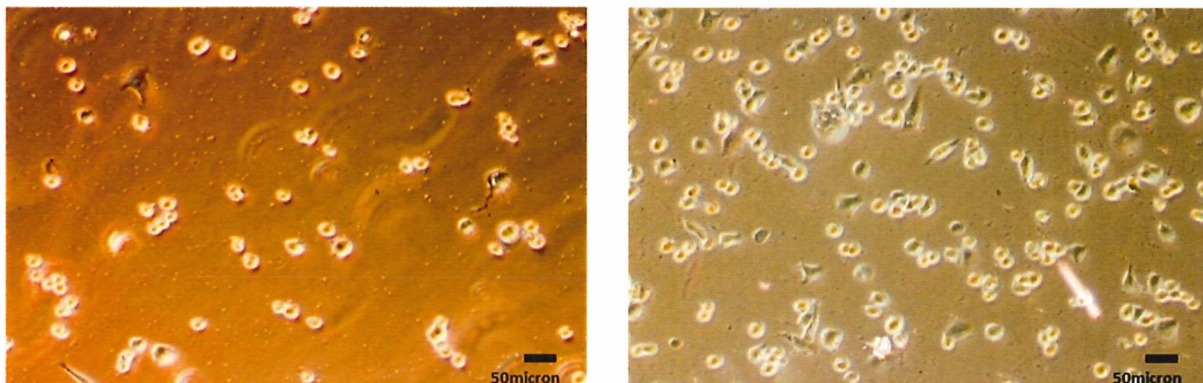
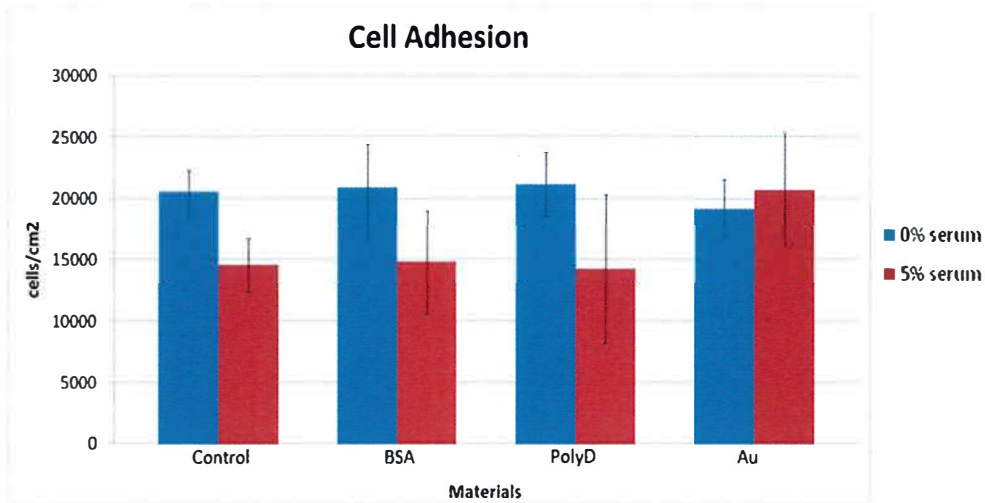


Figure 12. Cell adhesion Test (Day 0 after 4 hours); Control (Left) and Gold (Right)



*Error bars represent 95% confidence interval range

Figure 13. Adhesion Test (Day 0 after 4 hours): Quantitative comparisons of all substrates tested

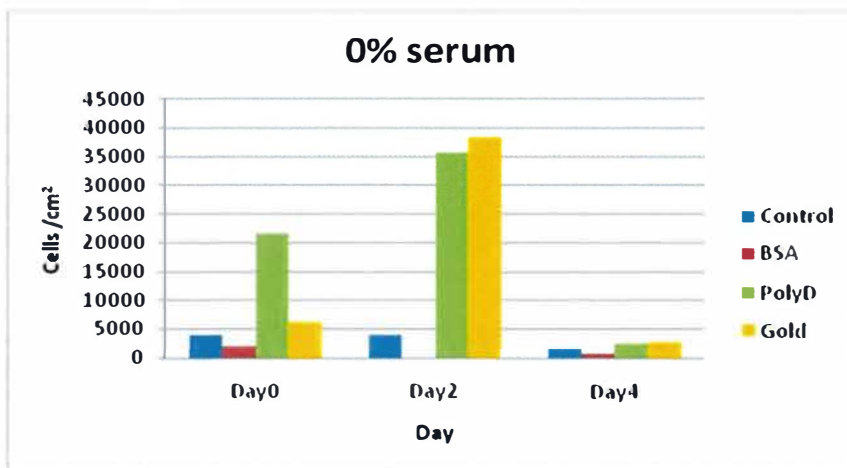


Figure 14. Cell Proliferation (0% serum)

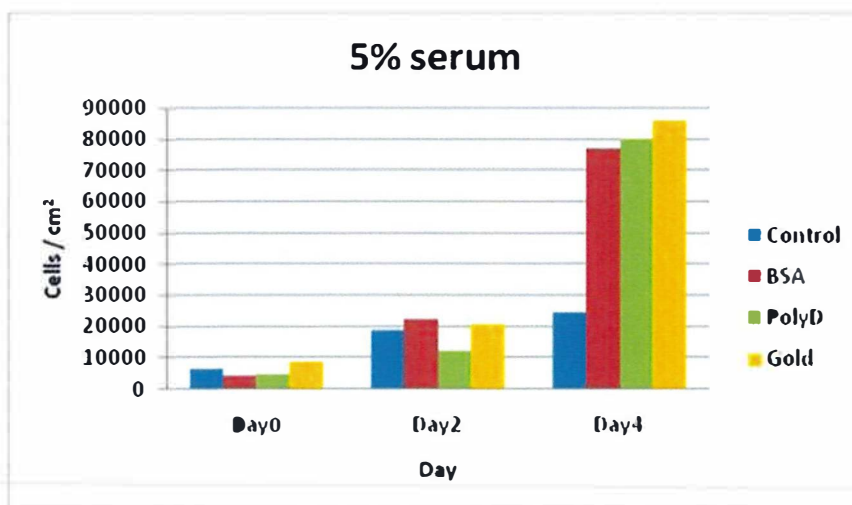


Figure 15. Cell Proliferation (5% serum)

In serum-free media, it can be seen that the number of cells on day 2 and day 4 on gold substrates are comparable to that on the PDL-coated substrates which is the experimental positive control. In 5% serum media the number of cells on gold substrates were even higher than that of PDL-coated substrates.

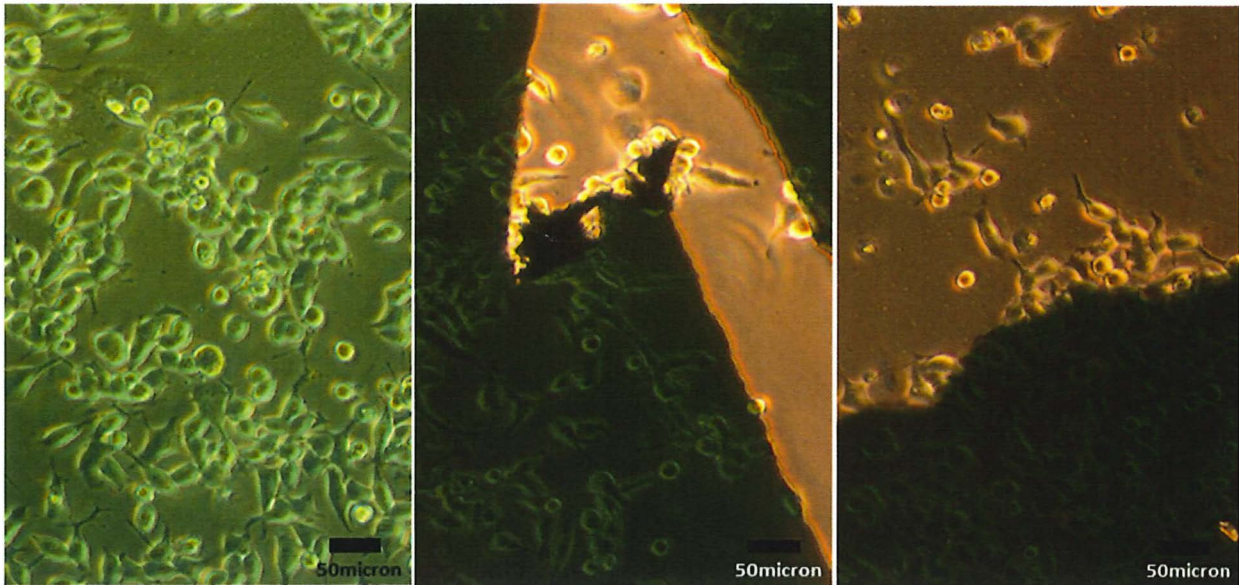


Figure 16. Differentiated Neuro2A on gold thin-film (Left), Preference of Neuro2A on gold-thin-film (Center and Right)

Figure 16 (Left) shows a surface of gold thin-film that has an abundance of healthy Neuro2A cells that have extensively adhered, proliferated, and differentiated. Figure 16 could be compared to Figure 16 (Center and Right) to visually portray how Neuro2A more preferably develops on gold thin-film in comparison to glass substrates. In Figure 16 (Center and Right), it is observed that a higher density of differentiated Neuro2A lies on the surface of gold thin-films than on the glass substrate (controlled group; bright area).

อภิปราย/วิจารณ์ (Discussion)

The best outcomes regarding Neuro2A cell adhesion and proliferation received were obtained from the first trial of the experimentation using materials fabricated in Batch A. Gold thin-film coated glass have shown a significantly higher number of cells adhered after 4 days compared to the negative controlled group. This illustrates the high potential of gold usage in nerve cell culture. The preference observation of Neuro2A for the first trial however showed impressive results in comparing the preferences of Neuro2A for gold thin-films than on controlled (glass) substrates. The team's investigation allowed simultaneous observations of two testing substrate conditions for a single environment; controlled (glass) and gold thin-film, repeated in a number of repeated 6-well plates used in the trial. These simultaneous

observations allowed the investigators to examine at a keener approach, therefore, obtaining more precise and reliable data. It was deduced that gold thin-film on substrates are potential candidates for nerve cell culture applications. The different results obtained in the second trial on the subjects of cell adhesion and cell proliferation could be accounted for by the different weight of gold used in the Thermal Evaporation process, which led to varying gold thin-film thicknesses and the different passages of Neuro2A used in the seeding process.

The porosity of gold will significantly reduce its conductivity and therefore casted doubts on the suitability of lithium dodecylsulfate (LDS) to produce the desired micro-patterning of gold. Therefore, it was evaluated that the process of thermal evaporation with the utilization of masks will fabricate micro-patterned gold on substrates that will potentially perform more effectively in terms of conductivity and neural development control.

From the results analyzed from Figure 14 and Figure 15, it was deductable that although for 0% serum where there was not enough nutrition to sustain the development of Neuro2A after two days, Neuro2A still had higher preference and enhanced cell proliferation on the surface of gold in comparison to the controlled, negative, and positive controlled groups. It is assumed that by day 4, the number of cells reached a threshold amount where it became inappropriate to sustain further development of neuro2A cells. Therefore, Neuro2A cells started to die after day 4 due to declining nutrient concentrations, depleting surface area for adhesion and proliferation, and increasing waste concentrations.

Originally, primitive Neuro2A cells will be circular in shape with somewhat turgid, continuous, and solid membrane boundaries. Differentiated Neuro2A however, will have an elongated body with extensions or branching of neuronal physiques. This was the main criteria for distinguishing one differentiated Neuro2A from one that has not. To obtain more detailed and highly comparable data of the preference of Neuro2A development on surface modified (hydrophilic) glass substrate and gold thin-film, investigations on both surfaces were made on the same substrate. This allowed the team to investigate keener on the preference of Neuro2A in a single system or environment. In Figure 16, it was revealed that Neuro2A prefers to adhere and proliferate on gold thin-film compared with glass substrate. In addition to greater adhesion and proliferation of Neuro2A, it could also be observed that the Neuro2A cells on gold thin-film are more extensively branched and developed that represents neuronal differentiation than those on the glass substrate.

สรุปและเสนอแนะเกี่ยวกับการวิจัย

The fabrication process encountered another obstacle regarding the peeling of gold thin-film before and during the investigations of the experiments in Batch A. The problem of gold

peeling off the glass substrate remains in Batch B. It is suspected that the source of this complication originated from the differences in the values of thermal expansion of glass and gold as in cell seeding experiments, variations in temperature were encountered. Otherwise, we are trying to evaluate cell adhesion and proliferation with Batch B.

For future pursuit, it is essential to alter the protocol in thin-film coating process. It is extrapolated that the thickness of the adhesive layer; chromium, should be significantly thinner than that of gold; possibly only a few nanometers thick. As for the thickness of gold thin-film, the aim is to increase its thickness by several folds achieving at least 20 nm.

ประโยชน์ในทางประยุกต์ของผลงานวิจัย

Listed below are some recommendations for future application

- Apply electrical current to gold substrate at various voltages and examine its effects on neural developments and differentiation
- Investigate different patterning techniques to construct microgrooves for axon guiding and neural behaviors

บรรณานุกรม (Bibliography)

- Anderson DE, Hinds MT. 2011. Endothelial cell micropatterning: methods, effects, and applications. *Ann Biomed Eng* 39(9):2329-45.
- Brunelli GA, Battiston B, Vigasio A, Brunelli G, Marocolo D. 1993. Bridging nerve defects with combined skeletal muscle and vein conduits. *Microsurgery* 14(4):247-51.
- Cemil B, Ture D, Cevirgen B, Kaymaz F, Kaymaz M. 2009. Comparison of collagen biomatrix and omentum effectiveness on peripheral nerve regeneration. *Neurosurg Rev* 32(3):355-62; discussion 362.
- Corey JM, Feldman EL. 2003. Substrate patterning: an emerging technology for the study of neuronal behavior. *Exp Neurol* 184 Suppl 1:589-96.
- Dvali L, Mackinnon S. 2003. Nerve repair, grafting, and nerve transfers. *Clin Plast Surg* 30(2):203-21.
- Geuna S, Papalia I, Tos P. 2006. End-to-side (terminolateral) nerve regeneration: a challenge for neuroscientists coming from an intriguing nerve repair concept. *Brain Res Rev* 52(2):381-8.
- Ichihara S, Inada Y, Nakamura T. 2008. Artificial nerve tubes and their application for repair of peripheral nerve injury: an update of current concepts. *Injury* 39 Suppl 4:29-39.
- Lin YL, Jen JC, Hsu SH, Chiu IM. 2008. Sciatic nerve repair by microgrooved nerve conduits made of chitosan-gold nanocomposites. *Surg Neurol* 70 Suppl 1:S1:9-18.
- Lohwongwatana B, Schroers J, Johnson WL. 2006. Strain rate induced crystallization in bulk metallic glass-forming liquid. *Phys Rev Lett* 96(7):503-506.

- Luis AL, Rodrigues JM, Amado S, Veloso AP, Armada-Da-Silva PA, Raimondo S, Fregnan F, Ferreira AJ, Lopes MA, Santos JD and others. 2007. PLGA 90/10 and caprolactone biodegradable nerve guides for the reconstruction of the rat sciatic nerve. *Microsurgery* 27(2):125-37.
- Meek MF, Coert JH. 2002. Clinical use of nerve conduits in peripheral-nerve repair: review of the literature. *J Reconstr Microsurg* 18(2):97-109.
- Myckatyn TM, Mackinnon SE, Hunter DA, Brakefield D, Parsadonian A. 2004. A novel model for the study of peripheral-nerve regeneration following common nerve injury paradigms. *J Reconstr Microsurg* 20(7):533-44.
- Strasberg SR, Hertl MC, Mackinnon SE, Lee CK, Watanabe O, Tarasidis G, Hunter DA, Wong PY. 1996. Peripheral nerve allograft preservation improves regeneration and decreases systemic cyclosporin A requirements. *Exp Neurol* 139(2):306-16.
- Yu H, Peng J, Guo Q, Zhang L, Li Z, Zhao B, Sui X, Wang Y, Xu W, Lu S. 2009. Improvement of peripheral nerve regeneration in acellular nerve grafts with local release of nerve growth factor. *Microsurgery* 29(4):330-6.
- Zorko B, Rozman J, Seliskar A. 1993. Multielectrode spiral cuff for ordered and reversed activation of nerve fibres. *J Biomed Eng* 15(2):113-20.

ประวัตินักวิจัยและคณะ

หัวหน้าโครงการวิจัย รองศาสตราจารย์ ดร.ศักนัน พงศ์พันธ์ผู้ภักดี

1. ชื่อ - นามสกุล (ภาษาไทย) ดร.ศักนัน พงศ์พันธ์ผู้ภักดี รองศาสตราจารย์
ชื่อ - นามสกุล (ภาษาอังกฤษ) Saknan Bongsebandhu-phubhakdi, Ph.D., Assistant Professor
2. เลขหมายบัตรประจำตัวประชาชน 3-1014-02236-60-7
3. ตำแหน่งปัจจุบัน รองศาสตราจารย์ระดับ A-3
4. หน่วยงาน ภาควิชาสรีรวิทยา คณะแพทยศาสตร์ จุฬาลงกรณ์มหาวิทยาลัย
โทรศัพท์ 0-2256-4267 โทรสาร 0-2252-7854
e-mail: saknan@live.jp
5. ประวัติการศึกษา
2544 B.Sc. Engineering (Bioengineering), Honors degree, Faculty of Bioscience and Biotechnology, Tokyo Institute of Technology, Tokyo, Japan
2546 M.Sc. Engineering (Biological Information), Graduate School Bioscience and Biotechnology, Tokyo Institute of Technology, Tokyo, Japan
2550 Ph.D. Medicine (Neuroscience), Graduate School of Medicine, The University of Tokyo, Tokyo, Japan
6. สาขาวิชาการที่มีความชำนาญพิเศษ (แตกต่างจากวุฒิการศึกษา) ระบุสาขาวิชาการ
Neurophysiology, Electrophysiology
7. ประสบการณ์ที่เกี่ยวข้องกับการบริหารงานวิจัยทั้งภายในและภายนอกประเทศ โดยระบุสถานภาพในการ
ทำการวิจัยว่าเป็นผู้อำนวยการแผนงานวิจัย หัวหน้าโครงการวิจัย หรือผู้ร่วมวิจัยในแต่ละผลงานวิจัย
 - 7.1. ผู้อำนวยการแผนงานวิจัย : ชื่อแผนงานวิจัย
ไม่มี
 - 7.2. หัวหน้าโครงการวิจัย : ชื่อโครงการวิจัย
 - Role of nociceptin in the rat trigeminal system evoked by cortical spreading depression (ทุนรัชดาภิเษกสมโภช คณะแพทยศาสตร์ จุฬาลงกรณ์มหาวิทยาลัย 2550-2552)
 - Role of endogenous nociceptin in migraine (ทุนพัฒนาอาจารย์ใหม่ จุฬาลงกรณ์มหาวิทยาลัย 2551-2553)
 - Effect of cortical spreading depression on synaptic transmission and synaptic plasticity (ทุนพัฒนาอาจารย์รุ่นใหม่ สำนักงานกองทุนสนับสนุนการวิจัย 2552-2554)
 - โครงการศึกษาพยาธิกำเนิดโรคของระบบประสาทกลางโดยวิธีทางไฟฟ้าสรีรวิทยา (ทุนส่งเสริมบัณฑิต มูลนิธิ “อานันท์มหิตล” แผนกแพทยศาสตร์ 2553-2556)
 - 7.3. งานวิจัยที่ทำเสร็จแล้ว : ชื่อผลงานวิจัย ปีที่พิมพ์ การเผยแพร่ และแหล่งทุน (อาจมากกว่า 1 เรื่อง)
 - 7.3.1. Haruyama T, Bongsebandhu-phubhakdi S, Nakamura I, Mottershead D, Keinanen K, Kobatake E, Aizawa M. A biosensing system based on extracellular potential recording

- of ligand-gated ion channel function. overexpressed in insect cells. *Analytical Chemistry*. 2003; 75: 918-921.
- 7.3.2. Bongsebandhu-phubhakdi S, Manabe T. The neuropeptide nociceptin is a synaptically released endogenous inhibitor of hippocampal long-term potentiation. *Journal of Neuroscience*. 2007; 27: 4850-4858.
- 7.3.3. Bongsebandhu-phubhakdi S, Haruyama T, Kobatake E. Electrophysiological methods for drug assessment. *Asian Biomedicine*. 2007; 1: 265-272.
- 7.3.4. Bongsebandhu-phubhakdi S, Phisonkulkasem D, Srikiatkachorn A. Enhancing effect of nociceptin in cortical spreading depression: electrophysiological study in animal model of migraine. *Asian Biomedicine*. 2009; 3: 325-329.
- 7.3.5. Bongsebandhu-phubhakdi S, Phisonkulkasem D, Srikiatkachorn A. Modulation of cortical spreading depression and trigeminal nociception by nociceptin/orphanin FQ. *Journal of Headache and Pain*. 2010; 11 (Supple 1): S10.
- 7.3.6. Maneepak M, Bongsebandhu-phubhakdi S, Le Grand SM, Srikiatkachorn A. Multiple cortical spreading depressions impair hippocampal long-term potentiation. *Journal of Headache and Pain*. 2010; 11 (Supple 1): S38.
- 7.3.7. Bongsebandhu-phubhakdi S, Phisonkulkasem D, Srikiatkachorn A. Nociceptin/Orphanin FQ modulates cortical activity and trigeminal nociception. *Headache*. 2011; 51:1245-1253.
- 7.3.8. Bongsebandhu-phubhakdi S, Srikiatkachorn A. Pathophysiology of Medication Overuse Headache: Implications from Animal Studies. *Current Pain and Headache Reports*. 2011; 16: 110-115.
- 7.3.9. Maneepark M, Srikiatkachorn A, Bongsebandhu-phubhakdi S. Involvement of AMPA receptors in CSD-induced impairment of LTP in the hippocampus. *Headache*. 2012; 52: 1535-1545.
- 7.3.10. Saleewong T, Srikiatkachorn A, Maneepark M, Chonwerayuth A, Bongsebandhu-phubhakdi S. Quantifying altered long-term potentiation in the CA1 hippocampus. *Journal of Integrative Neuroscience*. 2012; 11: 243-264.
- 7.3.11. Saleewong T, Srikiatkachorn A, Maneepark M, Chonwerayuth A, Bongsebandhu-phubhakdi S. Computational approach to long-term potentiation in hippocampal CA1 area describes the efficacy of stimulation patterns. *Asian Biomedicine*. 2013; 7: 347-356.
- 7.3.12. Junsre U, Bongsebandhu-phubhakdi S. ASICs Alteration by pH Change in Trigeminal Ganglion Neurons. *Journal of Physiology and Biomedical Sciences*. 2014; 27: 20-25.
- 7.3.13. Vibulyaseck S, Bongsebandhu-phubhakdi S, le Grand SM, Srikiatkachorn A. Potential risk of dihydroergotamine causing medication-overuse headache; preclinical evidence. *Asian Biomedicine*. 2014; 8: 323-331.
- 7.3.14. Hansrivijit P, Vibulyaseck S, Maneepark M, Srikiatkachorn A, Bongsebandhu-phubhakdi S. Cortical spreading depression increases NR2A/NR2B ratio by altering numbers of nr2a

- and nr2b subunit-containing nmda receptors in the hippocampus. *The Journal of Headache and Pain*. 2014; 15 (Suppl 1): F8.
- 7.3.15. Hansrivijit P, Vibulyaseck S, Maneepark M, Srikiatkachorn A, Bongsebandhu-phubhakdi S. NR2A/NR2B ratio elevation induced by cortical spreading depression: Electrophysiological and quantitative studies of the hippocampus. *Journal of Physiological Sciences*. 2015; Accepted.
- 7.3.16. Saleeon W, Jansri U, Srikiatkachorn A, Bongsebandhu-phubhakdi S. The estrous cycle modulates voltage-gated ion channels in TG neurons. *Journal of Physiological sciences*. 2015; Accepted.
- 7.3.17. Saleeon W, Jansri U, Srikiatkachorn A, Bongsebandhu-phubhakdi S. Estrous cycle induces peripheral sensitization in TG neurons: An animal model of menstrual migraine. *Journal of Medical Association Thailand*. 2015; Accepted.
- 7.4. งานวิจัยที่กำลังทำ: ชื่อข้อเสนอการวิจัย แหล่งทุน และสถานภาพในการทำวิจัยว่าได้ทำการวิจัย
 ล่วงแล้วประมาณร้อยละเท่าใด
- 7.4.1. Effect of acute and chronic ergotamine on cortical spreading depression and trigeminal nociception
 แหล่งทุน ทุนวิจัยรัชดาภิเษกสมโภช คณะแพทยศาสตร์ จุฬาลงกรณ์มหาวิทยาลัย
 สถานภาพในการทำวิจัย ร้อยละ 90
- 7.4.2. Involvement of low pH and estrous cycle in migraine; single-cell recording in primary-cultured trigeminal ganglionic neurons
 แหล่งทุน ทุนพัฒนามหาวิทยาลัยวิจัยแห่งชาติ: ชัยเฉลิมมหาวิทยาลัยโลก คลัสเตอร์
 สุขภาพ ปี 2557
 สถานภาพในการทำวิจัย ร้อยละ 90
- 7.4.3 The alteration of pain receptor and pain-related neurotransmitters in vagina of pre- and postmenopausal women
 แหล่งทุน ทุนวิจัยรัชดาภิเษกสมโภช คณะแพทยศาสตร์ จุฬาลงกรณ์มหาวิทยาลัย
 สถานภาพในการทำวิจัย ร้อยละ 40

อาจารย์ผู้วิจัยร่วม อาจารย์ ดร.บุญรัตน์ โล่ห์วงศ์วัฒน์

1. ชื่อ - นามสกุล (ภาษาไทย) ดร.บุญรัตน์ โล่ห์วงศ์วัฒน์ อาจารย์
ชื่อ - นามสกุล (ภาษาอังกฤษ) Dr. Boonrat Lohwongwatana, Ph.D., Lecturer
2. เลขหมายบัตรประจำตัวประชาชน 3-1002-02837-54-1
3. ตำแหน่งปัจจุบัน อาจารย์ระดับ A-5
4. หน่วยงาน ภาควิชาวิศวกรรมโลหการ คณะวิศวกรรมศาสตร์ จุฬาลงกรณ์มหาวิทยาลัย
โทรศัพท์ 0-2218-6939 โทรสาร 0-2218-6942
e-mail: boonrat@gmail.com
5. ประวัติการศึกษา
 - M.S. (พ.ศ.2545) และ Ph.D. (พ.ศ.2550) Materials Science and Engineering
California Institute of Technology, Pasadena, CA, ประเทศสหรัฐอเมริกา
 - B.E. (พ.ศ.2543) Materials Science and Engineering (Honors)
Northwestern University, Evanston, IL, ประเทศสหรัฐอเมริกา
 - มัธยมศึกษา จาก โรงเรียนสวนกุหลาบวิทยาลัย (พ.ศ.2538)
6. สาขาวิชาการที่มีความชำนาญพิเศษ (แตกต่างจากวุฒิการศึกษา) ระบุสาขาวิชาการ
Precious Metals, Solder Materials, Alloys Development, Thermodynamics Modeling, Nano-materials
7. ประสบการณ์ที่เกี่ยวข้องกับการบริหารงานวิจัยทั้งภายในและภายนอกประเทศ โดยระบุสถานภาพในการ
ทำการวิจัยว่าเป็นผู้อำนวยการแผนงานวิจัย หัวหน้าโครงการวิจัย หรือผู้ร่วมวิจัยในแต่ละผลงานวิจัย
 - 7.1 ผู้อำนวยการแผนงานวิจัย : ชื่อแผนงานวิจัย
ไม่มี
 - 7.2. หัวหน้าโครงการวิจัย : ชื่อโครงการวิจัย

1.	การพัฒนาโลหะผสมที่ไม่มีตะกั่วเพื่อการบัดกรีในงานอุตสาหกรรม อิเล็กทรอนิกส์	ดร.บุญรัตน์ โล่ห์วงศ์วัฒน์ ร.ศ.ดร.กอบบุญ หล่อทองคำ	สำนักงานกองทุนสนับสนุนการวิจัย (สกว.) TRF-MAG	2552-2554 (600,000)
2.	การปรับปรุงกระบวนการเชื่อมบัดกรีแบบเจ็ทบอนด์ตั้งในหัวอ่านฮาร์ดดิสก์ เพื่อปรับค่าระดับความเอียงของหัวอ่าน	อ.ดร.บุญรัตน์ โล่ห์วงศ์วัฒน์	Western Digital (Thailand) Co., Ltd.	2554 (328,670)
3.	เทคโนโลยีการตัด ชัดใส และขัดแบบละเอียด (การวิเคราะห์ความเค้นบนผิวในกระบวนการแปรรูปแผ่น ALTiC)	อ.ดร.บุญรัตน์ โล่ห์วงศ์วัฒน์ ผศ.ดร.ธัชชาย เหลือวรานันท์	Western Digital (Thailand) Co., Ltd.	2554-2555 (740,350)
4.	การขึ้นรูปแบบเทอร์โมพลาสติกของรัตนโลหะที่มีทองคำเป็นส่วนประกอบหลัก	อ.ดร.บุญรัตน์ โล่ห์วงศ์วัฒน์	สำนักงานกองทุนสนับสนุนการวิจัย (สกว.) ร่วมกับสมาคมผู้ค้าอัญมณีไทยและเครื่องประดับ	2554-2556 (400,000)
5.	การสังเคราะห์อนุภาคระดับนาโนโดยใช้รัตนโลหะทอง	อ.ดร.บุญรัตน์ โล่ห์วงศ์วัฒน์	สำนักงานกองทุนสนับสนุนการวิจัย (สกว.)	2552-2554 (480,000)

6.	การออกแบบพัฒนาโลหะผสมที่ไม่มีตะกั่วเพื่อการบัดกรีในงานอุตสาหกรรม โดยใช้กระบวนการวิเคราะห์แบบ Evolutionary Algorithm	อ.ดร.บุญรัตน์ โล่ห์วงศ์วัฒน์ รศ.ดร.กอบบุญ หล่อทองคำ	สำนักงานกองทุนสนับสนุนการวิจัย (สกว.) TRF-MAG	2551-2553 (600,000)
----	---	--	---	------------------------

7.3. งานวิจัยที่ทำเสร็จแล้ว : ชื่อผลงานวิจัย ปีที่พิมพ์ การเผยแพร่ และแหล่งทุน (อาจมากกว่า 1 เรื่อง)

- Lohwongwatana B, Lewan A, Thipayarat K, Akara-Apipokee N, and Nisaratanaporn E. Metals by design: From ultra-hard *in-situ* nano-composite gold jewelry articles to silver alloys castable in silicone mold. Invited speaker to the 26th SANTA FE SYMPOSIUM for jewelry manufacturing technology, Albuquerque, NM. May 20-23, 2012.
- Piyavatin P, Lothongkum G, and Lohwongwatana B. Characterization of eutectic Sn-Cu solder alloy properties improved by additions of Ni, Co & In MP Materials Testing, 06/2012, page 383-389.
- Thongprasom K, Suvanpiyasiri C, Wongs A, Iamaroon A, Korkij W, Lohwongwatana B, Sinpitaksakul S, and Nakpipat P. Nickel - Induced Oral Pemphigus Vulgaris -Like Lesions Acta Stomatol Croat. 2011;45(3):202-208.
- Lohwongwatana B, and Nisaratanaporn E. On Hardness Invited speaker to the 24th SANTA FE SYMPOSIUM for jewelry manufacturing technology, Albuquerque, NM. May 16-19, 2010.
- Lohwongwatana B, Nisaratanaporn E and Holstein J. Alloys By Design – Knowing the Answer before Spending money Invited speaker to the 22st SANTA FE SYMPOSIUM for jewelry manufacturing technology, Albuquerque, NM. May 18-21, 2008.
- Suh JY, Lohwongwatana B, Garland C, Conner R, Johnson WL, and Suh D. Novel Thermoplastic Bonding Using Bulk Metallic Glass Solder SCRIPTA MATERIALIA, 59 (2008) 905-908. (Impact Factor 2.481)
- Lohwongwatana B, Schroers J and Johnson WL. Hard 18K and .850 Pt. alloys that can be processed like plastics or blown like glass Invited speaker to the 21st SANTA FE SYMPOSIUM for jewelry manufacturing technology, Albuquerque, NM. May 20-23, 2007. (Received Outstanding Technical Presentation Award)
- Lohwongwatana B, Schroers J and Johnson WL. Strain rate induced crystallization in bulk metallic glass-forming liquid PHYSICAL REVIEW LETTERS 96 (7): Art. No. 075503 FEB 24 2006 (Impact Factor 7.072)
- Schroers J, Lohwongwatana B, Johnson WL and Peker A. Precious bulk metallic glasses for jewelry applications MATERIALS SCIENCE AND ENGINEERING A-STRUCTURAL MATERIALS PROPERTIES MICROSTRUCTURE AND PROCESSING 449: 235-238 MAR 25 2007 (Impact Factor 1.490)
- Xu DH, Lohwongwatana B, Duan G, Johnson WL and Garland C. Bulk metallic glass formation in binary Cu-rich alloy series - Cu_{100-x}Zr_x (x=34, 36 38.2, 40 at.%) and mechanical properties of bulk Cu₆₄Zr₃₆ glass ACTA MATERIALIA 52 (9): 2621-2624 MAY 17 2004. (Impact Factor 3.729)

11. Udomlertprecha S, Pavasant P, Lohwongwatana B. Surface modification of titanium alloys using alumina particles blasting for biomedical applications Advanced Materials Research 983: 135-140 2014. (Impact Factor 0.140)

12. Thumsoontorn S, Kuimalee S, Kuntalue B, Pintasiri S, Lohwongwatana B. Microstructure and Direct Measured Micro-strain by TEM of Hot Iso-static Pressed Alumina-Titanium Carbide (Al_2O_3-TiC) Composite Advanced Materials Research 983: 156-160 2014. (Impact Factor 0.140)

7.4. งานวิจัยที่กำลังทำ : ชื่อข้อเสนอการวิจัย แหล่งทุน และสถานภาพในการทำวิจัยว่าได้ทำการวิจัย ลุล่วงแล้วประมาณร้อยละเท่าใด

			Funding Agencies	Funding	สถานะ
1.	การพัฒนาโลหะผสมที่ไม่มีตะกั่วเพื่อการบัดกรีในงานอุตสาหกรรม อิเล็กทรอนิกส์	ดร.บุญรัตน์ โล่ห์วงศ์วัฒน์ รศ.ดร.กอบบุญ หล่อทองคำ	สำนักงานกองทุนสนับสนุนการวิจัย (สกว.) TRF-MAG	2552-2554 (600,000)	เสร็จสิ้น 100% ปิดโครงการแล้ว
2.	การปรับปรุงกระบวนการเชื่อมบัดกรีแบบเจ็ทบอนด์ตั้งในหัวอ่านฮาร์ดดิสก์ เพื่อปรับค่าระดับความเอียงของหัวอ่าน	อ. ดร. บุญรัตน์ โล่ห์วงศ์วัฒน์	Western Digital (Thailand) Co., Ltd.	2554-2555 (328,670)	เสร็จสิ้น 100% ระหว่างปิดโครงการ (ส่ง final report แล้ว)
3.	เทคโนโลยีการตัด ชัดใส และ ชัดแบบละเอียด (การวิเคราะห์ความเค้นบนผิวในกระบวนการแปรรูปแผ่น AlTiC)	อ. ดร. บุญรัตน์ โล่ห์วงศ์วัฒน์ ผศ. ดร. ธาชาย เหลือวารานันท์	Western Digital (Thailand) Co., Ltd.	2554-2555 (740,350)	เสร็จสิ้น 100% ระหว่างปิดโครงการ (ส่ง final report แล้ว)
4.	การขึ้นรูปแบบเทอร์โมพลาสติกของรัตนโลหะที่มีทองคำเป็นส่วนประกอบหลัก	อ. ดร. บุญรัตน์ โล่ห์วงศ์วัฒน์	สำนักงานกองทุนสนับสนุนการวิจัย (สกว.) ร่วมกับสมาคมผู้ค้าอัญมณีไทยและเครื่องประดับ	2554-2556 (400,000)	90%
5.	การสังเคราะห์อนุภาคระดับนาโนโดยใช้รัตนโลหะทอง	อ. ดร. บุญรัตน์ โล่ห์วงศ์วัฒน์	สำนักงานกองทุนสนับสนุนการวิจัย (สกว.)	2552-2554 (480,000)	ปิดโครงการแล้ว
6.	การออกแบบพัฒนาโลหะผสมที่ไม่มีตะกั่วเพื่อการบัดกรีในงานอุตสาหกรรม โดยใช้กระบวนการวิเคราะห์แบบ Evolutionary Algorithm	ดร.บุญรัตน์ โล่ห์วงศ์วัฒน์ รศ.ดร.กอบบุญ หล่อทองคำ	สำนักงานกองทุนสนับสนุนการวิจัย (สกว.) TRF-MAG	2551-2553 (600,000)	ปิดโครงการแล้ว

ที่ปรึกษาโครงการ ศาสตราจารย์ นายแพทย์อนันต์ ศรีเกียรติขจร

1. ชื่อ - นามสกุล (ภาษาไทย) นายแพทย์อนันต์ ศรีเกียรติขจร ศาสตราจารย์
ชื่อ - นามสกุล (ภาษาอังกฤษ) Dr. Anan Srikiatkachorn, M.D., Professor
2. เลขหมายบัตรประจำตัวประชาชน 3-1014-0185-2185
3. ตำแหน่งปัจจุบัน ศาสตราจารย์ระดับ 10 รองคณบดีฝ่ายวิจัย
4. หน่วยงาน ภาควิชาสรีรวิทยา คณะแพทยศาสตร์ จุฬาลงกรณ์มหาวิทยาลัย
โทรศัพท์ 0-2256-4267 โทรสาร 0-2252-7854
e-mail: Anan.S@Chula.ac.th
5. ประวัติการศึกษา
 - 2525 วิทยาศาสตร์บัณฑิต (วิทยาศาสตร์การแพทย์) คณะแพทยศาสตร์ ศิริราชพยาบาล มหาวิทยาลัยมหิดล
 - 2527 แพทยศาสตรบัณฑิต คณะแพทยศาสตร์ ศิริราชพยาบาล มหาวิทยาลัยมหิดล
 - 2533 วุฒิบัตร (ประสาทวิทยา) คณะแพทยศาสตร์ จุฬาลงกรณ์มหาวิทยาลัย / แพทยสภา
 - 2539 Research Fellow, Insitiute of Neurological Sciences, University of New South Wales, Australia
 - 2543 วิทยาศาสตรมหาบัณฑิต (ระบอบวิทยาคลินิก) คณะแพทยศาสตร์ จุฬาลงกรณ์มหาวิทยาลัย
6. สาขาวิชาการที่มีความชำนาญพิเศษ (แตกต่างจากวุฒิการศึกษา) ระบุสาขาวิชาการ ประสาทวิทยาศาสตร์
7. ประสบการณ์ที่เกี่ยวข้องกับการบริหารงานวิจัยทั้งภายในและภายนอกประเทศ โดยระบุสถานภาพในการทำการวิจัยว่าเป็นผู้อำนวยการแผนงานวิจัย หัวหน้าโครงการวิจัย หรือผู้ร่วมวิจัยในแต่ละผลงานวิจัย
 - 7.1. ผู้อำนวยการแผนงานวิจัย : ชื่อแผนงานวิจัย
Neuroscience of pain and headache
 - 7.2. หัวหน้าโครงการวิจัย : ชื่อโครงการวิจัย
Plasticity of trigeminal system and pathogenesis of primary headache
 - 7.3. งานวิจัยที่ทำเสร็จแล้ว : ชื่อผลงานวิจัย ปีที่พิมพ์ การเผยแพร่ และแหล่งทุน (อาจมากกว่า 1 เรื่อง)
 - 7.3.1. Srikiatkachorn A. Epidemiology of headache in the Thai elderly: a study in Bangkae Home for the Aged. *Headache* 1991;31:677-81.
 - 7.3.2. Phanthumchinda K, Srikiatkachorn A. Spinocerebellar degeneration. *J Med Assoc Thai* 1991;74:71-9
 - 7.3.3. Khaoropthum S, Phanthumchinda K, Srikiatkachorn A. Successful surgical removal of intrinsic medullary vascular malformation: a case presentation. *J Med Assoc Thai*1991;74:344-7
 - 7.3.4. Limthavon C, Srikiatkachorn A. Kotchabhakdi N, Govitrapong P. Age-related changes in 5-HT₂ serotonin receptor on human platelets. *Thai J Pharmacol* 1991;13:57-73
 - 7.3.5. Srikiatkachorn A. Phanthumchinda K. Headache in an out-patient department. *Chula Med J* 1992;36:701-13
 - 7.3.6. Govitrapong P, Limthavon C, Srikiatkachorn A. 5-HT₂ Serotonin receptor on platelet membrane of migraine patients. *Headache*1992;32:480-4
 - 7.3.7. Srikiatkachorn A. Govitrapong P, Limthavon C. Up-regulation of 5-HT₂ serotonin receptor: a possible mechanism of transformed migraine. *Headache*1994;34:8-11

- 7.3.8. Srikiatkhachorn A, Anthony M. Serotonin receptor adaptation in patients with analgesic induced headache. *Cephalalgia*1996;16:419-22
- 7.3.9. Srikiatkhachorn A, Anthony M. Platelet serotonin in patients with analgesic induced headache. *Cephalalgia*1996;16:423-26
- 7.3.10. Dumrongphol H, Srikiatkhachorn A, Hemachudha T, Kotchabhakdi N, Govitrapong P. Alteration of muscarinic acetylcholine receptors in rabies infected-dog brain. *J NeurolSci* 1996;137:1-6
- 7.3.11. Yang M, Srikiatkhachorn A, Anthony M, Chesterman CN, Chong BH. Serotonin uptake, storage and metabolism in megakaryoblasts. *Int J Hematol* 1996;63:137-42
- 7.3.12. Yang M, Srikiatkhachorn A, Anthony M, Chong BH. Serotonin stimulates megakaryocytopoiesis via 5HT₂ receptor. *Blood Coagul Fibrinolysis* 1996;7:127-33
- 7.3.13. Jitapunkul S, Lailert C, Worakul P, Srikiatkhachorn A, Ebrahim S. Chula Mental Test: a screening test for elderly people in less developed countries. *Int J GeriatrPsychiat* 1996;11:715-20
- 7.3.14. Puangniyom S, Srikiatkhachorn A, Kotchabhakdi N, Govitrapong P. Alteration of 5-HT₂ serotonin receptor in migraine patients with analgesic overuse. *Chula Med J*1996;40:557-66
- 7.3.15. Srikiatkhachorn A, Phanthumchinda K. Prevalence and clinical features of chronic daily headache in a headache clinic. *Headache* 1997;37:277-80
- 7.3.16. Tarasub N, Srikiatkhachorn A, Govitrapong P. Effect of paracetamol on central 5-HT_{2A} serotonin receptor. *Chula Med J* 1997;41:877-88
- 7.3.17. Srikiatkhachorn A, Kasantikul V, Maneesri S, Govitrapong P. Alteration of serotonergic transmission in migraine patients with analgesics abuse headache. In: *Proceeding of the Chulalongkorn University 80th Anniversary Research Conference*. Bangkok, Chulalongkorn University Press 1997;527-38
- 7.3.18. Srikiatkhachorn A, Govitrapong P, Kasantikul V. Role of serotonin in vascular headache: The platelet study. In: Bunnag SC, Srikiatkhachorn A, Patumraj S. eds. *Proceeding of the Third Asian Congress for Microcirculation*. Bologna: Manduzzi Editore;1997:151-7
- 7.3.19. Srikiatkhachorn A, Maneesri S, Govitrapong P, Kasantikul V. Derangement of serotonin system in migraine patients with analgesics abuse headache: clues from platelets. *Headache* 1998;38:43-9
- 7.3.20. Srikiatkhachorn A, Puangniyom S, Govitrapong P. Plasticity of 5-HT_{2A} serotonin receptor in patients with analgesic-induced transformed migraine. *Headache* 1998;38:534-9
- 7.3.21. Srikiatkhachorn A, Govitrapong P, Phanthumchinda K. Role of serotonin in pathogenesis of analgesic-induced headache. In: Boon-Long S, Covavisaruch S, eds. *Proceeding of the Sixth CU-of Seminar on "Medical Science Towards the Year 2000"*. Bangkok, Chulalongkorn University 1998; 19-34
- 7.3.22. Srikiatkhachorn A, Tarasub N, Govitrapong P. Acetaminophen-induced antinociception via central 5-HT_{2A} receptors. *NeurochemInt* 1999;34:491-8
- 7.3.23. Anuntasethakul T, Srikiatkhachorn A, Maneesri S, Patumraj S, Kasantikul V. Ultrastructural changes in endothelial cells of cerebral microvessels after exposure to nitric oxide donor. *Neuropathology* 1999;19:249-58
- 7.3.24. Srikiatkhachorn A, Anuntasethakul T, Maneesri S, Phansuwan-Pujito P, Patumraj S, Kasantikul V. Hyposerotonin-induced nitric oxide supersensitivity in the cerebral microcirculation. *Headache*2000;40:267-75
- 7.3.25. Srikiatkhachorn A, Tarasub N, Govitrapong P. Effect of chronic analgesic exposure on the central serotonin system. A possible mechanism of analgesic abuse headache. *Headache*2000;40:343-50
- 7.3.26. Govitrapong P, Chagkutip J, Turakiteanakan W, Srikiatkhachorn A. Platelet 5-HT_{2A} receptors in schizophrenic patients with and without neuroleptic treatment. *Psychiatry Res* 2000;96:41-50
- 7.3.27. Nudmamud S, Siripurkpong P, Chindaduangratana C, Harnyuttanakorn P, Lotrakul P, Laarbboonsarp W, Srikiatkhachorn A, Kotchabhakdi N, Casalotti SO. Stress, anxiety and peripheral benzodiazepine receptor mRNA levels in human lymphocytes. *LifeSci*2000;67:2221-31

- 7.3.28. [Srikiatkhachorn A](#), Anuntasethakul T, Phansuwan-Pujito P, Patumraj S, Kasantikul V. Effect of Serotonin Depletion on Nitric Oxide Induced Cerebrovascular Nociceptive Response. *Neuroreport* 2001;12:967-71
- 7.3.29. Anomasiri W, Sanguanrangsirikul S, [Srikiatkhachorn A](#), Chuntavan P. Changes of immune system in military recruits after the training program. *J Med Assoc Thai* 2002;85(Suppl 1):327-35
- 7.3.30. [Srikiatkhachorn A](#), Suwattanasophon C, Ruangpattanaatawee A, Phansuwan-Pujito P. 5-HT_{2A} receptor activation and nitric oxide synthesis: a possible mechanism determining migraine attacks. *Headache* 2002;42:566-74
- 7.3.31. Suwanwela NC, [Srikiatkhachorn A](#), Tangwongchai S, Phanthumchinda K. Cerebral autosomal dominant arteriopathy with subcortical infarcts and leukoencephalopathy (CADASIL) in a Thai family. *J Med Assoc Thai* 2003;86:178-82
- 7.3.32. Chuchareon P, Chetsawang B, Govitrapong P, [Srikiatkhachorn A](#). Melatonin receptor expression in rat cerebral artery. *Neurosci Lett* 2003; 341: 259-61
- 7.3.33. Suwattanasophon C, Phansuwan-Pujito P, [Srikiatkhachorn A](#). 5-HT(1B/1D) serotonin receptor agonist attenuates nitroglycerin-evoked nitric oxide synthase expression in trigeminal pathway. *Cephalalgia*. 2003 Oct;23(8):825-32
- 7.3.34. Maneesri S, Patamanont J, Patumraj S, [Srikiatkhachorn A](#). Cortical spreading depression, meningeal inflammation and trigeminal nociception. *Neuroreport* 2004;10:1623-7
- 7.3.35. Supornsilpchai W, Sanguanrangsirikul S, Maneesri S, [Srikiatkhachorn A](#). Serotonin depletion, cortical spreading depression and trigeminal nociception. *Headache* 2006;46:34-39
- 7.3.36. Le Grand SM, Patumraj S, Phansuwan-Pujito P, [Srikiatkhachorn A](#). Melatonin inhibits cortical spreading depression-evoked trigeminal nociception. *Neuroreport* 2006 Nov 6;17:1709-13
- 7.3.37. Chuchareon P, Chetsawang B, Putthaprasert C, [Srikiatkhachorn A](#), Govitrapong P. The presence of melatonin receptors and inhibitory effect of melatonin on hydrogen peroxide-induced endothelial nitric oxide synthase expression in bovine cerebral blood vessels. *J Pineal Res* 2007;43:35-41
- 7.3.38. Kaewwongse M, le Grand SM, [Srikiatkhachorn A](#). Involvement of 5-HT_{2A} receptor in chronic inflammatory pain. *Chula Med J* 2007;51:471-81
- 7.3.39. Maneepak M, le Grand SM, [Srikiatkhachorn A](#). Serotonin depletion increases nociception-evoked trigeminal NMDA receptor phosphorylation. *Headache* 2009;49:375-82
- 7.3.40. Bongsebandhu-phubhakdi S, Phisonkunkasem T, [Srikiatkhachorn A](#). Enhancing effect of nociceptin in cortical spreading depression: electrophysiological study using an animal model of migraine. *Asian Biomedicine* 2009;3:325-329
- 7.3.41. Supornsilpchai W, le Grand MS, [Srikiatkhachorn A](#). Involvement of pro-nociceptive 5-HT_{2A} receptor in the pathogenesis of medication-overuse headache. *Headache* 2010;50:185-197
- 7.3.42. Supornsilpchai W, le Grand MS, [Srikiatkhachorn A](#). Cortical hyperexcitability and mechanism of medication-overuse headache. *Cephalalgia* 2010;30:1101-1109
- 7.3.43. le Grand SM, Supornsilpchai W, Saengjaroentham C, [Srikiatkhachorn A](#). Depletion of serotonin leads to cortical hyperexcitability and trigeminal nociceptive facilitation via nitric oxide pathway. *Headache* 2011;51:1152-60
- 7.3.44. Bongsebandhu-phubhakdi S, Phisonkulkasem T, [Srikiatkhachorn A](#). Nociceptin/Orphanin FQ modulates cortical activity and trigeminal nociception. *Headache* 2011;51:1245-53
- 7.3.45. Kalandakanond-Thongsong S, Daendee S, [Srikiatkhachorn A](#). Effect of the acute and chronic estrogen on anxiety in the elevated T-maze. *Physiology & Behaviours* 2012;105:357-363
- 7.3.46. Nimnuan C, Asawawichienjinda T, [Srikiatkhachorn A](#). Potential risk factors for psychiatric disorders in patients with headache. *Headache* 2012;52:90-8
- 7.3.47. Maneepak M, [Srikiatkhachorn A](#), Bongsebandhu-phubhakdi S. Involvement of AMPA receptors in CSD-induced impairment of LTP in the hippocampus. *Headache* 2012;54:1821-1822

- 7.3.48. Saleewong T, Srikiatkachorn A, Maneepak M, Chonwerayuth A, Bongsebandhu-phubhakdi S. Computational approach to long-term potentiation in hippocampal CA1 area describes their efficacy of electrical stimulate patterns. *Asian Biomedicine* 2013;7:347-356
- 7.3.49. Saleewong T, Srikiatkachorn A, Maneepak M, Chonwerayuth A, Bongsebandhu-phubhakdi S. Quantifying altered long-term potentiation in the CA1 hippocampus. *J Integrative Neurosci* 2012;11:243-264
- 7.3.50. Srikiatkachorn A, le Grand SM, Supornsilpchai W, Storer RJ. Pathophysiology of medication overuse headache--an update. *Headache*. 2014;54(1):204-210
- 7.3.51. Saengjaroentham C, Supornsilpchai W, Ji-Au W, Srikiatkachorn A, Maneesri-le Grand S. Serotonin depletion can enhance the cerebrovascular responses induced by cortical spreading depression via the nitric oxide pathway. *Int J Neurosci*. 2014.
- 7.3.52. Yisarakun W, Supornsilpchai W, Chantong C, Srikiatkachorn A, Maneesri-le Grand S. Chronic paracetamol treatment increases alterations in cerebral vessels in cortical spreading depression model. *Microvasc Res*. 2014;94:36-46
- 7.3.53. Hansrivijit P, Vibulyaseck S, Maneepark M, Srikiatkachorn A, Bongsebandhu-phubhakdi S. NR2A/NR2B ratio elevation induced by cortical spreading depression: Electrophysiological and quantitative studies of the hippocampus. *Hippocampus*. 2014; submitted.
- 7.3.54. Vibulyaseck S, Bongsebandhu-phubhakdi S, le Grand MS, Srikiatkachorn A. Potential risk of dihydroergotamine causing medication-overuse headache: preclinical evidence. *Asian Biomedicine*. 2014; 8: 323-331.
- 7.3.55. Hansrivijit P, Vibulyaseck S, Maneepark M, Srikiatkachorn A, Bongsebandhu-phubhakdi S. Cortical spreading depression increases NR2A/NR2B ratio by altering numbers of nr2a and nr2b subunit-containing nmda receptors in the hippocampus. *The Journal of Headache and Pain*. 2014; 15 (Suppl 1): F8.
- 7.3.56. Hansrivijit P, Vibulyaseck S, Maneepark M, Srikiatkachorn A, Bongsebandhu-phubhakdi S. GluN2A/B ratio elevation induced by cortical spreading depression: Electrophysiological and quantitative studies of the hippocampus. *Journal of Physiological sciences*. 2015; Accepted
- 7.3.57. Saleeon W, Jansri U, Srikiatkachorn A, Bongsebandhu-phubhakdi S. The estrous cycle modulates voltage-gated ion channels in TG neurons. *Journal of Physiological sciences*. 2015; Accepted
- 7.3.58. Saleeon W, Jansri U, Srikiatkachorn A, Bongsebandhu-phubhakdi S. Estrous cycle induces peripheral sensitization in TG neurons: An animal model of menstrual migraine. *Journal of Medical Association Thailand*. 2015; Accepted
- 7.4. งานวิจัยที่กำลังทำ : ชื่อข้อเสนอการวิจัย แหล่งทุน และสถานภาพในการทำวิจัยว่าได้ทำการวิจัย
 ล่วงแล้วประมาณร้อยละเท่าใด
- 7.4.1. Effect of ergot exposure on cortical excitability and trigeminal nociceptive system
 แหล่งทุน สำนักงานกองทุนสนับสนุนการวิจัย และจุฬาลงกรณ์มหาวิทยาลัย
 สถานภาพในการทำวิจัย ร้อยละ 90
- 7.4.2. Plasticity of trigeminal ganglionic neurons and pathogenesis of primary headache
 แหล่งทุน สำนักงานกองทุนสนับสนุนการวิจัย และจุฬาลงกรณ์มหาวิทยาลัย
 สถานภาพในการทำวิจัย ร้อยละ 80

ภาคผนวก (Appendix)

บทความที่เผยแพร่ในวารสารวิชาการนานาชาติ

- Hansrivijit P, Vibulyaseck S, Maneepark M, Srikiatkachorn A, Bongsebandhu-phubhakdi S. Cortical spreading depression increases NR2A/NR2B ratio by altering numbers of nr2a and nr2b subunit-containing nmda receptors in the hippocampus. *The Journal of Headache and Pain.* 2014; 15 (Suppl 1): F8.
- Hansrivijit P, Vibulyaseck S, Maneepark M, Srikiatkachorn A, Bongsebandhu-phubhakdi S. GluN2A/B ratio elevation induced by cortical spreading depression: Electrophysiological and quantitative studies of the hippocampus. *Journal of Physiological sciences.* 2015; Accepted
- Saleeon W, Jansri U, Srikiatkachorn A, Bongsebandhu-phubhakdi S. The estrous cycle modulates voltage-gated ion channels in TG neurons. *Journal of Physiological sciences.* 2015; Accepted
- Saleeon W, Jansri U, Srikiatkachorn A, Bongsebandhu-phubhakdi S. Estrous cycle induces peripheral sensitization in TG neurons: An animal model of menstrual migraine. *Journal of Medical Association Thailand.* 2015; Accepted

MEETING ABSTRACT

Open Access

EHMTI-0308. Cortical spreading depression increases NR2A/NR2B ratio by altering numbers of nr2a and nr2b subunit-containing nmda receptors in the hippocampus

P Hansrivijit^{1*}, S Vibulyaseck¹, M Maneepark², S Bongsebandhu-Phubhakdi¹, A Srikiatkachorn¹

From 4th European Headache and Migraine Trust International Congress: EHMTIC 2014
Copenhagen, Denmark. 18-21 September 2014

Introduction

Cortical spreading depression (CSD), an underlying mechanism of migraine aura, that propagates to the hippocampus is believed to disrupt hippocampal metaplasticity owing to hippocampus-associated symptoms (e.g. amnesia) manifested by patients with chronic migraine. Our previous study showed that this aberration is mediated by AMPA receptors but roles of NMDA receptors are yet to be discovered.

Aims

To exhibit the alteration of NR2A/NR2B response ratio in terms of total numbers of individual NR2A and NR2B-subunits following CSD stimulation.

Methods

Adult Wistar rats were divided into CSD and control group for electrophysiological study (n = 6, each group) and Western blot analysis (n = 15, each group). Electrophysiological response of both NR2A and NR2B were recorded in terms of field-excitatory post-synaptic potentials (fEPSPs). The fEPSP of NR2A was divided by those of NR2B in both control and CSD groups. Western blot analysis was employed to quantify total numbers of hippocampal NR2A and NR2B.

Results

NR2A/NR2B ratio of CSD group significantly increased in comparison with control group (p = 0.018). From Western blot analysis, intensity of NR2A component

was significantly elevated (p = 0.048) whilst that of NR2B was diminished (p = 0.002).

Conclusions

As numerous studies demonstrated that increased hippocampal NR2A/NR2B ratio is linked to impaired long-term potentiation (LTP), our research adds that increase in NR2A/NR2B ratio following CSD stimulation is possibly due to transcriptional up/down-regulation of NR2A and NR2B, respectively. Combining with our previous study, we conclude that CSD impairs memory processes by disrupting both glutamate AMPA and NMDA receptors.

No conflict of interest.

Authors' details

¹Physiology, Faculty of Medicine Chulalongkorn University, Bangkok, Thailand. ²Physiology, Faculty of Science Srinakharinwirot University, Bangkok, Thailand.

Published: 18 September 2014

doi:10.1186/1129-2377-15-S1-F8

Cite this article as: Hansrivijit et al.: EHMTI-0308. Cortical spreading depression increases NR2A/NR2B ratio by altering numbers of nr2a and nr2b subunit-containing nmda receptors in the hippocampus. *The Journal of Headache and Pain* 2014 **15**(Suppl 1):F8.

¹Physiology, Faculty of Medicine Chulalongkorn University, Bangkok, Thailand
Full list of author information is available at the end of the article

GluN2A/B Ratio Elevation Induced by Cortical Spreading Depression: Electrophysiological and Quantitative Studies of the Hippocampus

Panupong Hansrivijit¹, Suteera Vibulyaseck^{1,2}, Montree Maneepark^{1,3}, Anan Srikiatkachorn¹, Saknan Bongsebandhu-phubhakdi¹

¹*Department of Physiology, Faculty of Medicine, Chulalongkorn University, Bangkok, Thailand*

²*Medical Research Institute, Tokyo Medical and Dental University, Tokyo, Japan*

³*Department of Biology, Faculty of Science, Srinakharinwirot University, Bangkok, Thailand*

Correspondence to: Saknan Bongsebandhu-phubhakdi, Ph.D., Department of Physiology, Faculty of Medicine, Chulalongkorn University, 1873 Rama IV Road, Pathumwan, Bangkok, 10330, Thailand. Tel: +66-83-986-0713, Fax: +66-2-252-7854, E-mail: saknan@live.jp

Abstract: Cortical spreading depression (CSD), an underlying mechanism of migraine aura, propagates to the hippocampus, and might explain hippocampus-associated symptoms during migraine attack. We hypothesized that the CSD-induced hippocampal impairment is mediated by NMDA receptors. By using a rat model, CSD was elicited by solid KCl for 45 minutes prior to electrophysiological and quantitative analyses. The result from electrophysiological study showed the ratio of glutamate NMDA receptor 2A and 2B subunits (GluN2A/B). Total NMDA receptor response was isolated using an AMPA antagonist, prior to a GluN2B receptor antagonist. The GluN2A/B ratio was calculated by dividing the remaining NMDA-mediated field-excitatory synaptic potentials (fEPSP) with the subtracted difference of NMDA-mediated fEPSP. Western blot analysis of the hippocampus was performed to confirm the quantitative change of GluN2A/B ratio. In electrophysiological study, the GluN2A/B ratio of hippocampal fEPSP was significantly increased in CSD group. Western blot analysis revealed an increase in GluN2A subunits and a decrease in GluN2B subunits in the ipsilateral hippocampus to the CSD induction. Our current study demonstrated that GluN2A/B ratio was shown to be elevated following CSD stimulation by increasing the total number of GluN2A while reducing the total number of GluN2B subunits. GluN2A/B ratio has been indicated to be associated with synaptic plasticity of the hippocampus. In conclusion, we showed that CSD increased GluN2A/B ratio, in turn, would result in impaired synaptic plasticity. Our findings provide a probable implication on the correlation of migraine aura and hippocampus-associated symptoms. No COI.

Keywords: Cortical spreading depression (CSD); migraine aura; NMDA receptors; GluN2A/2B ratio; synaptic plasticity

INTRODUCTION

Various cerebral insults (e.g. epileptic crises, trauma, ischemia, haemorrhage, and migraine) were shown to produce a transient disturbance in cortical activity, so-called cortical spreading depression (CSD). Cortical spreading depression is caused by massive redistribution of ions, particularly potassium and hydrogen ions between intracellular and extracellular compartments [1] resulting in cortical depolarisation that can spread to the adjacent

areas. By adopting a model of migraine with aura, spreading depression (SD) in each cortical area is accountable for different clinical manifestations seen in the patients. For instance, CSD in the occipital cortex can cause visual metamorphopsia [2,3], whereas those occur in the somatosensory cortex result in paraesthesia or hemi-anaesthesia [4].

Spreading depression propagated to the hippocampus is believed to cause amnesia, emotional and behavioural changes (e.g. hyperactivity, yawning) during migraine attack [5]. In case of acute amnesia, it seems to be transient (4-8 hours in duration) and may impair both anterograde and retrograde memory. Long-term association of migraine and amnesia was also demonstrated in a retrospective cohort study suggesting that migraine is a risk factor of developing transient global amnesia (TGA) [6]. For decades, Olesan and Jorgensen proposed that the association between migraine and TGA may be explained by presence of spreading depression in the hippocampus [7]. The hypothesis was later proven by groups of *ex vivo* and *in vitro* experiments showing that CSD propagated to the hippocampus. Limited studies were published regarding the presence of SD in the *in vivo* hippocampus following CSD except in familial hemiplegic migraine type 1 (FHM1) mutant mice [8]. Although the molecular mechanisms underlying the correlation of migraine and TGA are still unclear, existing evidence suggested that the process may involve actions of glutamatergic receptors [9].

Glutamatergic transmission is known to play an important role in inducing plastic change in the hippocampal synapse. Repetitive activation of the hippocampal synapse can result in a long-lasting change in synaptic activity known as long-term potentiation (LTP). This process is an important step in the registration and consolidation of new memories. Various classes of glutamatergic receptors are involved in LTP development, specifically α -amino-3-hydroxy-5-methyl-4-isoxazolepropionic acid (AMPA) and *N*-methyl-D-aspartic acid (NMDA) receptors. Previously, our group showed that CSD significantly reduced LTP magnitude by decreasing post-synaptic AMPA receptor response [9]. However, the effect of CSD on hippocampal NMDA receptor activity were not demonstrated. Differential subunits of NMDA receptors mainly detected in the hippocampus are GluN2A and GluN2B subunits [10]. Thus, these receptors are of our particular interest. Additional studies have demonstrated that GluN2A/B response ratio is strongly associated with synaptic plasticity by modifying LTP induction threshold [11-13].

In this study, we aimed to demonstrate the changes in synaptic transmission of NMDA receptors. We identified existence of SD observed in the rat hippocampus and compared their differences in electrical properties with the original CSD. Sequential changes in NMDA receptor activity were reported in term of GluN2A/B response ratio. Quantitative assays of GluN2A and GluN2B subunits were also performed using Western blot analysis. The findings of this study may imply a clinical correlation between migraine and hippocampus-associated symptoms.

METHODS

Animals. Adult male Wistar rats (National Laboratory Animal Centre, Mahidol University, Nakorn-Pathom, Thailand) weighing 200-350 g were recruited in this study (N = 50). The animals were acclimatised to the housing facility for at least seven days prior to the experiments. The study was conducted according to the guideline for

experimental animals suggested by the National Research Council of Thailand. The study protocol was approved by the Ethics Committee of the Faculty of Medicine, Chulalongkorn University.

Animal preparations. Each rat was anaesthetised with 60 mg/kg of sodium pentobarbital (Ceva Sante Animale, Libourne, France) intraperitoneally. We avoided using inhaled isoflurane or IV dexmedetomidine as surgical anaesthetics due to their effects on suppressing CSD frequency [14]. Physiological parameters were monitored and only animals that were in stable condition throughout the preparation were included in the experiment.

CSD induction. The rat's head was fitted to a stereotaxic apparatus (Narishige, Tokyo, Japan). After the right parietal bone had been exposed, a 2-mm craniotomy was performed at 6 mm posterior to the bregma and 2 mm lateral to the sagittal suture using an electric dental driller (NSK, Tokyo, Japan). Since propagation of CSD into the hippocampus usually occurred under hyper-excitability conditions, induced either pharmacologically or genetically, increased dose of KCl was employed in our study. For CSD induction, 3 mg of solid KCl (Sigma-Aldrich, St. Louis, MO, USA) was topically applied onto the dura mater for 45 minutes. In control rats, 3 mg of solid NaCl (Merck, Darmstadt, Germany) was used instead of solid KCl.

***In vivo* cortical DC recording.** For the DC recording ($n = 4$), a 2-mm diameter craniotomy was performed in the right frontal bone (from bregma: anterior-posterior, +3 mm; lateral, 2 mm; and dorsal-ventral, 0.5 mm). A recording glass microelectrode for detecting the DC potential was inserted into the frontal neocortex to a depth of 500 μm . Analogue data were converted into digital format using. The data were then analysed using MP100 (Biopac Systems Inc., Goleta, CA, USA) and AcqKnowledge acquisition software (Biopac Systems Inc., Goleta, CA, USA). The measured variables included the area under the curve (AUC) and the amplitude of each CSD wave as well as the number of CSD waves that occurred within a 45-minute period.

***In vivo* hippocampal DC recording.** In a separated set of experiments ($n = 4$), the DC potential was recorded in the CA1 region of the hippocampus instead of the neocortex (from bregma: anterior-posterior, -4 mm; lateral, 2 mm). A recording glass microelectrode was inserted with a depth of 2.2 mm with the aid of rat brain atlas [15] and previous electrophysiological study [16]. The histological position of the electrode was confirmed microscopically.

Hippocampal slice preparation. After 45 minutes of CSD stimulation using solid KCl, the animals ($n = 6$, each group) were decapitated and their ipsilateral hippocampal tissues were entirely dissected. These tissues were then quickly loaded and sectioned using a Vibratome tissue slicer (Vibratome, Richmond, IL, USA). The tissues were processed in cooled artificial CSF solution (119 mM NaCl, 26.2 mM NaHCO_3 , 11 mM glucose, 2.5 mM KCl, 2.5 mM CaCl_2 , 1.3 mM MgSO_4 , 1.0 mM NaH_2PO_4 , 0.1 mM picrotoxin; a GABA_A receptor antagonist), bubbled with carbogen (95% O_2 , 5% CO_2). Fresh slices were moved to a humidified interface-type holding chamber and recovered for at least 1.5 hours prior to the performance of the electrophysiological study.

Electrophysiological recording. A continuation between the CA1 and CA3 region was terminated in order to prevent epileptiform activity originating from the CA3 region. A bipolar tungsten-stimulating electrode was placed in the Schaffer collaterals to evoke a postsynaptic response by delivering a square-pulse stimulus at 0.1 Hz for 0.2 msec. Discharges from presynaptic fibres followed by fEPSPs were recorded using a glass microelectrode. Only

slices that produced fEPSP amplitudes of more than 1 mV and were stable for at least 15 minutes were included in this study.

Response ratio of GluN2A/B. After stable baseline fEPSPs were recorded for at least 15 minutes, NMDA receptor-mediated fEPSPs were isolated by bath application of a potent AMPA receptor antagonist, 6-cyano-7-nitroquinoxaline-2,3-dione; CNQX (10 μ M in 0.1% DMSO; Tocris Bioscience, Bristol, UK) to exclude signals from AMPA components. Ten minutes after application of the drug, input stimulation was delivered at 0.033 Hz and its intensity was adjusted to evoke stable NMDA receptor-mediated fEPSPs. Ten minutes later, the GluN2A component of NMDA receptor-mediated fEPSPs was isolated by bath application of CNQX (10 μ M) and GluN2B subunit-selective NMDA receptor antagonist, ifenprodil (3 μ M in 0.1% DMSO; Tocris Bioscience, Bristol, UK) for 1 hour.

Total component of NMDA receptor responses was the averaged AUC of the NMDA receptor-mediated fEPSPs during 10 minutes prior to ifenprodil application. The amplitude of NMDA receptor-mediated fEPSPs was normalised in the range of 0.5-1.5 mV. GluN2A component of NMDA receptor responses was the averaged AUC of the NMDA receptor-mediated fEPSPs during 50-60 minutes after ifenprodil application (i.e., ifenprodil-insensitive component). GluN2B component (i.e., ifenprodil-sensitive component) was the total component of NMDA receptor responses subtracted with GluN2A component. GluN2A/B ratio was then calculated by dividing GluN2A component with GluN2B component.

Western blot analysis. Another set of adult male Wistar rats was divided into control and CSD group (n = 15, each group). Protocols for CSD stimulation using 3 mg of solid KCl for 45 minutes, combined with solid NaCl in control groups, were repeated.

After 45 minutes of SD stimulation by solid KCl, the isolated hippocampi were then homogenised in a solution containing RIPA buffer (lysis buffer; 150 mM NaCl, 20 mM Tris-HCl, 2 mM EDTA, 1% Triton X-100, 0.05% SDS, 1 mM PMSF, pH 8; Cell Signaling Technology, Beverly, MA, USA) and Protease Inhibitor Cocktail (Cell Signaling Technology, Beverly, MA, USA). Tissue homogenates were centrifuged (Sigma-Aldrich, St. Louis, MO, USA) at 12,000 rpm; 4 °C for 15 minutes.

Fifteen micrograms of protein were loaded onto a 7.5% SDS-PAGE and electroblotted onto a polyvinylidene difluoride (PVDF) membrane (GE Healthcare Life Sciences, Little Chalfont, UK). Membranes that were intended to determine the quantity of GluN2A were blocked with 5% bovine serum albumin (BSA) prior to incubation with the primary antibody in 5% BSA at 4°C overnight and incubated with horseradish peroxidase (HRP)-conjugated secondary antibody (1:10,000 dilution; anti-rabbit IgG antibody; Sigma-Aldrich, St. Louis, MO, USA) for 1 hour. For GluN2B detection, the membranes were blocked with 5% TBST-MLK at room temperature for 1 hour and incubated with a primary antibody in 5% TBST-MLK at 4°C overnight, and incubated with a HRP-conjugated secondary antibody (1:10,000 dilution; anti-mouse IgG antibody; Sigma-Aldrich, St. Louis, MO, USA) for 1 hour. The dilutions of the primary antibodies were 1:500 for both GluN2A (rabbit monoclonal antibody; Millipore, Billerica, MA, USA) and GluN2B (mouse monoclonal antibody; Millipore, Billerica, MA, USA) and 1:2,000 for β -actin (mouse monoclonal antibody; Sigma-Aldrich, St. Louis, MO, USA). Protein bands were

sequentially detected using enhanced chemiluminescent (ECL) reagents (GE Healthcare Life Science, Little Chalfont, UK) exposed onto a hyperfilm (GE Healthcare Life Science, Little Chalfont, UK). The quantity of GluN2A and GluN2B were eventually measured using Image J software (NIH, Bethesda, MD, USA). These signals were normalised against β -actin bands.

Statistical analysis. All data were reported in the format of mean \pm standard error of the mean (SEM). Statistical analysis was performed using IBM SPSS software version 20. Independent sample t-tests was adopted in the analyses to establish a statistical correlation. Only probability values less than 0.05 ($p < 0.05$) were considered to be statistically significant.

RESULTS

***In vivo* cortical and hippocampal DC recordings**

Our data indicated that CSD propagated and reached the CA1 area of the hippocampus in an *in vivo* model with alteration of electrical properties. Several parameters characterising electrical properties of CSD and SD measured at the hippocampus (e.g. total number of SD waves, amplitude, duration, AUC, and wave interval) are displayed in **Table 1**. In the cortical DC recording, the results showed that multiple shifts of negative DC characterised as SD were detected in the frontal neocortex in all rats ($n = 4$) which indicated that solid KCl application consistently induced multiple waves of CSD (**Fig. 1A**). In hippocampal DC recording, we illustrated that a series of negative DC potentials characterised as SD was detected in the hippocampal CA1 in all rats ($n = 4$; **Fig. 1B**).

Ratio of GluN2A/B response

Analysis of our current study revealed that GluN2A/B ratio of the CSD group significantly increased in comparison with the control group. After application of ifenprodil, NMDA receptor-mediated fEPSPs were reduced in both control and CSD slices (**Fig. 2A**). The reduced magnitudes of NMDA receptor-mediated fEPSPs in CSD and control slices were 23.5 ± 2.1 and 34.4 ± 5.5 %, respectively ($p = 0.092$; independent samples two-tailed *t*-test). However, the extent of this reduction was not significantly different between the CSD and control groups. In control slices, ifenprodil decreased NMDA receptor-mediated fEPSPs on the hippocampal CA1 by a degree comparable to other studies [17]. The GluN2A/B ratios in CSD and control groups were 3.376 ± 0.361 and 1.968 ± 0.346 , respectively ($p = 0.018$; $n = 6$ each group; independent samples two-tailed *t*-test; **Fig. 2B**). This result showed that CSD altered the responses of NMDA receptors in the hippocampal CA1 towards greater GluN2A/B response ratio. After treatment with ifenprodil, we also demonstrated that isolated fEPSPs were mediated by NMDA receptors, because the remaining fEPSPs were abolished by the NMDA receptor antagonist, APV ($25 \mu\text{M}$). Importantly, this GluN2A/B ratio represents the 'response' of GluN2A over GluN2B subunits on the neuronal plasma membrane.

Quantitative assay of GluN2A and GluN2B receptors

Our results obtained from Western blotting analysis showed that the total number of both ipsilateral GluN2A and GluN2B subunits of the NMDA receptor were significantly altered in CSD groups ($n = 15$; right KCl-placed hippocampus) compared to control groups ($n = 15$). We observed a significant increase in total number of GluN2A

subunits and a reduction of those GluN2B subunits. The averaged intensity of GluN2A protein band relative to β -actin in ipsilateral CSD and control groups was 0.777 ± 0.040 and 0.655 ± 0.044 , respectively ($p = 0.048$; independent samples two-tailed t -test). The averaged intensity of GluN2B protein band relative to β -actin in ipsilateral CSD and control groups was 0.589 ± 0.027 and 0.713 ± 0.024 , respectively ($p = 0.002$; independent samples two-tailed t -test; **Fig. 3**).

We also compared the total number of GluN2A and GluN2B subunits of the NMDA receptor between ipsilateral and contralateral sides of the hippocampus in CSD group. Total number of GluN2A subunits was significantly increased in the ipsilateral side of the hippocampus ($p = 0.042$; independent samples two-tailed t -test). The averaged values of protein intensity in both ipsilateral and contralateral side of the hippocampus were 0.777 ± 0.040 and 0.650 ± 0.047 , respectively. In contrast, a significant reduction in the total number of GluN2B subunits was demonstrated with an averaged band intensity in both ipsilateral and contralateral side of 0.589 ± 0.027 and 0.699 ± 0.031 , respectively ($p = 0.012$; independent samples two-tailed t -test). In addition, we compared a number of GluN2A and GluN2B subunits in contralateral CSD-induced hippocampi with those control hippocampi. These results were undoubtedly insignificant for both GluN2A and GluN2B subunits ($p = 0.826$ for GluN2A component; $p = 0.805$ for GluN2B component; independent samples two-tailed t -test).

DISCUSSION

Our study demonstrated that induction of CSD resulted in trains of DC shifting, compatible with hippocampal spreading depression. The results are consistent with previous *ex vivo* studies that CSD was induced by 2M KCl microinjection [18,19], or 3 mg solid KCl [9]. However, microinjection of 0.5M KCl was shown not to produce DC shifting in the hippocampus [20]. Another study revealed that single CSD induced by 300 mM KCl topical application resulted in waves of SD in *in vivo* hippocampus only in FHM1 mutant mice, but not the wild-type mice [8]. These evidence support that propagation of SD from the neocortex into the hippocampus is increased in dose-dependent fashion.

According to the DC recordings, wave frequency and amplitude of hippocampal DC waves were diminished, while there were no significant changes in both duration and AUC. The duration of SD refers to how long ion channels remain open to enable prolongation of depolarisation. The AUC is the sum of the amplitude and duration. Wave frequency, which refers to the induction threshold, and amplitude were significantly diminished in hippocampal SD. Possible explanations may lie in anatomical difference [18,21] and conduction sensitivity of the two structures.

Based on our electrophysiological studies, we observed an enhanced GluN2A/B ratio secondarily to CSD stimulation. Combining this information with our previous research [9], we pointed that LTP magnitude was significantly reduced in CSD group compared to the control group. These findings suggest that CSD may be able to alter hippocampal synaptic transmission by interfering GluN2A/B response ratio. Some evidence strongly suggest that ratio of GluN2A/B response governs bidirectional modification of LTP induction threshold in the CA1 of

hippocampus [23,24]. An increase in GluN2A/B ratio was shown to impair LTP, in which an increase of GluN2A/B ratio by one unit is associated with approximately 9% reduction of LTP. [12,25]

Findings from Western blotting analysis support our electrophysiological result of enhanced GluN2A/B ratio. We demonstrated that the total number of GluN2A subunits of the NMDA receptor was elevated whilst those of GluN2B were significantly diminished in the CSD group. Because CSD was elicited for only 45 minutes, we hypothesised that CSD causes post-translational modifications to GluN2A and GluN2B proteins rather than interfering with transcriptional processes. Although little is known regarding the precise mechanism by which GluN2A/B ratio alters the plasticity threshold, we propose that it involves the individual properties of both GluN2A and GluN2B subunits. Furthermore, we also showed that CSD may not travel to the contralateral hippocampus, because we observed no significant changes of ipsilateral (right) and contralateral (left) in either the total number of individual GluN2A or GluN2B subunits.

Evidences from molecular experiments suggest that GluN2B receptors have longer activation duration than GluN2A, which results in a greater Ca^{2+} influx [26]; thus, overexpression of GluN2B led to the enhanced LTP in the hippocampus [27]. In addition, activation of GluN2B subunits of the NMDA receptor could generate LTP in GluN2A-knockout mice [23,28] and hippocampal LTP was not observed in GluN2B-knockout mice [29].

Some limitations should be considered. First, since we used CSD as a model, the interpretation of our study may not only be constrained to migraine with aura, since various cerebral insults has been shown to produce CSD. Second, although the knowledge obtained from this study may explain hippocampus-associated symptoms during migraine aura, the behaviour or memory in animals were not evaluated. This, however, are being studied in our further research.

Taken together, our study revealed that CSD increased GluN2A/B ratio by modifying the numbers of GluN2A and GluN2B subtypes. Our previous studies [9] showed that repetitive CSD resulted in a reduction of LTP which, in turn, is correlated to impaired memory processes. Thus, it is suggested that increased GluN2A/B ratio is associated with reduced LTP. This physiological finding may be used to imply a temporal correlation between migraine with aura and hippocampus-associated symptoms. However, our study was conducted in animals, whether or not the possibility of our findings hold true in human remains unanswered.

Acknowledgements. We thank Dr. Supang Maneesri-le Grand, Ph.D. for her laboratory facilities and Dr. Toshiya Manabe, M.D., Ph.D. for commenting on the preliminary version of this manuscript. This research was funded by Neuroscience of Headache Research Unit, “Integrated Innovation Academic Centre: IIAC”: 2012 Chulalongkorn University Centenary Academic Development Project, Anandamahidol Foundation, National Research University Project, Office of Higher Education Commission (WCU-008-HR-57), Government Research Budget 2014-2016 and Ratchadapiseksompotch Fund from Faculty of Medicine, Chulalongkorn University.

Conflict of interest: The authors declare that they have no conflict of interest.

References

1. Obrenovitch TP, Zilkha E (1995) High extracellular potassium, and not extracellular glutamate, is required for the propagation of spreading depression. *J Neurophysiol* 73: 2107–2114
2. Hadjikhani N, Sanchez del Rio M, Wu O, Schwartz D, Bakker D, Fischl B, Kwong KK, Cutrer FM, Rosen BR, Tootell RB, et al (2001) Mechanisms of migraine aura revealed by functional MRI in human visual cortex. *Proc Natl Acad Sci USA* 98: 4687-4692
3. Chen WT, Lin YY, Fuh JL, Hamalainen MS, Ko YC, Wang SJ (2011) Sustained visual cortex hyperexcitability in migraine with persistent visual aura. *Brain* 134: 2387-2395
4. Leao AAP (1944) Spreading depression of activity in the cerebral cortex. *J Neurophysiol* 7: 359-390
5. Crowell GF, Stump DA, Biller J, McHenry LC Jr, Toole JF (1984) The transient global amnesia-migraine connection. *Arch Neurol* 41: 75-79
6. Lin KH, Chen YT, Fuh JL, Li SY, Chen TJ, Tang CH, Wang SJ (2014) Migraine is associated with a higher risk of transient global amnesia: a nationwide cohort study. *Eur J Neurol* 21: 718-724
7. Olesen J, Jorgensen MB (1986) Leao's spreading depression in the hippocampus explains transient global amnesia. A hypothesis. *Acta Neurol Scand* 73: 219-220
8. Eikermann-Haerter K, Yuzawa I, Qin T, Wang Y, Baek K, Kim YR, Hoffmann U, Dilekoz E, Waeber C, Ferrari MD, van den Maagdenberg AMJM, Moskowitz MA, Ayata, C (2011) Enhanced Subcortical Spreading Depression in Familial Hemiplegic Migraine Type 1 Mutant Mice. *J Neurosci* 31: 5755–5763
9. Maneepark M, Srikiatkachorn A, Bongsebandhu-phubhakdi S (2012) Involvement of AMPA receptors in CSD-induced impairment of LTP in the hippocampus. *Headache* 52: 1535-1545
10. Laurie DJ, Bartke I, Schoepfer R, Naujoks K, Seeburg PH (1997) Regional, developmental and interspecies expression of the four NMDAR2 subunits, examined using monoclonal antibodies. *Brain Res Mol Brain Res* 51: 23-32
11. Philpot BD, Cho KK, Bear MF (2007) Obligatory role of NR2A for metaplasticity in visual cortex. *Neuron* 53: 495-502
12. Xu Z, Chen RQ, Gu QH, Yan JZ, Wang SH, Liu SY, Lu W (2009) Metaplastic regulation of long-term potentiation/long-term depression threshold by activity-dependent changes of NR2A/NR2B ratio. *J Neurosci* 29: 8764-8773
13. Kopp C, Longordo F, Nicholson JR, Luthi A (2011) Insufficient sleep reversibly alters bidirectional synaptic plasticity and NMDA receptor function. *J Neurosci* 26: 12456-12465
14. Kudo C, Toyama M, Boku A, Hanamoto H, Morimoto Y, Sugimura M, Niwa H (2013) Anesthetic effects on susceptibility to cortical spreading depression. *Neuropharmacology* 67: 32-36
15. Paxinos G, Watson C (1997) The rat brain in stereotaxic coordinates. Academic Press, New York, NY.
16. MacDougall MJ, Howland JG (2013) Acute stress and hippocampal output: exploring dorsal CA1 and subicular synaptic plasticity simultaneously in anesthetized rats. *Physiol Rep* 1: e00035
17. Scimemi A, Fine A, Kullmann DM, Rusakov DA (2004) NR2B-containing receptors mediate cross talk among hippocampal synapses. *J Neurosci* 24: 4767-4777

18. Wernsmann B, Pape H, Speckmann E, Gorji A (2006) Effect of cortical spreading depression on synaptic transmission of rat hippocampal tissues. *Eur J Neurosci* 23: 1103-1110
19. Martens-Mantai T, Speckmann E, Gorji A (2014) Propagation of cortical spreading depression into the hippocampus: the role of the entorhinal cortex. *Synapse* 68: 574-584
20. Kunkler PE, Kraig RP (2003) Hippocampal spreading depression bilaterally activates the caudal trigeminal nucleus in rodents. *Hippocampus* 13: 835-844
21. De Curtis M, Pare D (2004) The rhinal cortices: A wall of inhibition between the neocortex and the hippocampus. *Prog Neurobiol* 74: 101-110
22. Pelletier JG, Apergis J, Pare D (2004) Low probability transmission of neocortical and entorhinal impulses through the perirhinal cortex. *J Neurophysiol* 91: 2079-2089
23. Weitlauf C, Honse Y, Auberson YP, Mishina M, Lovinger DM, Winder DG (2005) Activation of NR2A-Containing NMDA Receptors Is Not Obligatory for NMDA Receptor-Dependent Long-Term Potentiation. *J Neurosci* 25: 8386-8390
24. Philpot BD, Cho KK, Bear MF (2007) Obligatory role of NR2A for metaplasticity in visual cortex. *Neuron* 53: 495-502
25. Cui Z, Feng R, Jacobs S, Duan Y, Wang H, Cao X, Tsien JZ (2013) Increased NR2A:NR2B ratio compresses long-term depression range and constrains long-term memory. *Sci Rep* 3: 1036
26. Erreger K, Dravid SM, Banke TG, Wyllie DJA, Traynelis SF (2005) Subunit-specific gating controls rat NR1/NR2A and NR1/NR2B NMDA channel kinetics and synaptic signaling profiles. *J Physiol* 563: 345-358
27. Tang YP, Shimizu E, Dube GR, Rampon C, Kerchner GA, Zhuo M, Liu G, Tsien JZ (1999) Genetic enhancement of learning and memory in mice. *Nature* 401: 63-69
28. Kiyama Y, Manabe T, Sakimura K, Kawakami F, Mori H, Mishina M (1998) Increased thresholds for long-term potentiation and contextual learning in mice lacking the NMDA-type glutamate receptor epsilon1 subunit. *J Neurosci* 18: 6704-6712
29. Sprengel R, Suchanek B, Amico C, Brusa R, Burnashev N, Rozov A, Hvalby O, Jensen V, Paulsen O, Andersen P, et al. (1998) Importance of the intracellular domain of NR2 subunits for NMDA receptor function in vivo. *Cell* 92: 279-289

Parameters	CSD (n = 4)	Hippocampal SD (n = 4)	<i>p</i> -value
Total number of SD (waves/45 min)	9.23 ± 1.74	3.67 ± 0.58	0.004*
Amplitude (mV)	34.62 ± 6.78	24.79 ± 3.51	0.04*
Wave interval (min)	5.10 ± 1.49	10.53 ± 2.27	0.03*
Duration (s)	69.67 ± 19.60	74.14 ± 28.93	0.83
AUC (mV*s)	712.35 ± 187.77	810.46 ± 217.11	0.56

Table 1 Comparison between CSD and Hippocampal SD. During 45 minutes of CSD elicitation using solid KCl, the glass electrodes were placed in both the neocortex (from bregma: anterior-posterior, +3 mm; lateral, 2 mm; and dorsal-ventral, 0.5 mm) and the ipsilateral hippocampus (from bregma: anterior-posterior, -4 mm; lateral, 2 mm). The measured variables included the area under the curve (AUC), the amplitude of each CSD wave as well as the number of CSD waves. These data were analysed using the AcqKnowledge acquisition software. Our results have revealed that total number of spreading depression and amplitude were significantly reduced in the hippocampus compared to those in the cortex. Meanwhile, wave interval has been shown to be significantly elevated in hippocampal SD. However, we observed no significant changes in terms of duration and AUC. $p < 0.05$ was considered to be statistically significant using independent sample two-tailed *t*-test.

Fig. 1 Cortical and hippocampal DC recordings. **A)** A representative tracing showing the DC shift in frontal cortex surface induced by KCl application (Scale bar: 5 min; 10 mV). **B)** A representative tracing showing the DC shift in hippocampus induced by KCl application (Scale bar: 5 min; 10 mV). These tracings illustrated that SDs originated from the neocortex were shown to be able to spread to the hippocampus. The waves also appeared to be morphologically different between CSD and hippocampal SD. Recorded parameters were previously described in **Table 1**.

Fig. 2 CSD induction affected functional GluN2A/B ratio in hippocampal slices. **A)** Isolation of GluN2A component from NMDA receptor-mediated fEPSPs in the control and CSD groups. The reduction of NMDA receptor-mediated fEPSPs was stabilised within 40-60 minutes after ifenprodil application. GluN2A component was isolated by bath application of 3 μ M ifenprodil, a GluN2B receptor antagonist, at time 0 to 60 min. Inset: Representative traces were recorded immediately prior to ifenprodil application and 60 minutes after ifenprodil application. Calibration: 50 millisecond, 0.4 mV. The traces were normalised in term of amplitude. **B)** Data plot of the GluN2A/B ratio. The ratio of GluN2A/B was calculated by dividing the averaged AUC values of ifenprodil-insensitive component with those of ifenprodil-sensitive component at time 50 to 60 minutes. The GluN2A/B ratio was significantly elevated in hippocampal slices obtained from the CSD rats. $n = 6$ each group; $p < 0.05$ independent samples two-tailed *t*-test. Bar and whisker plots indicate the mean \pm SEM.

Fig. 3 Total number of GluN2A and GluN2B subunits of the NMDA receptor measured by Western blot analysis. **A)** The protein band intensities were exposed and normalised in association to the β -actin bands at 43 kDa. For both GluN2A and GluN2B, the signals derived from contralateral and ipsilateral hippocampi are depicted as well as those for CSD and control group. **B)** Proportions of protein signal intensity over the β -actin were calculated and demographically presented in comparison with those of CSD and control groups. In CSD group, total number of GluN2A subunits of the NMDA receptor are significantly elevated while those of GluN2B are diminished. These findings are consistent with the result from our electrophysiological study towards greater GluN2A/B response ratio.

The estrous cycle modulates voltage-gated ion channels in TG neurons

Wachirapong Saleeon¹, Ukkrit Jansri², Anan Srikiatkachorn¹, Saknan Bongsebandhu-phubhakdi¹

(1) Department of Physiology, Faculty of Medicine, Chulalongkorn University, 1873 Rama IV Road, Pathumwan, Bangkok 10330, Thailand

(2) Research Affairs, Faculty of Medicine, Chulalongkorn University, 1873 Rama IV Road, Pathumwan, Bangkok 10330, Thailand

Correspondence to: Saknan Bongsebandhu-phubhakdi, Ph.D., Department of Physiology, Faculty of Medicine, Chulalongkorn University, 1873 Rama IV Road, Pathumwan, Bangkok, 10330, Thailand. Tel: +66-83-986-0713, Fax: +66-2-252-7854, E-mail: saknan@live.jp

Abstract

Migraines typically occur more frequently in women than men because of the effects of estrogen on both the frequency and severity of migraine attacks. Many women suffer from migraine attacks during menstruation, which are known as menstrual migraines. The pathophysiology of menstrual migraines can be explored by using the rat estrous cycle, which shows a cyclical fluctuation of estrogen levels that resembles the menstrual cycle. The aim of this study was to investigate whether each stage of the estrous cycle is involved in migraine development by comparing the susceptibility of trigeminal ganglion (TG) neurons in each stage of the estrous cycle by using action potential (AP) parameter assessments. The stages of the estrous cycle were identified by a vaginal smear and measuring the estrogen levels in collected blood. The proestrus and estrus stages had higher estrogen levels compared with the diestrus and metestrus stages. Whole-cell patch clamp recordings demonstrated that TG neurons in the proestrus and estrus stage had lower AP thresholds, decreased rheobases, enhanced AP heights, shorter falling times of AP and deeper after-hyperpolarization (AHP) depth. Our results revealed that the high level of estrogen in the proestrus and estrus stage alters the AP properties of TG neurons. Estrogen may increase membrane sensitivity and the summation of cellular responses, which alters the AP properties. The alterations of the AP properties in the proestrus and estrus stage are due to a modification of voltage-gated ion channels in TG neurons, which may be a pathogenesis for menstrual migraine. No COI.

Keywords: Menstrual migraine, estrous cycle, trigeminal ganglion (TG) neurons, whole-cell patch clamp recording, voltage-sensitive ion channels

Introduction

Migraine occurs more often in women than in men. More than 50% of women experience menstrual cycle-related migraine, particularly during adulthood [1, 2]. The menstrual cycle enhances various parameters of a migraine, such as the severity, duration and frequency of painful migraine attacks. Previous research suggests that altered estrogen levels during the menstrual cycle can affect menstrual migraine [3]. The incidence of migraine attacks peaks on the days before and after the onset of menstruation [4]. Estrogen levels fluctuate during each stage of the menstrual cycle, which is divided into follicular and luteal phases. In female rats, the menstrual cycle is called the estrous cycle and occurs in four stages, diestrus, proestrus, estrus, and metestrus. Estrogen levels peak during proestrus and estrus. The rat estrous cycle is used to model the effects of estrogen during the menstrual cycle in women.

Cyclical fluctuation of estrogen levels occur during estrous cycle progression. Estrogen levels steadily rise during the diestrus stage and peak during the proestrus stage. Subsequently, estrogen levels rapidly drop and then slowly rise to reach a plateau at the estrus stage. From the plateau during the estrus stage, the estrogen level steeply decreases during the metestrus stage and then increases during the progression towards the diestrus stage. Menstrual cycle activity has been implicated as a cause of migraine because high levels of estrogen during the proestrus and estrus stage can enhance the susceptibility of neurons in the trigeminal nucleus caudalis (TNC), which results in migraine attacks [5]. Furthermore,

estrogen exposure also increases the sensitization of the temporomandibular branch, which is innervated by TG neurons [6]. These results demonstrated that estrogen can affect the trigeminal system.

In the trigeminal nociceptive system, estrogen activates the estrogen receptor (ER) on TG neurons via either genomic or non-genomic pathways. Estrogen modulates neuronal activity through the expression of ion channels or by increasing intracellular cascades, such as extracellular-signal-regulated kinase (ERK) signaling, which phosphorylates ion channels [7, 8]. In addition, previous research has demonstrated that voltage-gated Na channels [9-11] and voltage-gated K channels [12] in dorsal root ganglion (DRG) cells are activated by exogenous estrogen. Activation of voltage-gated ion channels affects AP development in TG neurons, which is a major nociceptive signal from the periphery to higher cortical neurons. Thus, estrogen may induce AP by stimulating TG neurons, which activate nociceptive signals from the trigeminal system.

Our study aims to investigate the AP properties of TG neurons in various stages of the estrous cycle. The AP properties reflect the activation of voltage-gated ion channels that affect the susceptibility of TG neurons. Our results suggest that modulation of the trigeminal system underlies the pathophysiology of menstrual migraine.

Materials and Methods

Animals

Female Sprague–Dawley rats, 6-8 weeks old, have a sufficient estrogen level for observing the estrous cycle [13, 14]. Animals used in all experiments were from the National Laboratory Animal Center, Mahidol University, Nakorn-Pathom, Thailand. Rats were housed in stainless cages in a ventilated room under a 12-hour dark-light cycle and were fed ad libitum. All of the protocols were approved by the Animal Care and Use Committee of the Faculty of Medicine, Chulalongkorn University, Thailand (No. 4/58).

Immunoassay of Estrogen levels

Immediately after decapitation, we collected arterial blood from the left cardiac ventricle for storage in a 1.5-ml microcentrifuge tube. The collection tubes were centrifuged at 3,200 rpm for 10 min. Then, serum was collected and stored at -20° C. The serum concentration of estradiol (E2) was analyzed using the Chemiluminescent Microparticle Immunoassay (CMIA) method.

Estimation of estrous cycle stages

Using a dropper, we flushed the vagina with normal saline. Subsequently, one drop of vaginal fluid was placed on a slide and stained with 1% methylene blue. In this manner, vaginal smears were performed under a light microscope (with a 40X objective lens). Classification of the estrous cycle was determined according to the staining of three cell types in the vaginal smear, nucleated epithelial cells (Fig. 2B), cornified epithelial cells (Fig. 2C) and leukocytes (Fig. 2D)[15].

Primary cultured of TG neurons

Primary dissociated TG neurons were cultured as described previously [16-18]. Briefly, rats were anesthetized with an overdose intra-peritoneal injection of sodium pentobarbital before decapitation. Both trigeminal ganglia were removed and cultured in a 35-mm culture dish of ice-cold Hank's Balance Salt Solution (HBSS) with penicillin/streptomycin, washed 2 times in HBSS, and sectioned into small pieces with a sterile razor blade in 1 ml of HBSS. Collagenase and dispase were filtrated using a 0.22- μ m filter and then added to the sample. Immediately following filtration, the sample was incubated at 37° C for 20 min. Papain was filtered and added, and then, the sample was incubated at 37° C for 20 min again. Afterwards, the sample was centrifuged at 1,500 rpm for 2 min, and the supernatant was removed. The precipitate was triturated 3 times in L-15 complete medium using a glass pipette. Next, the sample was centrifuged at 1,500 rpm for 8 min. The precipitate was collected and washed with F-12 complete medium 2 times. Finally, 400 μ l of F-12 complete medium was added to the sample and placed into a 35-mm Laminin/PDL dish for incubation in an incubator (37° C, 5% CO₂) for 3 hours. The sample was washed with F-12 2 times for further electrophysiological study [19].

Electrophysiological recording

Whole-cell patch clamp recording was used to estimate the electrophysiological properties of dissociated TG neurons that were maintained in primary culture for 3 hours. Plastic chambers containing trigeminal neurons were placed on the microscope sample stand (Olympus BX51WI microscope, Olympus, USA), after which the cells were superfused with extracellular solution flowing into the plastic chamber at a flow rate of 1 ml/min at room temperature. The extracellular solution was composed of 145 mM NaCl, 5 mM KCl, 2 mM CaCl₂, 1 mM MgCl₂, 10 mM D-Glucose, and 10 mM HEPES; the pH value was adjusted to 7.40 with 1 M NaOH, and the osmolarity adjusted to 320 mOsm/kg with glucose. Glass microelectrodes with an outer diameter of 1.5 mm and an inner diameter of 0.86 mm (Sutter Instruments, Navato, CA, USA) were pulled on a microelectrode puller (Sutter Instrument) and heat polished using a microforge (Narashige, Tokyo, Japan) to a resistance of 4-5 mega-ohm.

Next, we filled microelectrodes with an intracellular solution (composed of 140 mM K-gluconate, 1 mM CaCl₂, 2 mM MgCl₂, 10 mM EGTA, 10 mM HEPES, and 10 mM ATP; osmolality adjusted to 280 ± 5 with glucose) and inserted the microelectrodes to the headstage of an Axopatch amplifier (Axon, Sunnyvale, CA, USA). We approached a TG neuron with a microelectrode and attached the electrode to the neuron. Then, we ruptured the cell membrane to establish a whole-cell patch clamp recording in the current-clamp mode and measured the resting membrane potential (RMP in mV) of the TG neuron.

In current-clamp recording, to evaluate AP properties in response to the estrous cycle stage, the membrane potential was manually held at -60 mV and injected with a current of 10 pA/step with 100 ms duration. The criteria for successful recording were a minimum 10 min recording time, with a stable RMP of more negative than -40 mV; an amplitude of the action potential that was greater than 70 mV; and an input resistance that was higher than 100 mega-ohm. The protocol we followed was adapted from previous reports [20, 21]. The cell diameter was evaluated as the average of the longest and shortest axis in a BX51WI upright microscope (Olympus, Tokyo, Japan). Only cells with diameter < 38 μm were analyzed.

Assessment of the AP properties

The current clamp injected with brief (100 ms) current pulses from a holding potential at -60 mV is shown in Fig. 1A. The threshold (mV) was the lowest membrane potential that yielded the first depolarization phase of an AP. Rheobase (pA) was the minimal current injection that was able to cause the depolarization phase of an AP. The AP height (AP_{height}; mV) was measured as the elevation of an AP measured from the holding potential to peak amplitude of the AP. The AP overshoot (mV) was measured as the elevation of an AP measured from 0 mV to peak amplitude of the AP. The rising time (ms) was measured as the duration of the depolarization phase, which was measured from the threshold to peak amplitude of an AP. The falling time (ms) was measured as the duration of the less positive phase, which was measured from a peak amplitude of an AP to the holding potential (Fig. 1B). The depth of after-hyperpolarization (AHP_{depth}; mV) is the de-escalation of an AP measured from the holding potential to the negative peak of an AHP. The AHP duration (AHP_{duration}; ms) is the duration time from the negative peak of an AHP to 50% of the recovery of the holding potential (Fig. 1C).

Data analysis

All data are presented as the mean ± standard errors of the mean (SEM). Statistical analysis was performed using Student's t test. $p < 0.05$ was accepted as statistically significant.

Results

After decapitation, we immediately collected blood serum to analyze the estrogen level. A comparison of the estrogen levels at each stage of the estrous cycle (Fig. 2A) demonstrated that the estrogen level at the proestrus stage (61.00 ± 1.41 pg/ml, $n = 5$) was the highest among the estrous cycle stages (comparing with diestrus, 31.00 ± 2.18 pg/ml, $n = 5$; $p < 0.05$). Furthermore, the estrogen level at the estrus stage was significantly higher than the level at the diestrus stage (46.33 ± 2.89 pg/ml, $n = 5$; $P < 0.05$), whereas the estrogen level at the metestrus stage was almost the same as the level at the diestrus stage (21.00 ± 2.65 pg/ml, $n = 5$; N.S.).

The vaginal smear demonstrated that the cytological properties of the vaginal cells changed according to the estrogen level at each stage of the estrous cycle. At the diestrus stage, there were several more leukocytes than nucleated epithelial cells (Fig. 2E). In the proestrus stage, there were only clusters of round nucleated epithelial cells, which included a granular cytoplasm and a nucleus (Fig. 2F). In the estrus stage, there were only clusters of cornified epithelial cells (Fig. 2G). In the metestrus stage, there were more leukocytes than cornified epithelial cells (Fig. 2H). However, there were no differences in the morphology of TG neurons at each estrous cycle stage (Figs. 2I, 2J, 2K and 2L).

At each stage of the estrous cycle, the dissociated TG neurons in the primary culture were estimated using a whole-cell patch clamp configuration, of which depolarizing current steps were used to stimulate TG neurons to analyze the AP properties (Fig. 3). The TG neurons at each stage of the estrous cycle had similar RMP values (Table 1). The threshold at the proestrus (-27.46 ± 0.52 mV, $n = 24$) and estrus stages (-27.00 ± 2.20 mV, $n = 35$) was significantly lower than thresholds at the diestrus stage (-19.14 ± 1.76 mV, $n = 52$; $p < 0.05$, $p < 0.05$, respectively). The rheobase at the proestrus (55.63 ± 0.27 pA, $n = 24$) and estrus stages (49.58 ± 2.70 pA, $n = 35$) was also lower than the rheobase at the diestrus stage (73.33 ± 3.54 pA, $n = 52$; $p < 0.05$, $p < 0.05$, respectively). The AP height and overshoot at the proestrus stage (AP height; 116.66 ± 1.16 mV and AP overshoot; 67.41 ± 1.02 mV, $n = 24$) were significantly higher compared to the diestrus stage (AP height; 109.21 ± 3.35 mV and AP overshoot; 52.41 ± 2.76 mV, $n = 52$; $p < 0.05$, $p < 0.05$, respectively). The rising time of the AP was not significant at any stage, and the falling time of the AP at the proestrus (3.22 ± 0.56 ms, $n = 24$) and estrus stages (2.43 ± 0.31 ms, $n = 35$) were significantly shorter compared to the diestrus stage (5.21 ± 0.4 ms, $n = 52$; $p < 0.05$, $p < 0.05$, respectively). Moreover, the duration of the AP at the proestrus (4.48 ± 0.20 ms, $n=24$) and estrus stage (3.67 ± 0.31 ms, $n = 35$) was also significantly shorter compared to the diestrus stage (6.46 ± 0.46 ms, $n = 52$; $p < 0.05$, $p < 0.05$, respectively). The depth of the AHP at the proestrus (-12.15 ± 2.36 mV, $n = 24$) and estrus stages (-13.56 ± 1.00 mV, $n=35$) was significantly deeper compared to the diestrus stage (-5.10 ± 0.49 mV, $n = 52$; $P < 0.05$, $P < 0.05$, respectively), whereas the duration of the AHP was not changed at any stage (Table 1).

Discussion

The present study investigated the effects of the estrogen level during the estrous cycle on the alteration of the AP properties linked to the trigeminal nociceptive system. Each stage of the estrous cycle was associated with differences in the morphology of the vaginal epithelium, which was influenced by the level of estrogen. Our findings are consistent with Goldman, et al. [16]; however, the morphology of the TG neurons did not change, while the properties of the AP were changed.

Estrogen, which binds to ER-alpha and ER-beta receptors, acts via both genomic and non-genomic mechanisms to modulate the pain response, neurotransmitter systems, and other modulatory systems [22, 23]. For AP development in the trigeminal system, voltage-gated Na channels have a key role in response to depolarization, eliciting an AP in TG neurons, which leads to pain perception. Voltage-gated Na channels Nav1.1 to 1.9 are expressed in TG neurons, including Nav1.7 (a tetrodotoxin-sensitive Na channel; TTX-S), Nav1.8 (a tetrodotoxin-resistant Na channel; TTX-R), and Nav1.9 (TTX-R), which can be stimulated to induce an AP [24, 25].

Our results demonstrated that the high levels of estrogen at the proestrus and estrus stages reduced the AP threshold and rheobase and increased the AP height. These findings are consistent with a previous study demonstrating that high estrogen levels increase the excitability of trigeminal ganglion neurons by reducing the AP threshold and rheobase and that estrogen also increases the height of the AP [18]. In addition, estrogen has been shown to increase the expression of ERK [14], which phosphorylates voltage-gated Na channels in TG neurons [26]. Moreover, a previous study reported that exogenous estrogen can increase the specific expression of Nav1.8 and Nav 1.9 in DRG cells of ovariectomized rat [11]. Thus, high levels of estrogen during the proestrus and estrus stages may increase the expression of Nav1.8 and Nav1.9, as well as ERK, which enhances the susceptibility of AP development in TG neurons.

Additionally, voltage-gated K channels play a key role during the less positive and repolarization phases. Our findings demonstrated that high estrogen levels at the proestrus and estrus stages reduced the falling time and increased the depth of AHP. Previous research has demonstrated that estrogen alters the duration of an AP via a large conductance through the calcium-activated K channel (BK_{Ca}) and changes the depth of AHP via a small conductance through the calcium-activated K channel (SK_{Ca}) in the hippocampal pyramidal neurons [27]. Moreover, estrogen also activates L-type Ca channels to allow Ca²⁺ influx, which increases intracellular Ca²⁺ and activates voltage-gated K channels [25, 26]. Consequently, a high level of estrogen at the proestrus and estrus stages may potentiate the activation of voltage-gated K channels, which increases K efflux during AP development in TG neurons.

Conclusion

The present study demonstrates that the estrogen level at each stage of the estrus cycle correlates with the morphology of vaginal epithelial cells, but not the morphology of TG neurons. Interestingly, modification of AP development in TG neurons at each stage of the estrous cycle may be induced by the cyclical fluctuation of estrogen levels, which modulate the activation of voltage-gated ion channels. The results of this study reveal that the susceptibility of the trigeminal system increases during menstruation, which may be the fundamental mechanism underlying menstrual migraine.

Acknowledgements

The research was supported by the Neuroscience of Headache Research Unit, Integrated Innovation Academic Center, the 2012 Chulalongkorn University Centenary Academic Development Project, the National Research University Project, the Office of Higher Education Commission (WCU-008-HR-57), the Government Research Budget 2014 and the Ratchadapiseksompoj Fund from the Faculty of Medicine, Chulalongkorn University.

Conflict of interest

None

References

1. Couturier EG, Bomhof MA, Neven AK, van Duijn NP (2003) Menstrual migraine in a representative Dutch population sample: prevalence, disability and treatment. *Cephalalgia* 23: 302-308
2. Stovner LJ, Zwart JA, Hagen K, Terwindt GM, Pascual J (2006) Epidemiology of headache in Europe. *Eur J Neurol* 13: 333-45
3. Dao TT, LeResche L (2000) Gender differences in pain. *J Orofac Pain* 14:169-84
4. Tassorelli C, Greco R, Allena M, Terreno E, Nappi RE (2012) Transdermal hormonal therapy in perimenstrual migraine: why, when and how? *Curr Pain Headache Rep* 16: 467-73
5. Martin VT, Lee J, Behbehani MM (2007) Sensitization of the trigeminal sensory system during different stages of the rat estrous cycle: implications for menstrual migraine. *Headache* 47: 552-63
6. LeResche L, Mancl L, Sherman JJ, Gandara B, Dworkin SF (2003) Changes in temporomandibular pain and other symptoms across the menstrual cycle. *Pain* 106: 253-61
7. Amandusson A, Blomqvist A (2013) Estrogenic influences in pain processing. *Front Neuroendocrinol* 34: 329-49
8. Martin VT, Behbehani M (2006) Ovarian hormones and migraine headache: Understanding mechanisms and pathogenesis - Part I. *Headache* 46: 3-23
9. Bi RY, Ding Y, Gan YH (2015) A new hypothesis of sex-differences in temporomandibular disorders: estrogen enhances hyperalgesia of inflamed TMJ through modulating voltage-gated sodium channel 1.7 in trigeminal ganglion? *Med Hypotheses* 84: 100-3
10. Wang Q, Cao J, Hu F, Lu R, Wang J, Ding H, Gao R, Xiao H (2013) Effects of estradiol on voltage-gated sodium channels in mouse dorsal root ganglion neurons. *Brain Res* 1512: 1-8
11. Hu F, Wang Q, Wang P, Wang W, Qian W, Xiao H, Wang L (2012) 17beta-Estradiol regulates the gene expression of voltage-gated sodium channels: role of estrogen receptor alpha and estrogen receptor beta. *Endocrine* 41: 274-80
12. Du J, Wang Q, Hu F, Wang J, Ding H, Gao R, Xiao H, Wang L (2014) Effects of estradiol on voltage-gated potassium channels in mouse dorsal root ganglion neurons. *J Membr Biol* 247: 541-8
13. Norris ML, Adams CE (1979) Exteroceptive factors, sexual maturation and reproduction in the female rat. *Lab Anim* 13: 283-6
14. Puri V, Puri S, Svojanovsky SR, Mathur S, Macgregor RR, Klein RM, Welch KM, Berman NE (2006) Effects of oestrogen on trigeminal ganglia in culture: implications for hormonal effects on migraine. *Cephalalgia* 26: 33-42

15. Yener T, Turkkani Tunc A, Aslan H, Aytan H, Cantug Caliskan A (2007) Determination of oestrous cycle of the rats by direct examination: how reliable? *Anat Histol Embryol* 36: 75-7
16. Malin SA, Davis BM, Molliver DC (2007) Production of dissociated sensory neuron cultures and considerations for their use in studying neuronal function and plasticity. *Nature Protocols* 2: 152-160
17. Eckert SP, Taddese A, McCleskey EW (1997) Isolation and culture of rat sensory neurons having distinct sensory modalities. *J Neurosci Methods* 77: 183-90
18. Flake NM, Bonebreak DB, Gold MS (2005) Estrogen and inflammation increase the excitability of rat temporomandibular joint afferent neurons. *J Neurophysiol* 93: 1585-97
19. Junsre U, Bongsebandhu-phubhakdi S (2014) ASICs Alteration by pH Change in Trigeminal Ganglion Neurons. *J Physiol Biomed Sci* 27: 20-25
20. Catacuzzeno L, Fioretti B, Pietrobon D, Franciolini F (2008) The differential expression of low-threshold K (+) currents generates distinct firing patterns in different subtypes of adult mouse trigeminal ganglion neurones. *Journal of Physiology-London* 586: 5101-5118
21. Adams JP, Anderson AE, Varga AW, Dineley KT, Cook RG, Pfaffinger PJ, Sweatt JD (2000) The A-type potassium channel Kv4.2 is a substrate for the mitogen-activated protein kinase ERK. *Journal of Neurochemistry* 75: 2277-2287
22. Martin VT (2009) Ovarian hormones and pain response: a review of clinical and basic science studies. *Gend Med* 6 Suppl 2: 168-92
23. Fillingim RB, Maixner W (1995) Gender differences in the responses to noxious stimuli. *Pain Forum* 4: 209-221
24. Dib-Hajj SD, Black JA, Waxman SG (2009) Voltage-gated sodium channels: therapeutic targets for pain. *Pain Med* 10: 1260-9
25. Rush AM, Dib-Hajj SD, Liu S, Cummins TR, Black JA, Waxman SG (2006) A single sodium channel mutation produces hyper- or hypoexcitability in different types of neurons. *Proc Natl Acad Sci U S A* 103: 8245-50
26. Filardo EJ, Quinn JA, Bland KI, Frackelton AR Jr (2000) Estrogen-induced activation of Erk-1 and Erk-2 requires the G protein-coupled receptor homolog, GPR30, and occurs via trans-activation of the epidermal growth factor receptor through release of HB-EGF. *Mol Endocrinol* 14: 1649-60
27. Carrer HF, Araque A, Buno W (2003) Estradiol regulates the slow Ca^{2+} -activated K^+ current in hippocampal pyramidal neurons. *J Neurosci* 23: 6338-44

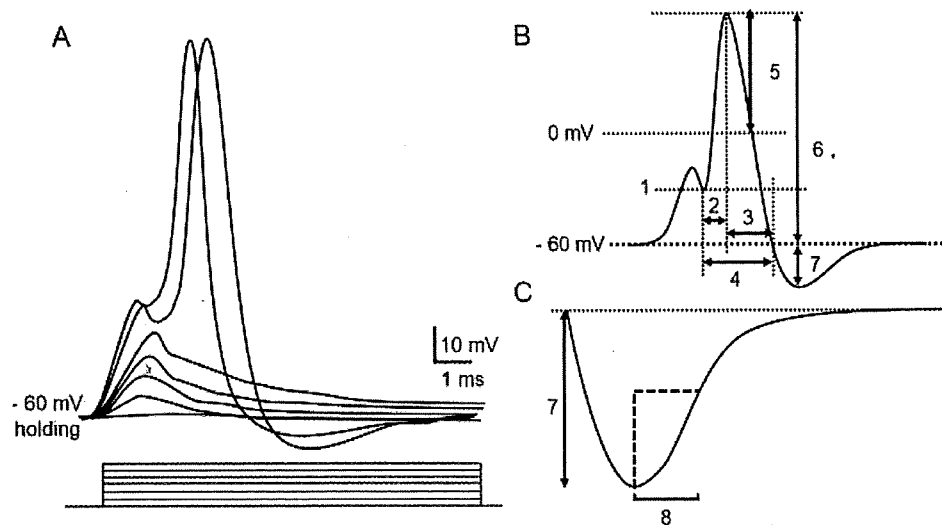


Fig. 1 Assessment of the AP properties. (A) Step current from the 1st to 7th step with increases of 10 pA per step. (B) 1 = Threshold, 2 = Rising time, 3 = Falling time, 4 = Duration, 5 = AP overshoot, 6 = AP height and 7 = the depth of AHP. (C) 7 = the depth of AHP and 8 = AHP duration

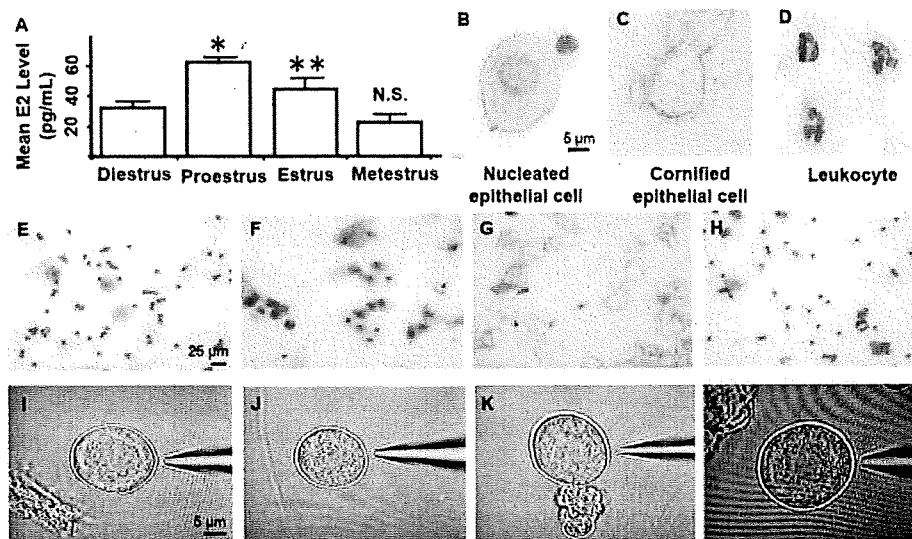


Fig. 2 Evaluation of estrous cycling female rats. Panel (A), the concentration of estrogen at each stage of estrous cycle. * $p < 0.05$, ** $p < 0.005$ compared with diestrus stage. Panel (B-D), representative microphotographs of vaginal cytological samples. (B) Nucleated epithelial cells; (C) cornified epithelial cells; and (D) leukocytes. Panel (E-H), representative samples taken from vaginal smears at each stage of the estrous cycle. (E) Diestrus stage, leukocytes appear more than nucleated epithelial cells; (F) proestrus stage, only nucleated epithelial cells are found; (G) estrus stage, only cornified epithelial cells are found; (H) metestrus stage, leukocytes appear more than cornified epithelial cells. Panel (I-L), representative characterization of primary cultured TG neurons at different stages of the estrous cycle. (I) Diestrus stage; (J) proestrus stage; (K) estrus stage; and (L) metestrus stage. The morphology of TG neurons do not change due to estrogen level or stage of the estrous cycle.

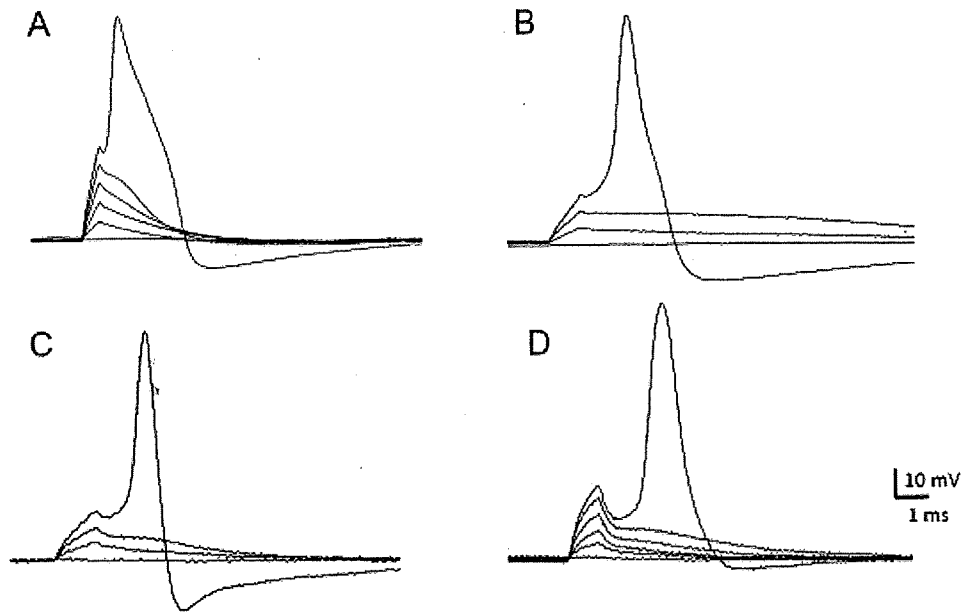


Fig. 3 Representative traces of AP development in TG neurons at each stage of the estrous cycle. (A) Diestrus stage; (B) proestrus stage; (C) estrus stage; and (D) metestrus stage.

Table 1 RMP and AP properties of TG neurons at each stage of the estrous cycle. Each variable is shown as the mean \pm SEM. * $p < 0.05$ compared with the diestrus stage.

Variables	Diestrus (n = 52)	Proestrus (n = 24)	Estrus (n = 35)	Metestrus (n = 27)
RMP (mV)	-46.57 \pm 1.13	-47.88 \pm 2.38	-49.39 \pm 2.46	-41.98 \pm 1.86
Threshold (mV)	-19.14 \pm 1.76	-27.46 \pm 0.52*	-27.00 \pm 2.20*	-29.95 \pm 3.14
Rheobase (pA)	73.33 \pm 3.54	55.63 \pm 0.27*	49.58 \pm 2.70*	66.36 \pm 8.00
AP height (mV)	109.21 \pm 3.35	116.66 \pm 1.16*	98.24 \pm 4.97	92.53 \pm 6.40
AP overshoot (mV)	52.41 \pm 2.76	67.41 \pm 1.02*	51.63 \pm 3.84	39.10 \pm 6.56
AP Rising time (ms)	1.52 \pm 0.63	1.26 \pm 0.39	1.24 \pm 0.62	1.95 \pm 0.93
AP Falling time (ms)	5.21 \pm 0.4	3.22 \pm 0.56*	2.43 \pm 0.31*	4.41 \pm 0.66
Duration (ms)	6.46 \pm 0.46	4.48 \pm 0.20*	3.67 \pm 0.31*	5.99 \pm 0.82
AHP depth (mV)	-5.10 \pm 0.49	-12.15 \pm 2.36*	-13.56 \pm 1.00*	-6.85 \pm 1.78
AHP duration (ms)	7.46 \pm 1.10	7.92 \pm 1.12	5.20 \pm 0.82	7.62 \pm 2.23

Estrous cycle induces peripheral sensitization in TG neurons: An animal model of menstrual migraine

Wachirapong Saleeon¹, Ukkrit Jansri², Anan Srikiatkhachorn¹, Saknan Bongsebandhu-phubhakdi¹

(1) Department of Physiology, Faculty of Medicine, Chulalongkorn University, 1873 Rama IV Road, Pathumwan, Bangkok 10330, Thailand

(2) Research Affairs, Faculty of Medicine, Chulalongkorn University, 1873 Rama IV Road, Pathumwan, Bangkok 10330, Thailand

Correspondence to: Saknan Bongsebandhu-phubhakdi, Ph.D., Department of Physiology, Faculty of Medicine, Chulalongkorn University, 1873 Rama IV Road, Pathumwan, Bangkok, 10330, Thailand. Tel: +66-83-986-0713, Fax: +66-2-252-7854, E-mail: saknan@live.jp

Abstract

Background: Many women have experienced menstrual migraines that develop into recurrent migraine attacks during menstruation. In the human menstrual cycle, the estrogen level fluctuates according to changes in the follicular and luteal phases. The rat estrous cycle is used as an animal model to study the effects of estrogen fluctuation.

Objective: To investigate whether each stage of the estrous cycle is involved in migraine development by comparing the neuronal excitability of trigeminal ganglion (TG) neurons in each stage of the estrous cycle.

Material and Method: Female rats were divided into four experimental groups based on examinations of the cytologies of vaginal smears and serum analyses of estrogen levels following each stage of the estrous cycle. The rats in each stage of the estrous cycle were anesthetized and their trigeminal ganglia were removed. The collections of trigeminal ganglia were cultured for 2-3 h and then in whole-cell patch clamp recording experiments to estimate the electrophysiological properties of the TG neurons.

Results: There were many vaginal epithelial cells and high estrogen levels in the proestrus and estrus stages of the estrous cycle. Electrophysiological studies revealed that the TG neurons in the proestrus and estrus stages exhibited significantly lower thresholds of stimulation and significant increases in total spikes compared to the TG neurons that were collected in the diestrus stage.

Conclusion: Our results revealed that high estrogen levels in the proestrus and estrus stages altered the thresholds, rheobases and total spikes of the TG neurons. High estrogen levels in the estrous cycle induce increases in neuronal excitability and the peripheral sensitization of TG neurons. These findings may provide an explanation for the correlation of estrogen fluctuations during the menstrual cycle with the pathogenesis of menstrual migraines.

Keywords: menstrual migraine, peripheral sensitization, estrous cycle, trigeminal ganglion (TG) neurons, whole-cell patch clamp recording

Introduction

Migraine is a neurological disorder that is accompanied by migraine attacks that include recurrent painful headache. Migraine attacks occur at a higher prevalence in females than in males^(1,2), and migraine attacks related to the menstrual cycle are called menstrual migraines. The gonadal hormones progesterone and estrogen fluctuate in each stage of the menstrual cycle. These fluctuations in gonadal hormones have been suggested to cause menstrual migraines. Consistent with the hormonal changes in the menstrual cycle⁽³⁾, the estrous cycle comprises the recurring physiological changes that are induced by gonadal hormones in mammalian therian females. The estrous cycle of rats is used as an animal model that exhibits enhancing effects of estrogen on peripheral pain modulation.

The estrous cycle is divided into four stages: diestrus, proestrus, estrus and metestrus. Estrogen fluctuations are synchronized with the development of the stages of the estrous cycle. The systemic estrogen level is constant at a baseline level during the diestrus stage and increases dramatically to its peak level in the proestrus stage. Next, the estrogen level slightly decreases but remains at a considerably high level in the estrus stage. Finally, the estrogen level returns to the baseline level during the metestrus stage and remains steady until the proestrus stage of the next estrous cycle. Previous studies have demonstrated that high levels of estrogen can augment pain perception in the trigeminal nociceptive pathway, which is related to the induction of migraine attacks⁽⁴⁾. Estrogen may intensify the activation of trigeminal ganglion neurons via estrogen receptors, and this process results in peripheral sensitization^(5,6). Additionally, electrophysiological studies have shown that the chronic administration of estrogen increases the total numbers of action potentials in TG neurons.

This study aimed to investigate the electrophysiological properties of TG neurons in various stages of the estrous cycle. Estrogen fluctuations may affect the excitability of TG neurons that have been implicated in peripheral sensitization in the trigeminal system. The results of this study may reveal the involvement of peripheral sensitization in the pathophysiology of menstrual migraine.

Materials and Methods

Female Sprague–Dawley rats at the age of 6–8 weeks old were obtained from the National Laboratory Animal Center, Mahidol University, Nakorn-Pathom, Thailand. The animals were adults and exhibited high estrogen levels. The rats used in all experiments were housed in stainless cages in a ventilated on a 12-h dark-light cycle, and they were fed ad libitum. All of the procedures of the experiments were approved by the Animal Care and Use Committee of the Faculty of Medicine, Chulalongkorn University, Thailand. The rats were divided into four experimental groups according to the following four stages of the estrous cycle: diestrus, proestrus, estrus and metestrus. The estrous cycle stage of for each female rat was identified based on histological examinations of cells in vaginal smears that have been widely used for the detection of estrous cycle stages. The vaginal smears were typically taken with a plastic dropper and 0.9% saline. The plastic dropper was filled with 0.9% saline and inserted into the vagina. The saline was allowed to fill the vagina and then

mixed two to three times until the saline became turbid. The turbid fluid was placed on a glass slide. The samples were fixed with fire or air dried and stained with 1% methylene blue for 5 min. The slides were rinsed in water. The resulting samples were examined under a light microscope. The characterization of each stage of the estrous cycle was performed by discriminating three types of cells in the vaginal smear (i.e., epithelial cells, cornified cells and leukocytes). The stage of the estrous cycle was confirmed by measuring hormone concentrations in the serum. Blood (400 – 500 μ l) was collected in clot blood tubes from the hearts of the rats prior to anesthesia. The blood samples were centrifuged at 3200 rpm for 10 min, and the serum was then stored at -20 °C. The serum was analyzed for the level of estradiol (E2) using the chemiluminescent microparticle immunoassay (CMIA) method.

The primary cell culture process was modified from a dissociated primary sensory neuron protocol. The rats were examined in each estrous stage with vaginal smears. The rats were anesthetized with intra-peritoneal injection overdoses of sodium pentobarbital prior to decapitation. Both of the trigeminal ganglia were removed and cultured in a 35-mm culture dish with ice-cold Hank's balanced salt solution (HBSS) with penicillin/streptomycin. Next, the trigeminal ganglia were washed 2 times in HBSS and cut into small pieces with a blade in 1 ml of HBSS. Collagenase and dispase were filtrated through a 0.22- μ m filter and added to the sample, and the sample was then immediately incubated at 37°C for 20 min. Papain was filtrated through a 0.22- μ m filter and added to the sample, and the sample was then immediately incubated at 37°C for 20 min. Next, the sample was centrifuged at RCF 400 g for 2 min, and the supernatant was removed. The first precipitate was ground in L-15 complete medium using a glass pipette 3 times and was then centrifuged at RCF 400 g for 8 min. The second precipitate was collected and washed with F-12 complete medium twice. Finally, 400 μ l F-12 completed medium was added into the sample, and the sample was placed in a 35-mm laminin/PDL dish. The sample was incubated in an incubator (37°C, 5% CO₂) for 3 hr. For further electrophysiological studies, the sample was washed in F12 twice.

The patch-clamp recordings were performed at room temperature (26 \pm 0.5°C) using TG neurons that had been maintained in primary culture for 3 h after isolation. The patch-clamp recordings were performed on an Axopatch 200B amplifier (Axon Instruments, Foster City, CA, USA) and recorded in a computer for data analysis with pClampfit 10.2 software (Axon instruments, Foster City, CA, USA). The output signal was filtered at 2 kHz, and the sampling rate was 5 kHz. The glass pipettes were 1.5 mm in outer diameter and 0.86 mm in inner diameter (Sutter Instruments, Navato, CA, USA). The glass pipettes were pulled with a Flaming/Brown micropipette puller (P-97; Sutter Instruments, Navato, CA, USA) with a resistance of 3-5 M Ω ^(7,8) and filled with internal solution. The internal solution was prepared with nuclease-free water that contained the following (in mM): 144 potassium gluconate, 3 MgCl₂, 10 HEPES, 0.2 EGTA, 2 K₂-ATP and 0.3 Na₃-GTP (pH 7.2 and 285-295 mOsm). The plastic chamber that included the primary-cultured TG neurons was placed on the sample stand of upright microscope (Olympus BX51WI microscope, Olympus, USA). Next, the extracellular superfusion solution was added to the plastic chamber (composition in mM: 1 M CaCl, 1M MgCl, D-gluta and 10% HEPES; adjusted to a pH of 7.40 with 1 M NaOH and an

osmolality of 320 mOsm/kg with glucose) at an initial flow rate of 1 ml/min at room temperature. In current-clamp recording mode, the membrane potentials of the TG neurons were manually held at -60 mV and injected with -30 to 70 (10 pA/step) in 11 steps of 500 msec duration. Only the TG neurons with diameters <38 μm were analyzed⁽⁹⁾. The measurement of electrophysiological properties is shown in Fig. 1. Threshold was considered as the depolarizing potential that triggered the first action potential (dash line 1, Fig. 1). Rheobase was the lowest injecting current that produced the first action potential (line 3, Fig. 1).

Data analysis

All data are presented as the means \pm the standard errors of means (SEM). The statistical analyses were performed using Student's t tests. $P < 0.05$ was accepted as statistically significant.

Results

Morphological studies revealed that the TG neurons in various stages of the estrous cycle exhibited similar structures (Figs. 2A, 2B, 2C and 2D). TG neurons had a diameter approximately 24 μm , and contained clear nucleus and nucleolus. In contrast, the cytological studies of vaginal smears demonstrated differences in the distributions of vaginal cells. There were many leukocytes and few epithelial nucleated cells in the diestrus stage (Fig. 2E), and only clusters of nucleated epithelial cells were observed in the proestrus stage (Fig. 2F). The nucleated epithelial cells differentiated to the clusters of cornified epithelial cells in the estrus stage (Fig. 2G). The changes in the cell distributions completed with many leukocytes and few cornified epithelial cells in the metestrus stage (Fig. 2H). The representative structure of nucleated epithelial cells, cornified epithelial cells and leukocyte are shown in Fig. 2I, 2J and 2K, respectively.

We estimated the estrogen levels of the sera from each stage of the estrous cycle (Fig. 2L; $n=8$ in each stage). We found that the estrogen levels were stable at the baseline level in the diestrus stage (32.00 ± 1.00 pg/ml) and then immediately increased to the highest level in the proestrus stage (63.43 ± 2.99 pg/ml; $P < 0.005$ compared with the diestrus stage). In the estrus stage, the estrogen level had decreased slightly from the highest level but remained significantly higher than in the diestrus stage (45.71 ± 2.98 pg/ml; $P < 0.005$ compared with the diestrus stage). In the metestrus stage, the estrogen level significantly decreased to below the baseline level (24.29 ± 3.90 pg/ml; $P < 0.05$ compared with the diestrus stage).

Next, we applied 500-msec step pulses and examined the electrophysiological properties of the TG neurons with whole-cell patch clamp techniques ($n=15$ in each stage). The TG neurons in each stage of the estrous cycle exhibited similar RMP values that were not significantly different from those of the diestrus stage (Table 1). Interestingly, the TG neurons in each stage of the estrous cycle exhibited different neuronal excitabilities (Fig. 3). The threshold of the TG neurons in the diestrus stage was -29.31 ± 0.69 mV, whereas the threshold of the TG neurons in the high-estrogen conditions were significantly lower than those in the diestrus stage (proestrus stage: -43.85 ± 0.04 mV; $P < 0.005$ compared with the

diestrus stage and estrus stage -39.99 ± 0.71 mV; $P < 0.005$ compared with the diestrus stage). However, the threshold of the TG neurons in the metestrus stage was not significantly different from that in the diestrus stage (-27.57 ± 2.18 mV; $P = 0.50$). The rheobase values in each stage of the estrous cycle paralleled the thresholds of the TG neurons. The rheobase of the TG neurons in the diestrus stage was 45.33 ± 2.45 pA. Although the rheobases in the proestrus and estrus stages were significantly lower than that in the diestrus stage (16.00 ± 0.11 pA, 19.33 ± 1.62 pA; $P < 0.005$, $P < 0.005$, respectively), the rheobase in the metestrus stage was not significantly different from that in the diestrus stage (45.33 ± 4.89 ; $P = 1.00$). Additionally, the summations of peripheral sensitization as indicated by the total spikes of the TG neurons varied according to the stage of the estrous cycle. The total spikes over the 11 stimulation steps were 6.13 ± 0.78 . Peripheral sensitizations were observed as enhancements in the total numbers of spikes in the proestrus and estrus stages compared with the diestrus stage (111.00 ± 7.43 , 81.80 ± 8.14 ; $P < 0.005$, $P < 0.005$, respectively); however, there was no change in the total number of spikes in the metestrus stage compared with the diestrus stage (6.53 ± 0.91 ; $P = 0.51$).

Discussion

In the present study, we showed that the stages of the estrous cycle could be determined via cytological examinations of the vaginal epithelium cells that are influenced by the level of estrogen. The high systemic estrogen level conditions of the proestrus and estrus stages increases the numbers of nucleated epithelium cells and cornified epithelium cells, whereas there were many leukocytes in the diestrus and metestrus stages during which estrogen is stable at the baseline level. The change of vaginal cytology in our study is consistent with previous studies^(10, 11). The estrogen level had no effect on the morphologies of the TG neurons, but the electrophysiological properties of the TG neurons were altered according to the fluctuations in the estrogen levels across the estrous cycle. The TG neurons exhibited increased excitability in the proestrus and estrus stages during which the estrogen levels were high. These alterations in TG neuron excitability may be related to peripheral sensitization in the trigeminal nociceptive system.

Following exposure to estrogen, cells are activated by the process of protein expression. Estrogen binds to the ER-alpha and ER-beta receptors, which function via both genomic and non-genomic mechanisms⁽¹²⁾. Systemic high estrogen levels activate the ER receptors in vaginal cells, which results in the proliferation of nucleated epithelium cells and cornified epithelium cells. Estrogen receptors are also expressed in TG neurons⁽¹³⁾. Our results revealed that the high estrogen levels of the proestrus and estrus stages reduced the thresholds and rheobases of stimulation required to evoke action potentials in TG neurons. The thresholds and rheobases reflect the neuronal excitability of TG neurons, which are modulated by various neurotransmitters and neuropeptides. It has been demonstrated that the administration of estrogen decreases trigeminal pain thresholds in female rats and also increases the excitability of TG neurons⁽¹⁴⁾. Estrogen increases peripheral sensitization in the trigeminal system by enhancing bradykinin signaling in TG neurons^(15, 16). In addition, estrogen also augments endothelial NOS (eNOS) levels, and these levels directly modify peripheral sensitization⁽¹⁷⁾.

Because estrogen increases calcitonin gene-related peptide (CGRP) and serotonin (5-HT) that are known to have important roles in pain perception in the trigeminal system, estrogen is thought to be a modulatory factor in menstrual migraines^(4, 18). Other studies have reported enhanced effects of estrogen in CGRP synthesis due to nerve growth factor (NGF)-mediated mechanisms and activation of the transient receptor potential cation channel V1 (TRPV1) in dorsal root ganglia⁽¹⁹⁾. The chronic administration of estrogen increases CGRP levels in dorsal root ganglia⁽²⁰⁾. Estrogen also modulates nociceptive responses through its effects on other neuropeptides, such as galanin and neuropeptide Y⁽²¹⁾. Thus, it is highly possible that fluctuation of estrogen level during estrus cycle induces the alteration of neurotransmitters, which results in the peripheral sensitization in our study.

Additionally, our results also revealed that the total numbers of spikes during the proestrus and estrus stages increased. These findings indicate that estrogen may modulate the activation of several voltage-gated ion channels. Estrogen has been found to increase the activity of Ca²⁺-dependent K⁺ channels and induce augmented depolarization in dorsal root ganglion cells^(22, 23). Estrogen increases the activation of mitogen-activated protein (MAP) kinase and extracellular signal-regulated kinase (ERK), which result in the phosphorylation of voltage-gated sodium channels and voltage-gated potassium channels⁽⁶⁾. These effects are involved in the regulation of neuronal excitability⁽²⁴⁾. Thus, the fluctuations of estrogen levels during the estrous cycle are correlated with neuronal excitability and peripheral sensitization in the trigeminal system. Our findings suggest the possible adverse effect of estrous cycle in causing peripheral sensitization of TG neurons that may be the fundamental mechanism underlying menstrual migraine in human.

Conclusion

Our results revealed that the fluctuations in estrogen levels during the various stages of the estrous cycle are related to the cytology of vaginal epithelial cells; however, the estrous cycle did not affect the morphologies of TG neurons. Interestingly, the high estrogen levels of the proestrus and estrus stages induced peripheral sensitization by lowering the thresholds and rheobases of stimulation and by increasing the total spikes numbers in the TG neurons. We conclude that the estrous cycle induces peripheral sensitization, which is an animal model of menstrual migraine.

Acknowledgments

This research was supported by the Research Unit and Center of Excellence for Neuroscience of Headache, “Integrated Innovation Academic Centre: IIAC”, 2012; the Chulalongkorn University Centenary Academic Development Project, the National Research University Project, the Office of Higher Education Commission (WCU-008-HR-57), Anandamahidol Foundation, the Government Research Budget 2014-2019 and the Ratchadapiseksompoj Fund from the Faculty of Medicine, Chulalongkorn University.

References

1. Stewart WF, Wood C, Reed ML, Roy J, Lipton RB, Ampp Advisory Group. Cumulative lifetime migraine incidence in women and men. *Cephalalgia* 2008; 28:1170-1178.
2. Lipton RB, Bigal ME, Diamond M, Freitag F, Reed M L, Stewart WF, Ampp Advisory Group. Migraine prevalence, disease burden, and the need for preventive therapy. *Neurology* 2007; 68:343-349.
3. Emanuele MA, Wezeman F, Emanuele NV. Alcohol's effects on female reproductive function. *Alcohol Res Health* 2002; 26:274-281.
4. Bolay H, Berman NE, Akcali D. Sex-related differences in animal models of migraine headache. *Headache*, 2011. 51(6): p. 891-904.
5. Flake NM, Bonebreak DB, Gold MS. Estrogen and inflammation increase the excitability of rat temporomandibular joint afferent neurons. *J Neurophysiol* 2005; 93:1585-1597.
6. Puri V, Puri S, Svojanovsky SR, Mathur S, Macgregor RR, Klein RM, Welch KM, Berman NE. Effects of oestrogen on trigeminal ganglia in culture: implications for hormonal effects on migraine. *Cephalalgia* 2006; 26: 33-42.
7. Hullugundi SK, Ansuini A, Ferrari MD, van den Maagdenberg AM, Nistri A. A hyperexcitability phenotype in mouse trigeminal sensory neurons expressing the R192Q Cacna1a missense mutation of familial hemiplegic migraine type-1. *Neuroscience* 2014; 266: 244-254.
8. Hullugundi SK, Ferrari MD, van den Maagdenberg AM, Nistri A. The mechanism of functional up-regulation of P2X3 receptors of trigeminal sensory neurons in a genetic mouse model of familial hemiplegic migraine type 1 (FHM-1). *PLoS One* 2013; 8: e60677.
9. Junsre U, Bongsebandhu-phubhakdi S. ASICs Alteration by pH Change in Trigeminal Ganglion Neurons. *J Physiol Biomed Sci* 2014; 27: 20-25.
10. McLean, AC, Valenzuela N, Fai S, Bennett SA. Performing vaginal lavage, crystal violet staining, and vaginal cytological evaluation for mouse estrous cycle staging identification. *J Vis Exp* 2012; 15: e4389.
11. Shannon L. Byers, Michael V. Wiles et al., Mouse Estrous Cycle Identification Tool and Images. *PLoS One* 2012; 7: e35538.
12. Martin VT. Ovarian hormones and pain response: a review of clinical and basic science studies. *Gend Med* 2009; 6 Suppl 2: 168-192.
13. Papka RE, Storey-Workley M, Shughrue PJ, Merchenthaler I, Collins JJ, Usip S, Saunders PT, Shupnik M. Estrogen receptor-alpha and beta- immunoreactivity and mRNA in neurons of sensory and autonomic ganglia and spinal cord. *Cell Tissue Res* 2001; 304: 193-214.
14. Martin VT, Lee J, Behbehani MM. Sensitization of the trigeminal sensory system during different stages of the rat estrous cycle: implications for menstrual migraine. *Headache* 2007; 4: 552-563.

15. Rowan MP, Berg KA, Roberts JL, Hargreaves KM, Clarke WP. Activation of estrogen receptor alpha enhances bradykinin signaling in peripheral sensory neurons of female rats. *J Pharmacol Exp Ther* 2014; 349: 526-532.
16. Rowan MP, Berg KA, Milam SB, Jeske NA, Roberts JL, Hargreaves KM, Clarke WP. 17beta-estradiol rapidly enhances bradykinin signaling in primary sensory neurons in vitro and in vivo. *J Pharmacol Exp Ther* 2010; 335: 190-196.
17. Brandes JL. The influence of estrogen on migraine: a systematic review. *JAMA* 2006; 295:1824-1830.
18. Averbeck B, Izydorczyk I, Kress M. Inflammatory mediators release calcitonin gene-related peptide from dorsal root ganglion neurons of the rat. *Neuroscience* 2000; 98: 135-140.
19. Gangula PR, Lanlua P, Wimalawansa S, Supowit S, DiPette D, Yallampalli C. Regulation of calcitonin gene-related peptide expression in dorsal root ganglia of rats by female sex steroid hormones. *Biol Reprod* 2000; 62: 1033-1039.
20. Gangula PR, Chauhan M, Reed L, Yallampalli C. Age-related changes in dorsal root ganglia, circulating and vascular calcitonin gene-related peptide (CGRP) concentrations in female rats: effect of female sex steroid hormones. *Neurosci Lett* 2009; 454: 118-123.
21. Puri V, Cui L, Liverman CS, Roby KF, Klein RM, Welch KM, Berman NE. Ovarian steroids regulate neuropeptides in the trigeminal ganglion. *Neuropeptides* 2005; 39: 409-417.
22. Scholz A, Gruss M, Vogel W. Properties and functions of calcium-activated K⁺ channels in small neurones of rat dorsal root ganglion studied in a thin slice preparation. *J Physiol* 1998; 513: 55-69.
23. Valverde MA, Rojas P, Amigo J, Cosmelli D, Orio P, Bahamonde MI, Mann GE, Vergara C, Latorre R. Acute activation of Maxi-K channels (hSlo) by estradiol binding to the beta subunit. *Science* 1999; 285: 1929-1931.
24. Ji RR, Baba H, Brenner GJ, Woolf CJ. Nociceptive-specific activation of ERK in spinal neurons contributes to pain hypersensitivity. *Nat Neurosci* 1999; 2: 1114-1119.

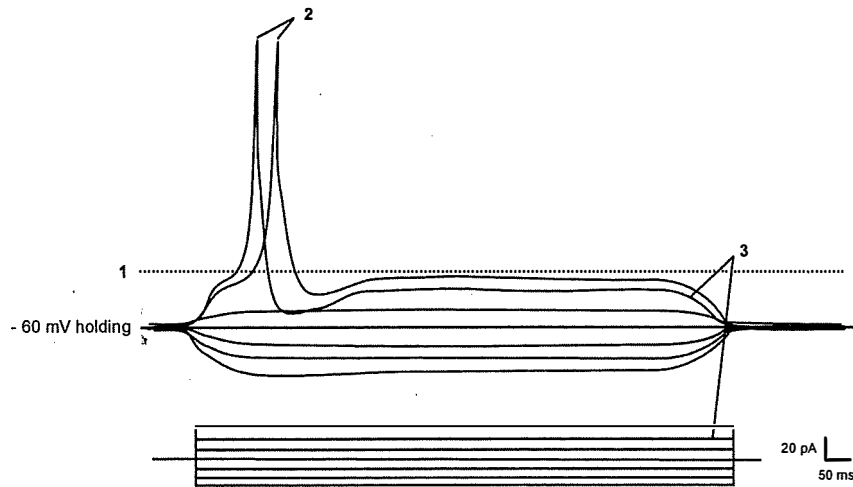


Figure 1. Electrophysiological parameters. A: The 1st to 7th current steps; the currents were incremented 10 pA per step. 1 = threshold, 2 = spikes (2 total spikes), 3 = rheobase.

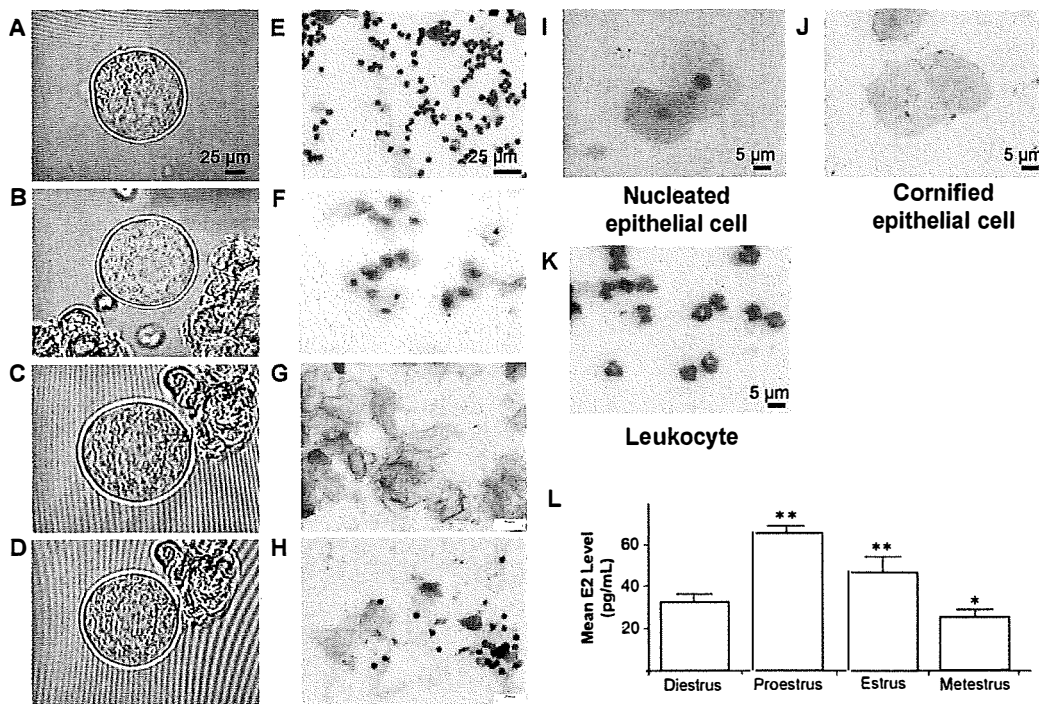


Figure 2. Evaluation of the estrous cycles of female rats. (A-D) Representative morphologies of primary cultured TG neurons at each stage of the estrous cycle. (A) Diestrus stage, (B) proestrus stage, (C) estrus stage, and (D) metestrus stage. (E-H) Representative cytologies of the vaginal cells in each stage of the estrous cycle. (E) Diestrus stage, (F) proestrus stage, (G) estrus stage, and (H) metestrus stage. (I-K) Representative vaginal cell types. (I) Nucleated epithelial cells, (J) cornified epithelial cells, and (K) leukocytes. (L) The concentrations of estrogen at each stage of the estrous cycle (N = 8 per stage). * $P < 0.05$, ** $P < 0.005$ compared with the diestrus stage.

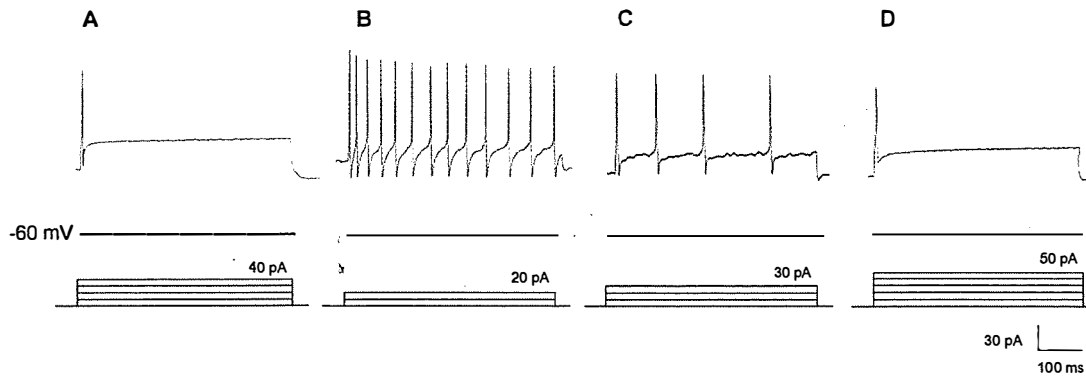


Figure 3. Neuronal excitabilities of the TG neurons at each stage of the estrous cycle. A: In the diestrus stage, the rheobase of 40 pA induced the first response. B: In the proestrus stage, the rheobase of 20 pA induced the first response. C: In the estrus stage, the rheobase of 30 pA induced the first response. D: In the metestrus stage, the rheobase of 50 pA induced the first response.

Table 1 Electrophysiological properties of the TG neurons in each stage of the estrous cycle. The values are presented as the means \pm the SEMs. * $P < 0.05$ compared with the diestrus stage.

	Diestrus (N = 15)	Proestrus (N = 15)	Estrus (N = 15)	Metestrus (N = 15)
RMP (mV)	-48.93 ± 0.68	-47.90 ± 1.83	-48.35 ± 1.03	-44.32 ± 1.53
Threshold (mV)	-29.31 ± 0.69	$-43.85 \pm 0.04^*$	$-39.99 \pm 0.71^*$	$-27.57 \pm 2.18^*$
Rheobase (pA)	45.33 ± 2.45	$16.00 \pm 0.11^*$	$19.33 \pm 1.62^*$	45.33 ± 4.89
Total spikes	6.13 ± 0.78	$111.00 \pm 7.43^*$	$81.80 \pm 8.14^*$	6.53 ± 0.91

บทคัดย่อภาษาไทย

วงจรความเป็นสัดเหนียวทำให้เกิด *peripheral sensitization* ในเซลล์ปมประสาทไทรเจมินัล:

แบบจำลองในสัตว์สำหรับโรคไมเกรนในช่วงที่มีรอบเดือน

วชิรพงศ์ สลืออ่อน, อุกกฤษฎ์ จันทร์ศรี, อนันต์ ศรีเกียรติขจร, ศักนัน พงศ์พันธุ์ผู้ภักดี

ที่มา: ผู้หญิงส่วนมากมักจะเคยมีประสบการณ์เกี่ยวกับโรคไมเกรนในช่วงที่มีรอบเดือน ซึ่งจะมีอาการปวดหัวซ้ำไปมา เกิดขึ้นในช่วงดังกล่าว ในวงจรรอบเดือนของมนุษย์เพศหญิง จะมีการเปลี่ยนแปลงของระดับฮอร์โมนเอสโตรเจนสอดคล้องกับการเปลี่ยนแปลงระหว่างระยะ follicular phase และ luteal phase มักจะมีการนำวงจรความเป็นสัดของหนูแรทมาศึกษาเป็นแบบจำลองในสัตว์ เพื่อทดสอบผลของการเปลี่ยนแปลงระดับฮอร์โมนเอสโตรเจน

วัตถุประสงค์: เพื่อทดสอบระยะต่างๆ ในวงจรความเป็นสัดจะเกี่ยวข้องกับการเกิดไมเกรนได้จริงหรือไม่ โดยเปรียบเทียบระดับการกระตุ้นของเซลล์ปมประสาทไทรเจมินัล ในหลากหลายระยะของวงจรความเป็นสัด

วิธีดำเนินการวิจัย: นำหนูแรทเพศเมียมาแบ่งเป็น 4 กลุ่ม ตามระยะของวงจรความเป็นสัด ตัดสินการแบ่งกลุ่มโดยการทำสเมียร์ช่องคลอด และวิเคราะห์ระดับเอสโตรเจนในซีรัม หนูแรทในแต่ละกลุ่มจะได้รับการฉีดยาสลบ และผ่าตัดนำปมประสาทไทรเจมินัลออกมา จากนั้นจะนำเซลล์ในปมประสาทมาผ่านกระบวนการเพาะเลี้ยง 2-3 ชั่วโมง และนำไปทดลองด้วยวิธี whole-cell patch clamp เพื่อวัดผลคุณสมบัติทางไฟฟ้าสรีรวิทยาของเซลล์ปมประสาทไทรเจมินัล

ผลการทดลอง: ในระยะ proestrus และ estrus พบเซลล์เยื่อเป็นจำนวนมากในช่องคลอด ควบคู่กับการเพิ่มระดับของเอสโตรเจน ในการศึกษาทางไฟฟ้าสรีรวิทยาพบว่า เซลล์ปมประสาทไทรเจมินัลในระยะ proestrus และ estrus แสดงค่า threshold สำหรับการกระตุ้นที่ต่ำลง และมีจำนวนการเกิดศักยไฟฟ้าทำงานเพิ่มขึ้น เมื่อเทียบกับเซลล์ในระยะ diestrus

บทสรุป: ผลการทดลองของงานวิจัยนี้ บ่งชี้ว่าเอสโตรเจนที่มีระดับสูงขึ้นในระยะ proestrus และ estrus มีผลเปลี่ยนแปลงค่า threshold และ rheobases สำหรับการกระตุ้น รวมถึงการเกิดศักยไฟฟ้าทำงานในเซลล์ปมประสาทไทรเจมินัล ซึ่งนำไปสู่การเพิ่มระดับการกระตุ้น และ peripheral sensitization ในเซลล์ปมประสาทไทรเจมินัล การค้นพบนี้น่าจะนำไปสู่ความเชื่อมโยงของการเปลี่ยนแปลงระดับเอสโตรเจนระหว่างช่วงรอบเดือน กับพยาธิกำเนิดของโรคไมเกรนในช่วงที่มีรอบเดือน

สรุป รายงานการรับ-จ่ายเงิน

โครงการวิจัย การใช้ศักย์ไฟฟ้ากระตุ้นการยึดเส้นแอกซอน
และการเกาะติดของเซลล์ประสาทบนแผ่นทองขนาดเล็ก

เอกสารแนบท้ายสัญญา ๘

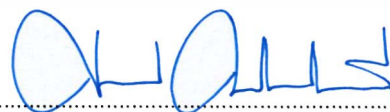
สัญญาเลขที่ GRB_APS_๐๙_๕๘_๓๐_๐๖
โครงการวิจัย เรื่อง โครงการวิจัยการใช้ศักยภาพฟ้ากระตุ้นการยึดเส้นแอกซอน
และการเกาะติดของเซลล์ประสาทบนแผ่นทองขนาดเล็ก

รายงานการรับ-จ่ายเงิน *

	<u>ประมาณการ</u>	<u>งบที่เกิดขึ้นจริง</u>
รายได้		
เงินอุดหนุนงบประมาณแผ่นดิน	650,000.00	650,000.00
รวมรายได้	<u>650,000.00</u>	<u>650,000.00</u>
รายจ่าย		
หมวดค่าจ้างชั่วคราว		
- ค่าจ้างเหมาบริการปฏิบัติการทางวัสดุวิทยาศาสตร์	50,000.00	50,000.00
- ค่าจ้างงานธุรการ	36,000.00	36,000.00
	<u>86,000.00</u>	<u>86,000.00</u>
หมวดค่าตอบแทน		
ค่าตอบแทนคณะผู้วิจัย (3,600 บาทx12 เดือนx 3 คน)		
- รศ.ดร ศักนัน พงศ์พันธุ์ผู้ภักดี (3,600x12)	43,200.00	43,200.00
- อ.ดร. บุญรัตน์ โล่ห์วงศ์วัฒน์ (3,600x12)	43,200.00	43,200.00
- ศ.นพ.อนันต์ ศรีเกียรติขจร (3,600x12)	43,200.00	43,200.00
	<u>129,600.00</u>	<u>129,600.00</u>
- หมวดค่าใช้สอย		
- ค่าพาหนะและที่จอดรถ	18,800.00	30,000.00
	<u>18,800.00</u>	<u>30,000.00</u>
หมวดค่าวัสดุ		
- ค่าวัสดุวิทยาศาสตร์,	120,000.00	135,709.80
- ค่าวัสดุสารเคมี	160,000.00	146,908.60
- ค่าสัตว์ทดลองและเซลล์เพาะเลี้ยง	54,000.00	27,900.00
- ค่าวัสดุคอมพิวเตอร์	40,000.00	57,584.30
- ค่าวัสดุสำนักงาน	21,600.00	3,122.00
- ค่าหนังสือ วารสาร ตำราและถ่ายเอกสาร	20,000.00	33,175.30
	<u>415,600.00</u>	<u>404,400.00</u>
รวมรายจ่าย	<u>650,000.00</u>	<u>650,000.00</u>

รายรับสูงกว่ารายจ่าย นำส่งส่วนการคลังจุฬาลงกรณ์มหาวิทยาลัย (เอกสารแนบ)	0.00
ดอกเบี้ย (ถ้ามี)	<u>972.28</u>
รวมจำนวนเงินที่นำส่งส่วนการคลังทั้งสิ้น	<u>972.28</u>

ขอรับรองว่ารายงานการรับ-จ่ายเงินข้างต้นเป็นความจริงทุกประการ

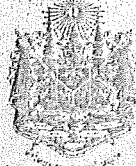


(รศ.ดร. ศักนัน พงศ์พันธุ์ผู้ภักดี)

หัวหน้าโครงการวิจัย

...../..... ม.ค...../....2559

หมายเหตุ : รายงานตลอดโครงการเมื่อสิ้นสุดโครงการ/ปิดโครงการ



20/02/14 13:20 0415D*2350 045-596503 BY BR0045
 NEW P/B NO.-0008730441 (OLD P/B NO.-0008730440)

พระบาทสมเด็จพระปรมินทรมหาจุฬาลงกรณ์พระจุลจอมเกล้าเจ้าอยู่หัว
 ได้ทรงพระกรุณาโปรดเกล้าโปรดกระหม่อมพระราชทานพระบรมราชานุญาตให้

บริษัท แวงก๊วยสามกัมมาจอล จำกัด

ใช้ตราแผ่นดินนี้ เป็นตราประจำธนาคาร เมื่อ ร.ศ.125 (พ.ศ. 2449)

ชื่อบัญชี
 NAME

รศ.ดร. ศักดิ์กัน พงศ์กันธัฐวิภาติ (วงษ์ประภณีเป็นต้น)

ธนาคารไทยพาณิชย์ จำกัด (มหาชน)
 SIAM COMMERCIAL BANK PUBLIC COMPANY LIMITED

0045 สาขาสะพานตากสิน ไทย

เลขที่บัญชี 045-596503-3
 ACCOUNT NO.

บัญชีเงินฝากออมทรัพย์
 SAVINGS ACCOUNT

8730441

- เงินฝากนี้ได้รับความคุ้มครองจากสถาบันคุ้มครองเงินฝากตามจำนวนที่กำหนดไว้ในกฎหมาย
- การทำรายการโดยมิใช่สมุดคู่มือฝากที่มีระยะเวลาเกินกว่า 6 เดือนขึ้นไป ธนาคารจะสรุปรวมรายการฝากและรายการถอนอย่างละเอียดรวมรายการเป็นรายเดือน

วันที่ DATE	รายการ TIC	ถอน WITHDRAWAL	ฝาก DEPOSIT	ยอดคง BALANCE	ยอดคง M.T. USD
1 20/02/14	BF			+++++260,800.00	0415D
2 19/05/14	CW	ถอน 334,978.00		++++145,820.10	04100
3 25/06/14	IN	+++++409.05		++++146,229.15	0000A
4 28/07/14	QN	+++++260,800.00		++++407,029.15	0418D
5 16/09/14	CW	-----66,163.77		++++340,865.38	1316C
6 29/09/14	CW	-----307,230.00		++++33,635.38	0418D
7 25/12/14	IN	+++++444.14		++++34,079.52	0000A
8 12/03/15	QD	+++++260,200.00		++++294,279.52	0415C
9 23/03/15	CW	-----34,079.52		++++260,200.00	0418D
10 03/06/15	CW	-----153,252.80		++++106,947.20	0418D
11 25/06/15	IN	+++++370.15		++++107,317.35	0000A
12 04/08/15	QD	+++++158,400.00		++++265,717.35	0412C
13 07/09/15	CW	-----180,873.09		+++++84,844.26	0415C
14 09/09/15	QN	+++++260,200.00		++++345,044.26	0413D
15 19/10/15	XW	-----146,036.21		+++++199,008.05	0417C
16 30/10/15	XD	+++++132,126.00		+++++331,134.05	0415C
17 13/11/15	CW	-----100,000.00		+++++231,134.05	0826D
18 25/12/15	IN	+++++602.13		+++++231,736.18	0000A
19 19/01/16	CW	-----45,748.00		+++++185,988.18	0413D
20 26/01/16	QD	+++++335,200.00		+++++521,188.18	0420C
21					
22					

ข้อมูลแสดงรายการฝากและถอนที่เกิดขึ้นจริงตามบัญชีฝากเงินของธนาคารแห่งประเทศไทย โดยข้อมูลดังกล่าวอาจมีความคลาดเคลื่อนได้บ้างเนื่องจากข้อมูลดังกล่าวเป็นข้อมูลเบื้องต้น
 Should show the transactions recorded without the use of a passbook for 6 months. The deposit and withdrawal transactions will be separately summarized and shown in the passbook on a monthly basis.

หมายเหตุ (TIC):
 DI, CR ฝาก, ถอน โอนเงิน โอนบัญชี
 CD, XD โอนเงิน โอนบัญชี โอนบัญชี
 CD, CW ฝาก โอนเงิน โอนเงิน
 CC, XC โอนบัญชี โอนบัญชี โอนบัญชี
 CH, OH โอนบัญชี โอนบัญชี โอนบัญชี
 OD, MO โอนบัญชี โอนบัญชี โอนบัญชี
 PF โอนบัญชี โอนบัญชี โอนบัญชี
 EC โอนบัญชี โอนบัญชี โอนบัญชี
 FE โอนบัญชี โอนบัญชี โอนบัญชี

DI, TX โอนบัญชี โอนบัญชี Interest Tax
 MO, OD โอนบัญชี โอนบัญชี Deposit Deposit
 PF โอนบัญชี โอนบัญชี Interest Returned
 RT โอนบัญชี โอนบัญชี Deposit Returned
 VO โอนบัญชี โอนบัญชี Deposit New A/C
 VD, VW ฝาก โอนบัญชี โอนบัญชี
 XB โอนบัญชี โอนบัญชี โอนบัญชี
 XI, XZ ฝาก, ถอน โอนบัญชี โอนบัญชี
 XD, XW ฝาก โอนบัญชี โอนบัญชี
 Transfer Deposit Withdrawal

XR ฝาก โอนบัญชี โอนบัญชี Real Time Fund Transfer
 PW, FX โอนบัญชี โอนบัญชี โอนบัญชี Portal Cash Transfer Withdrawal
 P1 โอนบัญชี โอนบัญชี โอนบัญชี Conditioned no book deposits
 P2 โอนบัญชี โอนบัญชี โอนบัญชี Conditioned no book withdrawal